ETSI TR 102 376-1 V1.2.1 (2015-11)

Digital Video Broadcasting (DVB);
Implementation guidelines for the second generation system for Broadcasting, Interactive Services, News Gathering and other broadband satellite applications;
Part 1: DVB-S2

EBU
OPERATING EUROVISION

DVB
Digital Video Broadcasting

Reference
RTR/JTC-DVB-354-1

Keywords
broadband, broadcasting, digital, satellite, TV, video

ETSI

650 Route des Lucioles
F-06921 Sophia Antipolis Cedex - FRANCE

Tel.: +33 4 92 94 42 00 Fax: +33 4 93 65 47 16

Siret N° 348 623 562 00017 - NAF 742 C
Association à but non lucratif enregistrée à la
Sous-Préfecture de Grasse (06) N° 7803/88

Contents

Intellectual Property Rights

IPRs essential or potentially essential to the present document may have been declared to ETSI. The information pertaining to these essential IPRs, if any, is publicly available for **ETSI members and non-members**, and can be found in ETSI SR 000 314: *"Intellectual Property Rights (IPRs); Essential, or potentially Essential, IPRs notified to ETSI in respect of ETSI standards"*, which is available from the ETSI Secretariat. Latest updates are available on the ETSI Web server (http://ipr.etsi.org).

Pursuant to the ETSI IPR Policy, no investigation, including IPR searches, has been carried out by ETSI. No guarantee can be given as to the existence of other IPRs not referenced in ETSI SR 000 314 (or the updates on the ETSI Web server) which are, or may be, or may become, essential to the present document.

Foreword

This Technical Report (TR) has been produced by Joint Technical Committee (JTC) Broadcast of the European Broadcasting Union (EBU), Comité Européen de Normalisation ELECtrotechnique (CENELEC) and the European Telecommunications Standards Institute (ETSI).

The work of the JTC was based on the studies carried out by the European DVB Project under the auspices of the Ad Hoc Group on DVB-S2 of the DVB Technical Module. This joint group of industry, operators and broadcasters provided the necessary information on all relevant technical matters (see clause 2).

NOTE: The EBU/ETSI JTC Broadcast was established in 1990 to co-ordinate the drafting of standards in the specific field of broadcasting and related fields. Since 1995 the JTC Broadcast became a tripartite body by including in the Memorandum of Understanding also CENELEC, which is responsible for the standardization of radio and television receivers. The EBU is a professional association of broadcasting organizations whose work includes the co-ordination of its members' activities in the technical, legal, programme-making and programme-exchange domains. The EBU has active members in about 60 countries in the European broadcasting area; its headquarters is in Geneva.

European Broadcasting Union
CH-1218 GRAND SACONNEX (Geneva)
Switzerland
Tel: +41 22 717 21 11
Fax: +41 22 717 24 81

The Digital Video Broadcasting Project (DVB) is an industry-led consortium of broadcasters, manufacturers, network operators, software developers, regulatory bodies, content owners and others committed to designing global standards for the delivery of digital television and data services. DVB fosters market driven solutions that meet the needs and economic circumstances of broadcast industry stakeholders and consumers. DVB standards cover all aspects of digital television from transmission through interfacing, conditional access and interactivity for digital video, audio and data. The consortium came together in 1993 to provide global standardization, interoperability and future proof specifications.

The present document is part 1 of a multi-part deliverable covering Digital Video Broadcasting (DVB); Implementation guidelines for the second generation system for Broadcasting, Interactive Services, News Gathering and other broadband satellite applications, as identified below:

Part 1: "DVB-S2";

Part 2: "S2 Extensions (DVB-S2X)".

Modal verbs terminology

In the present document "**shall**", "**shall not**", "**should**", "**should not**", "**may**", "**need not**", "**will**", "**will not**", "**can**" and "**cannot**" are to be interpreted as described in clause 3.2 of the ETSI Drafting Rules (Verbal forms for the expression of provisions).

"**must**" and "**must not**" are **NOT** allowed in ETSI deliverables except when used in direct citation.

1 Scope

The present document is part 1 of a multipart deliverable and gives an overview of the technical and operational issues relevant to the system specified in ETSI EN 302 307-1 [i.2], including service quality and link availability evaluation for typical DSNG and fixed contribution links, with the purpose to facilitate its interpretation.
Correspondingly, ETSI TR 102 376-2 [i.45] considers technical and operational issues relevant to the system specified in ETSI EN 302 307-2 [i.44], but it can be applied also to DVB-S2, when enhanced S2 receivers and channel models are implemented.

2 References

2.1 Normative references

References are either specific (identified by date of publication and/or edition number or version number) or non-specific. For specific references, only the cited version applies. For non-specific references, the latest version of the reference document (including any amendments) applies.

Referenced documents which are not found to be publicly available in the expected location might be found at http://docbox.etsi.org/Reference.

NOTE: While any hyperlinks included in this clause were valid at the time of publication, ETSI cannot guarantee their long term validity.

The following referenced documents are necessary for the application of the present document.

Not applicable.

2.2 Informative references

References are either specific (identified by date of publication and/or edition number or version number) or non-specific. For specific references, only the cited version applies. For non-specific references, the latest version of the reference document (including any amendments) applies.

NOTE: While any hyperlinks included in this clause were valid at the time of publication, ETSI cannot guarantee their long term validity.

The following referenced documents are not necessary for the application of the present document but they assist the user with regard to a particular subject area.

[i.1] ETSI EN 300 421: "Digital Video Broadcasting (DVB); Framing structure, channel coding and modulation for 11/12 GHz satellite services".

[i.2] ETSI EN 302 307-1: "Digital Video Broadcasting (DVB); Second generation framing structure, channel coding and modulation systems for Broadcasting, Interactive Services, News Gathering and other broadband satellite applications; Part 1: DVB-S2".

[i.3] ISO/IEC 13818 (parts 1 and 2): "Information technology - Generic coding of moving pictures and associated audio information".

[i.4] ETSI EN 301 210: "Digital Video Broadcasting (DVB); Framing structure, channel coding and modulation for Digital Satellite News Gathering (DSNG) and other contribution applications by satellite".

[i.5] ETSI EN 301 192: "Digital Video Broadcasting (DVB); DVB specification for data broadcasting".

[i.6] ETSI EN 300 429: "Digital Video Broadcasting (DVB); Framing structure, channel coding and modulation for cable systems".

[i.7] ETSI TR 101 221: "Digital Video Broadcasting (DVB); User guideline for Digital Satellite News Gathering (DSNG) and other contribution applications by satellite".

[i.8] U. Reimers, A. Morello: "DVB-S2, the second generation standard for satellite broadcasting and unicasting", International Journal on Satellite Communication Networks, Volume 22, Issue 3.

[i.9] R. Gallager: "Low Density Parity Check Codes", IRE Transactions on Information Theory, January 1962.

[i.10] M. Eroz, F.-W. Sun and L.-N. Lee: "DVB-S2 Low Density Parity Check Codes with near Shannon Limit Performance", International Journal on Satellite Communication Networks, Volume 22, Issue 3.

[i.11] E. Casini, R. De Gaudenzi and A. Ginesi: "DVB-S2 modem algorithms design and performance over typical satellite channels", International Journal on Satellite Communication Networks, Volume 22, Issue 3.

[i.12] F.-W. Sun Y. Jiang and L.-N. Lee: "Frame synchronization and pilot structure for DVB-S2" International Journal on Satellite Communication Networks, Volume 22, Issue 3.

[i.13] R. Rinaldo, M. Vazquez-Castro and A. Morello: "DVB-S2 ACM modes for IP and MPEG unicast applications", International Journal on Satellite Communication Networks, Volume 22, Issue 3.

[i.14] S. Cioni, R. De Gaudenzi and R. Rinaldo: "Channel estimation and physical layer adaptation techniques for satellite networks exploiting adaptive coding and modulation", International Journal of Satellite Communications, John Wiley & Sons, Volume 26, pp. 157-188, January/February 2008.

[i.15] H. Bischl, H. Brandt, T. de Cola, R. De Gaudenzi, E. Eberlein, N. Girault, E. Alberty, S. Lipp, R. Rinaldo, B. Rislow, J. A. Skard, J. Tousch and G. Ulbricht: "Adaptive coding and modulation for satellite broadband networks: From theory to practice", International Journal of Satellite Commun., John Wiley & Sons, Volume 28, pp. 59-111, March/April 2010.

[i.16] Final Report of ESA Contract No. 19572/06/NL/JA, DVB-S2 Satellite Experiment, EADS Astrium, September 2010.

[i.17] R. Rinaldo and R. De Gaudenzi: "Capacity analysis and system optimization for the forward link of multi-beam satellite broadband systems exploiting adaptive coding and modulation", International Journal on Satellite Communication Networks, Volume 22, Issue 3.

[i.18] M.A. Vazquez-Castro et Al.: "Scheduling issues in ACM DVB-S2 systems: performance assessment through a comprehensive OPNET simulator", under preparation.

[i.19] C.E. Gilchriest: "Signal to Noise Monitoring" JPL Space Programs Summary, No 37-27, Volume IV, pp 169-176.

[i.20] D. J. MacKay and R. M. Neal: "Good codes based on very sparse matrices", 5th IMA Conf. 1995, pp.100-111.

[i.21] D. J. MacKay and R. M. Neal: "Near Shannon limit performance of low density parity check codes", Electronics Letters, March 1997, Volume 33, no.6, pp. 457-458.

[i.22] T. Richardson and R. Urbanke: "Efficient encoding of low-density parity check codes", IEEE Transactions on Information Theory, Volume 47, pp.638-656, February 2001.

[i.23] T. Richardson, A. Shokrollahi and R. Urbanke: "Design of capacity approaching irregular low density parity check codes", IEEE Transactions on Information Theory, February 2001, Volume 47, pp. 619-637.

[i.24] U. Mengali and A.N. D'Andrea: "Synchronization Techniques for Digital Receivers", Plenum Press, New York, USA, 1997.

[i.25] R. De Gaudenzi, A. Guillen i Fabregas and A. Martinez Vicente: "Turbo-coded APSK Modulations for Satellite Broadcasting and Multicasting- Part I: Coded Modulation Design", submitted to IEEE Transactions On Wireless Communications 2004.

[i.26] R. De Gaudenzi, A. Guillen i Fabregas and A. Martinez Vicente: "Turbo-coded APSK Modulations for Satellite Broadcasting - Part II: End-to-End Performance" submitted to IEEE Transactions on Wireless Communications 2004.

[i.27] R. De Gaudenzi and M. Luise: "Design and Analysis of an All-Digital Demodulator for Trellis Coded 16-QAM Transmission over a Non-linear Satellite Channel", IEEE Transactions on Communications, Volume 43, No. 2/3/4, February/March/April 1995, part 1.

[i.28] F. M. Gardner: "A BPSK/QPSK timing-error detector for sampled receivers", IEEE Transactions On Communications, Volume COM-34, no. 5, May 1986.

[i.29] M. Luise and R. Reggiannini: "Carrier Frequency Recovery in All Digital Modems for Burst Mode Transmissions", IEEE Transactions on Communications, COM-43, pp. 1169-1178, February/March/April 1995.

[i.30] M. Oerder and H. Meyr: "Digital Filter and Square Timing Recovery", IEEE Transactions on Communications, COM-36, May 1988.

[i.31] A. Morello, V. Mignone: "DVB-S2 ready to lift-off", IBC'04 Conference, Amsterdam, 9-13 September, 2004.

[i.32] D.R. Pauluzzi and N.C. Beaulieu: "A Comparison of SNR Estimation Techniques for the AWGN channel", IEEE Transactions on Communications, Volume 48, pp. 1681-1691, October 2000.

[i.33] L. Castanet et al.: "Comparison of Various Methods for Combining Propagation Effects and Predicting Loss in Low-Availability Systems in the 20-50 GHz Frequency Range", International Journal on Satellite Communications, Volume 19, pp. 317-334, 2001.

[i.34] E. Casini: "DVB-S2 end-to-end performance with linearized and non-linearized TWT amplifiers" ESA document Reference TEC-ETC/2004.84/EC/ec.

[i.35] F. J. Williams, N.J.A. Sloane: "The Theory of error correction coding", Elsevier, New York, 1977.

[i.36] ETSI EN 301 790: "Digital Video Broadcasting (DVB); Interaction channel for satellite distribution systems".

[i.37] ETSI ETS 300 801: "Digital Video Broadcasting (DVB); Interaction channel through Public Switched Telecommunications Network (PSTN)/ Integrated Services Digital Networks (ISDN)".

[i.38] ETSI EN 301 195: "Digital Video Broadcasting (DVB); Interaction channel through the Global System for Mobile communications (GSM)".

[i.39] ETSI ES 200 800: "Digital Video Broadcasting (DVB); DVB interaction channel for Cable TV distribution systems (CATV)".

[i.40] Recommendation ITU-R SNG.770-1: "Uniform operational procedures for satellite news gathering (SNG)".

[i.41] ETSI TS 102 606: "Digital Video Broadcasting (DVB); Generic Stream Encapsulation (GSE) Protocol".

[i.42] ETSI TS 102 771: "Digital Video Broadcasting (DVB); Generic Stream Encapsulation (GSE) implementation guidelines".

[i.43] Recommendation ITU-T H.264 (11-2009): "Advanced video coding for generic audiovisual services | ISO/IEC 14496-10:2008, Information technology - Coding of audio-visual objects (MPEG-4) - Part 10: Advanced video coding", Version 13.

[i.44] ETSI EN 302 307-2: "Digital Video Broadcasting (DVB); Second generation framing structure, channel coding and modulation systems for Broadcasting, Interactive Services, News Gathering and other broadband satellite applications; Part 2: DVB-S2 Extensions (DVB-S2X)".

[i.45] ETSI TR 102 376-2: "Digital Video Broadcasting (DVB); Implementation guidelines for the second generation system for Broadcasting, Interactive Services, News Gathering and other broadband satellite applications; Part 2: DVB-S2X".

[i.46] Recommendation ITU-R P.618-11 (09/2013): "Propagation data and prediction methods required for the design of Earth-space telecommunication systems".

[i.47] Recommendation ITU-R P.837-6 (02/2012): "Characteristics of precipitation for propagation modelling".

[i.48] Recommendation ITU-R P.839-4 (09/2013): "Rain height model for prediction methods".

3 Symbols and abbreviations

3.1 Symbols

For the purposes of the present document, the following symbols apply:

α	Roll-off factor
B_S	Bandwidth of the frequency Slot allocated to a service
BUFS	Maximum size of the requested receiver buffer to compensate delay variations
c	codeword
C/N	Carrier-to-noise power ratio (N measured in a bandwidth equal to symbol rate)
C/(N+I)	Carrier-to-(Noise + Interference) ratio
C_{SAT}	Un-modulated pure carrier saturated power
C_{SAT}/N	Ratio of the Un-modulated pure carrier saturated power and the Noise power in the receiver bandwidth
DFL	Data Field Length
D_S	Source Delay
E_b/N_0	Ratio between the energy per information bit and single sided noise power spectral density
E_s/N_0	Ratio between the energy per transmitted symbol and single sided noise power spectral density
$E_s/(N_0+I_0)$	Ratio between the energy per transmitted symbol and single sided noise plus interference power spectral density
ΔD_{TOT}	Total Delay variations
Φ	Antenna diameter
$\psi_{MPEG}(L)$	MPEG encapsulation efficiency
$\psi_{DVB-S2}(L)$	Overall DVB-S2 encapsulation efficiency
$\psi_{MS}(\eta, L)$	DVB-S2 Mode and Stream adaptation efficiency
$\psi_{\text{framing}}(\eta)$	DVB-S2 Physical layer framing efficiency
i	LDPC code information block
$i_0, i_1, ..., i_{k_{ldpc}-1}$	LDPC code information bits
$H_{(N-K)\times N}$	LDPC code parity check matrix
I, Q	In-phase, Quadrature phase components of the modulated signal
K_{BCH}	number of bits of BCH uncoded Block
N_{BCH}	number of bits of BCH coded Block
k_{ldpc}	number of bits of LDPC uncoded Block
n_{ldpc}	number of bits of LDPC coded Block
N_I	zero-mean Gaussian noise contribution to the phase estimate
η	Spectral efficiency
η_c	code efficiency
η_{MOD}	number of transmitted bits per constellation symbol
L	IP packet length
m	BCH code information word
m(x)	BCH code message polynomial
$p_0, p_1, ... p_{n_{ldpc}-k_{ldpc}-1}$	LDPC code parity bits
P_R	Total received power
q	code rate dependant constant for LDPC codes
r_m	In-band ripple (dB)
R_s	Symbol rate corresponding to the bilateral Nyquist bandwidth of the modulated signal
R_{TS}	Transport Stream Bit rate

R_u	Useful bit rate at the DVB-S2 system input
S	Number of Slots in a XFECFRAME
T_s	Symbol period
T_{loop}	loop delay
T_{prop}	propagation time
T_q	waiting time
T_{ST}	Threshold on SOF in Tentative state
T_{PL}	Threshold of PLSCODE in Locked mode
T_{PT}	Threshold on PLSCODE in Tentative state
T_{SL}	Threshold on SOF in Locked state

3.2 Abbreviations

For the purposes of the present document, the following abbreviations apply:

16APSK	16-ary Amplitude and Phase Shift Keying
32APSK	32-ary Amplitude and Phase Shift Keying
8PSK	8-ary Phase Shift Keying
ACI	Adjacent Channel Interference
ACM	Adaptive Coding and Modulation
ADSL	Asymmetric Digital Subscriber Line
AFR	Array Fed Reflector
AGC	Automatic Gain Control
ALC	Automatic Level Control
AM/AM	Amplitude Modulation/Amplitude Modulation
AM/PM	Amplitude Modulation/Phase Modulation
APSK	Amplitude Phase Shift Keying
ATM	Asynchronous Transfer Mode
AVC	Advanced Video Coding
AWGN	Additive White Gaussian Noise
BB	Baseband
BCH	Bose-Chaudhuri-Hocquenghem multiple error correction binary block code
BER	Bit Error Ratio
BPSK	Binary Phase Shift Keying
BS	Broadcast Service
BW	Bandwidth
CBR	Constant Bit Rate
CCM	Constant Coding and Modulation
CDF	Cumulative Distribution Function
CRC	Cyclic Redundancy Check
DA	Data Aided
DAGC	Digital AGC
DA-VT	Data Aided- Vector-Tracker
DA-VT AGC	Data-Aided version of the Vector-Tracker Automatic Gain Control
DBFN	Digital Beam Forming Network
DC	Direct Current
DD	Decision Directed
DD-PLL	Decision Directed-Phase Lock Loop
DNP	Deleted Null Packets
DPLL	Digital Phase Lock Loop
DSM-CC	Digital Storage Media - Command and Control
DSNG	Digital Satellite News Gathering
DTH	Direct To Home
DTT	Digital Terrestrial Television
DTV	Digital TeleVision
DVB	Digital Video Broadcasting project
DVB-CM	DVB Commercial Module
DVB-S	DVB System for satellite broadcasting

NOTE: As specified in ETSI EN 300 421 [i.1].

DVB-S2 DVB-S2 System

NOTE: As specified in ETSI EN 302 307-1 [i.2].

EBU European Broadcasting Union
EIRP Effective Isotropic Radiated Power
EN European Norm
EOC Edge Of Coverage
EPG Electronic Program Guide
ES ETSI Standard
ETS European Telecommunication Standard
FDM Frequency Division Multiplex
GEO Geostationary
FEC Forward Error Correction
FED Frequency Error Detector
FER Frame Error Rate
FF Feed Forward
FIFO First In First Out
FPGA Field Programmable Gate Array
GEO Geostationary
GS Generic Stream
GSE Generic Stream Encapsulation
GW GateWay
HDTV High Definition Television
HPA High Power Amplifier
IBO Input Back Off
IF Intermediate Frequency
IIR Infinite Impluse Response
IMUX Input MUltipleXer - Filter
IP Internet Protocol
IPFD Isotropic Power Flux Density
IRD Integrated Receiver Decoder
IS Interactive Services
ISCR Input Stream Clock Reference
ISI InterSymbol Interference
ITU International Telecommunications Union
ITU-R International Telecommunication Union - Radiocommunication Sector
LDPC Low Density Parity Check (codes)
LNB Low Noise Block
LP Low Priority
LPF Low Pass Filter
LTWTA Linearized Travelling Wave Tube Amplifier
MAC Media Access Control
ML Maximum Likelihood
MOD Modulation
MODCOD MODulation and CODing Mode
MPE Multi-Protocol Encapsulation
MPEG Moving Pictures Experts Group
MUX Multiplex
NA Not Applicable
NASA National Aeronautics and Space Administration
NCO Numerically Controlled Oscillator
NDA Non-Data Aided
NG Nominal Gain
NL Non-Linear
NP Null Packets
NPR Noise Power Ratio
OBO Output Back Off
OMUX Output Multiplexer - Filter
PCR Programme Clock Reference
PER (MPEG TS) Packet Error Rate
PFA Probability of False Alarm

PID	Packet Identifier
PL	Physical Layer
PLL	Phase-Locked Loop
PLR	Packet Loss Rate
PLS	Physical Layer Signalling
PLSCODE	PLS code
PM	Phase Modulation
PND	Probability of Non Detection
PS	Professional Services
PSD	Power Spectral Density
PSK	Phase Shift Keying
QAM	Quadrature Ampliture Modulation
QEF	Quasi-Error-Free
QoS	Quality of Service
QPSK	Quaternary Phase Shift Keying
r.m.s.	root mean square
RF	Radio Frequency
RF/IF	Radio Frequency to Intermediate Frequency Conversion
RMS	Root Mean Square
RR	Round Robin
RRM	Radio Resource Management
RS	Reed Solomon
RX	Receiver
SDTV	Standard Definition Television
SISO	Single Input Single Output
SMATV	Satellite Master Antenna TeleVision
SMF	Signal Matched Filter
SNG	Satellite News Gathering
SNIR	Signal to Noise plus Interference Ratio
SNORE	Signal to NOise Ratio Estimation
SNR	Signal to Noise Power Ratio
SOF	Start of Frame
SRRC	Square Root Raised Cosine Filter
ST	Satellite Terminal
SYNC	Synchronisation
SYNCD	SYNC Distance
TCP	Transmission Control Protocol
TCP/IP	Transmission Control Protocol / Internet Protocol
TDM	Time Division Multiplex
TS	Transport Stream
TSN	Time Slice Number
TV	Television
TWT	Travelling Wave Tube
TWTA	Travelling Wave Tube Amplifier
TX	Transmitter
UDP	User Datagram Protocol
UMTS	Universal Mobile Telecommunication System
UP	User Packet
UPL	User Packet Length
USA	United States of America
VBR	Variable Bit Rate
VCM	Variable Coding and Modulation
VL-SNR	Very Low-Signal to Noise Ratio
VPN	Virtual Private Network
XPD	Cross Polar Discrimination

4 General description of the technical characteristics of the DVB-S2 system

4.0 Overview

DVB-S2 is the second-generation DVB specification for broadband satellite applications, developed on the success of the first generation specifications, DVB-S for broadcasting and DVB-DSNG for satellite news gathering and contribution services, benefiting from the technological achievements of the last decade. It has been designed for:

- Broadcast Services for standard definition TV and HDTV.
- Interactive Services including Internet Access for consumer applications.
- Professional Applications, such as Digital TV contribution and News Gathering, TV distribution to terrestrial VHF/UHF transmitters, Data Content distribution and Internet Trunking.

The DVB-S2 standard has been specified around three key concepts: best transmission performance, total flexibility and reasonable receiver complexity.

To achieve the best performance-complexity trade-off, DVB-S2 benefits from more recent developments in channel coding (adoption of LDPC codes) and modulation (use of QPSK, 8PSK, 16APSK and 32APSK). The result is typically a 30 % capacity increase over DVB-S under the same transmission conditions. In addition, for broadcast applications, DVB-S2 is not constrained to the use of QPSK and therefore it can deliver significantly higher bit rates over high power satellites, thus still increasing capacity gain with respect to DVB-S. Furthermore, when used for interactive point-to-point applications like IP unicasting, the gain of DVB-S2 over DVB-S is even greater: Variable Coding and Modulation (VCM) functionality allows different modulations and error protection levels to be used and changed on a frame-by-frame basis. This may be combined with the use of a return channel to achieve closed-loop Adaptive Coding and Modulation (ACM), thus allowing the transmission parameters to be optimized for each individual user, dependant on its own link conditions.

DVB-S2 is so flexible that it can cope with any existing satellite transponder characteristics, with a large variety of spectrum efficiencies and associated C/N requirements. Furthermore, it is not limited to MPEG-2 video and audio source coding, but it is designed to handle a variety of audio-video and data formats including formats which the DVB Project is currently defining for future applications. DVB-S2 accommodates any input stream format, including continuous bit-streams, single or multiple MPEG Transport Streams, IP as well as ATM packets. This future proofing will allow other current and future data schemes to be used without the need for a new specification. An optional transmission format for high symbol-rate satellite carriers for broadcasting, professional and interactive services is also specified, that may optionally be adopted for wideband satellite transponders (e.g. 200 MHz to 500 MHz), where the transmission of a single or few wide-band carriers is preferable to the transmission of a multiplicity of narrow-band carriers, for power and efficiency optimization or other needs.

It is based on the "tool-kit" approach that allows to cover all the application areas while still keeping the single-chip decoder at reasonable complexity levels, thus enabling the use of mass market products also for professional applications.

4.1 Commercial requirements

4.1.0 DVB commercial requirements for Advanced Coding and Modulation Schemes for Broadband Satellite Services

For clause 4.1 the content in italic is extracted from document DVB CM373r1 BSS17r1 on "Advanced Coding and Modulation Schemes for Broadband Satellite Services - Commercial Requirements".
The DVB-S standard was developed primarily with unidirectional broadcast applications in mind, but has been adopted for other purposes, such as point-to-point data transmission. One of the reasons for this is the availability of inexpensive receive silicon as a result of the high volume broadcast receiver market. The Commercial Module of DVB (DVB-CM) foresaw a similar process for the new system, where the volume driver is expected to remain broadcast applications.

To avoid confusion in the distinction between broadcast and non-broadcast applications, with increasing provision of entertainment services over IP networks, and increasing use of interactivity with TV, DVB-CM introduced the following definitions:

- Broadcast services are defined as TV, radio and associated data (e.g. teletext, EPG, etc.) in contribution (e.g. DSNG), distribution (e.g. SMATV and cable feeds) and direct to home applications. In the case of interactive services, it is intended only the forward path.
- Non-broadcast services are defined as point-to-point and point-to-multipoint data services.

4.1.1 Commercial Requirements for Broadcast Services

Broadcast services *are characterized by having a large coverage area and providing audio-visual and data services to an extensive base of similar reception systems (both antennas and receivers) with a high degree of availability. For broadcasters there are various reasons to use higher order modulation and/or advanced coding schemes, including:*

- *Increased data throughput in a given bandwidth.*
- *Increased availability through improved link margin.*
- *Increased coverage area.*

At the launch of DVB-S2 a *key factor for many established broadcasters was the issue of backwards-compatibility. Large populations of DVB-S receivers in the field must continue to provide service to customers for at least several years. This was particularly important where there was a subsidy. Backwards-compatible modulation systems that allow DVB-S receivers to continue operating, while providing additional capacity and services to new, advanced receivers, are seen as the only commercially viable way forward for some operators. Backwards-compatible systems however suffer from two disadvantages:*

- *Compatibility will cause the overall performance to fall short of that achievable by non backwards compatible systems.*
- *There will be some performance penalty in the behaviour of existing QPSK receivers. Note that some operators are reluctant to accept even a slight performance penalty, as this increases service call-outs and churn.*

On the basis of the above considerations, DVB-CM concluded that the technical specification should provide for two approaches:

- A non backwards compatible scheme, *intended for use in systems requiring the highest efficiency, and not requiring that transmissions should be receivable by existing receiver populations.*
- A backwards-compatible scheme *that can be received by existing receiver populations, but provides additional capacity to enhanced receivers.* This should have the capability of migrating to a more efficient non backwards-compatible mode once all DVB-S receivers have been replaced.

The above considerations are no longer applicable; therefore DVB-CM concluded that the backward-compatible scheme is obsolete and is not included in the revised version of the ETSI EN 302 307-1 [i.2].

Furthermore the technical specification should also take into account the following:

- *A bit-rate increase of at least 35 % over DVB-S should be achieved.*
- Service availability targets remain no more than one uncorrected error per hour.
- For DVB-S2 transmissions, reliable reception should be possible using receive antenna diameters in the range 0,4 m to 0,8 m. *Due account shall be taken of anticipated satellite system characteristics (e.g. power, bandwidth, interference) over the next ten years.*
- *While the technical specification is concerned with the transmission format, it is important that this does not impose an undue burden on receiver costs.* New receiver silicon, enabling multi-mode reception, including DVB-S, DVB-S2, in volume should cost no more than 15 % more than current DVB-S devices.

4.1.2 Commercial Requirements for Non-Broadcast Services

In general, DVB-CM stated that *characteristics that are desirable exclusively for non-broadcast services should only be included in the base specification if the burden of cost to the broadcast receiver is negligible. The specification should be available for consideration as an alternative forward path for DVB-RCS Ku- and Ka-band systems and other data systems currently using DVB-S.* In the future non-broadcast *two-way services will need to take advantage of such techniques as adaptive modulation, adaptive coding* and adaptive power systems. The services provided will include:

- *Point-to-point services* (e.g. IP-backbone).
- *Point-to-multipoint services* (e.g. VPN services).
- *Two way mass market services (e.g. Internet access via satellite).*

The above services are differentiated from broadcast services by the following requirements and characteristics:

- The possibility of targeting particular receivers with particular content *within the common transport system. It is therefore not necessary to be able to decode the entire data stream at a typical user terminal.*
- The possibility of establishing different quality of service targets for services to different customers in different areas.
- *Receiver network volumes may not be as high as broadcast applications, but could benefit from inexpensive silicon arising from broadcast applications.*
- *Satellite capacity is generally the most expensive part of a link, always more expensive* compared to the equipment behind it.
- *Business users may be able to accept significantly larger receive antennas that residential users. In such cases it would be desirable to use this to allow greater user data rates to be transmitted.*

The technical specifications shall additionally take into account the following requirements:

- *Non-broadcast services should be receivable on antennas down to typical consumer sizes.*
- A wide range of *system parameters shall be available to address applications across consumer to business antenna sizes, and telecom to broadcast satellite powers.*
- *As in the case of broadcast applications, it should be possible to manufacture low cost receivers. If the impact of advanced features such as adaptive coding and modulation that are not relevant to broadcast applications is to raise broadcast receiver costs excessively, then these features could exist in an enhanced profile, available as an option.*
- *The technology shall aim to optimize the use of the transponder (keeping all other technical parameters the same, a minimum capacity increase of 100 % is targeted for the professional, non-broadcast market case using adaptive technologies).*
- *The target BER shall be at least as good as for broadcast applications.*
- The system has to allow for power control technologies, adaptive modulation and adaptive coding.

4.1.3 Common Commercial Requirements

The primary goal of new broadband satellite systems is to deliver a significantly higher net data rate in a given transponder bandwidth than the current DVB-S standard. Technical specifications for such a new standard should not prevent operators from taking into account all issues covered by local, national, and international laws, especially those related to security (protection of personal data, encryption of data and services). The new specification will cover transmit-end functions only, but take into account the consequent cost of receive silicon. The market will determine what features are actually implemented in receive silicon. For the protection of existing business, the current DVB-S standard will not be modified, nor will changes to other standards cause any existing feature to become invalid. The new specification will contain a range of options for coding that are appropriate to a wide range of applications. The new specifications will be application neutral and media content independent. The specifications will be transmission frequency neutral, or contain the elements allowing for an adaptation to the specifics of certain frequency ranges (e.g. Ka Band). Specifications for broadcast and non-broadcast applications will be provided by the definition of a limited number of profiles. The specification will not prevent the use of any kind of scrambling and security system at the transport layer.

4.2 Application scenarios

The DVB-S2 system has been optimized for the following broadband satellite application scenarios.

- Broadcast Services (BS): digital multi-programme Television (TV)/High Definition Television (HDTV) broadcasting services

  DVB-S2 is intended to provide Direct-To-Home (DTH) services for consumer Integrated Receiver Decoder (IRD), as well as collective antenna systems (Satellite Master Antenna Television - SMATV) and cable television head-end stations (possibly with remodulation, see ETSI EN 300 429 [i.6]). DVB-S2 may be considered a successor to the current DVB-S standard ETSI EN 300 421 [i.1], and may be introduced for new services and allow for a long-term migration. BS services are transported in MPEG Transport Stream format. VCM may be applied on multiple transport stream to achieve a differentiated error protection for different services (TV, HDTV, audio, multimedia).

- Interactive Services (IS): interactive data services including internet access

  DVB-S2 is intended to provide interactive services to consumer IRDs and to personal computers, where DVB-S2's forward path supersedes the DVB-S standard ETSI EN 300 421 [i.1] for interactive systems. No recommendation is included in the DVB-S and DVB-S2 standards as far as the return path is concerned. Therefore, interactivity can be established either via terrestrial connection through telephone lines, or via satellite. DVB offers a variety of return link specifications, such as for example DVB-RCS (ETSI EN 301 790 [i.36]), DVB-RCP (ETSI ETS 300 801 [i.37]), DVB-RCG (ETSI EN 301 195 [i.38]), DVB-RCC (ETSI ES 200 800 [i.39]). Data services are transported in (single or multiple) Transport Stream format according to ETSI EN 301 192 [i.5] (e.g. using Multiprotocol Encapsulation), or in (single or multiple) generic stream format. DVB-S2 can provide Constant Coding and Modulation (CCM), or Adaptive Coding and Modulation (ACM), where each individual satellite receiving station controls the protection mode of the traffic addressed to it.

- Digital TV Contribution and Satellite News Gathering (DTVC/DSNG)

  Digital television contribution applications by satellite consist of point-to-point or point-to-multipoint transmissions, connecting fixed or transportable uplink and receiving stations. They are not intended for reception by the general public. According to Recommendation ITU-R SNG.770-1 [i.40], SNG is defined as "Temporary and occasional transmission with short notice of television or sound for broadcasting purposes, using highly portable or transportable uplink earth stations, etc.". Services are transported in single (or multiple) MPEG Transport Stream format. DVB-S2 can provide Constant Coding and Modulation (CCM), or Adaptive Coding and Modulation (ACM). In this latter case, a single satellite receiving station typically controls the protection mode of the full multiplex.

- Data content distribution/trunking and other professional applications (PS)

  These services are mainly point-to-point or point-to-multipoint, including interactive services to professional head-ends, which re-distribute services over other media. Services may be transported in (single or multiple) generic stream format. The system can provide Constant Coding and Modulation (CCM), Variable Coding and Modulation (VCM) or Adaptive Coding and Modulation (ACM). In this latter case, a single satellite receiving station typically controls the protection mode of the full TDM multiplex, or multiple receiving stations control the protection mode of the traffic addressed to each one. In either case, interactive or non-interactive, the present document is only concerned with the forward broadband channel.

For all these applications, DVB-S2 benefits from more recent developments in channel coding and modulation, achieving typically a 30 % capacity increase over DVB-S ETSI EN 300 421 [i.1]. When used for point-to-point applications like IP unicasting or DSNG, the gain of DVB-S2 is even greater. Adaptive Coding and Modulation (ACM) functionality allows different modulation formats and error protection levels (i.e. coding rates) to be used and changed on a frame-by-frame basis within the transmitted data stream. By means of a return channel, informing the transmitter of the actual receiving condition, the transmission parameters may be optimized for each individual user, dependant on path conditions.

Furthermore DVB-S2 is compatible with Moving Pictures Experts Group (MPEG-2 and MPEG-4) coded TV services ISO/IEC 13818 [i.3], with a Transport Stream packet multiplex. Multiplex flexibility allows the use of the transmission capacity for a variety of TV service configurations, including sound and data services. All service components are Time Division Multiplexed (TDM) on a single digital carrier.

4.3 System architecture

4.3.0 Main features

To achieve the best performance, DVB-S2 is based on LDPC (Low Density Parity Check) codes, simple block codes with very limited algebraic structure, discovered by R. Gallager in 1962 [i.9]. LDPC codes have an easily parallelizable decoding algorithm which consists of simple operations such as addition, comparison and table look-up [i.20] and [i.21]; moreover the degree of parallelism is "adjustable" which makes it easy to trade-off throughput and complexity (see note 1).

NOTE 1: For the purpose of FEC technology selection during standardization, the maximum decoder complexity was set to correspond to 14 mm^2 of silicon using a 0,13 µm technology, and the reference symbol rate was 55 Mbaud.

Their key characteristics, allowing quasi-error free operation at only 0,6 to 1,2 dB from the modulation constrained Shannon limit [i.10], are:

- the very large LDPC code block length (64 800 bits for the normal frame, and 16 200 bits for the short frame);
- the large number of decoding iterations (around 50 SISO iterations);
- the presence of a concatenated BCH outer code (without any interleaver), defined by the designers as a "cheap insurance against unwanted error floors at high C/N ratios".

In comparison, the DVB-S and DVB-DSNG soft-decision Viterbi decoder takes decisions on blocks of only 100 symbols, without iterations, and the RS code over blocks of about 1 600 bits (interleaving factor 12), offering already quite good performance (see figure 4), around 3 dB from the Shannon limit.

Digital transmissions via satellite are affected by power and bandwidth limitations. Therefore DVB-S2 provides for many transmission modes (FEC coding and modulations), giving different trade-offs between power and spectrum efficiency. Code rates of 1/4, 1/3, 2/5, 1/2, 3/5, 2/3, 3/4, 4/5, 5/6, 8/9 and 9/10 are available depending on the selected modulation and the system requirements. Coding rates 1/4, 1/3 and 2/5 have been introduced to operate, in combination with QPSK, under exceptionally poor link conditions, where the signal level is below the noise level. Computer simulations demonstrated the superiority of such modes over BPSK modulation combined with code rates 1/2, 2/3 and 4/5. The introduction of two FEC code block length (64 800 and 16 200) was dictated by two opposite needs: the C/N performance improves for long block lengths, but the end-to-end modem latency increases as well. Therefore for applications not critical for delays (such as for example broadcasting) the long frames are the best solution, while for interactive applications a shorter frame may be more efficient when a short information packet has to be forwarded immediately by the transmitting station. Four modulation modes can be selected for the transmitted payload (see figure 1).

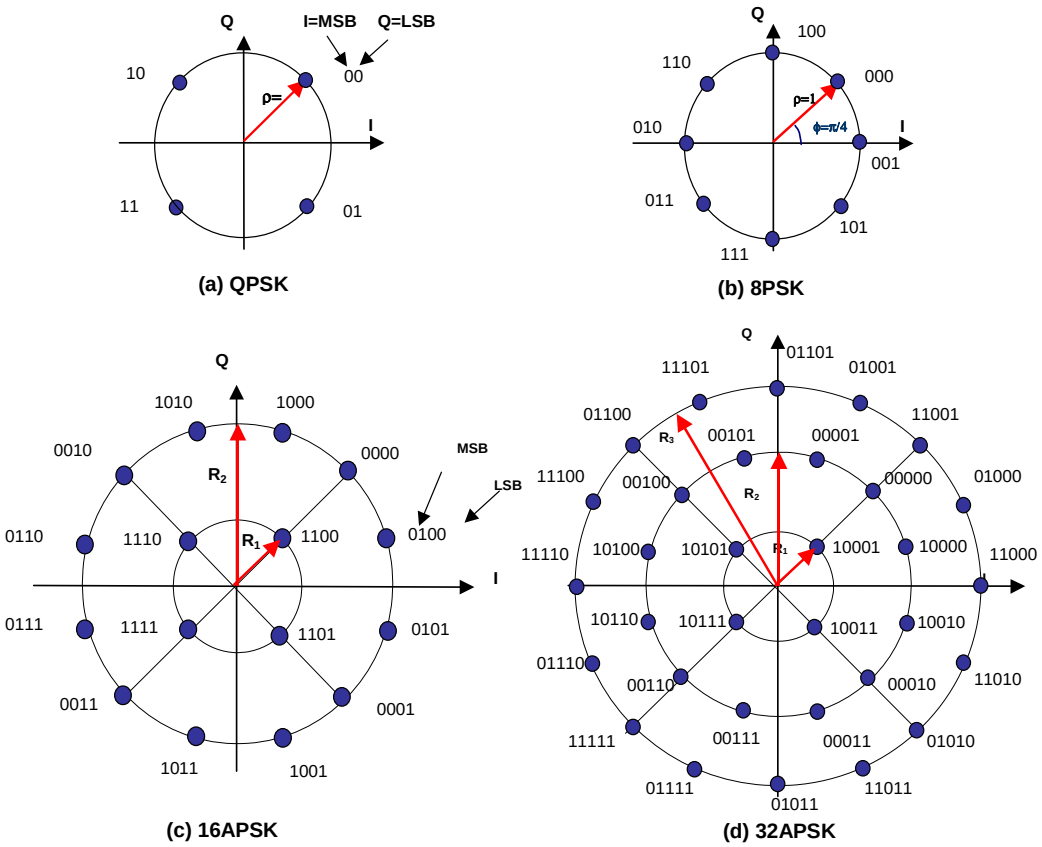

Figure 1: The four possible DVB-S2 constellations before physical layer scrambling

QPSK and 8PSK are typically proposed for broadcast applications, since they are virtually constant envelope modulations and can be used in non-linear satellite transponders driven near saturation. For some specific broadcasting applications (i.e. regional spot beams) and interactive application operating with multi-beam satellites, 16APSK provides extra spectral efficiency with very limited linearity requirements if proper pre-distortion schemes are employed. 32APSK modes, mainly targeted to professional applications, can also be used for broadcasting, but these require a higher level of available C/N and the adoption of advanced pre-distortion methods in the up-link station to minimize the effect of transponder non-linearity. Whilst these modes are not as power efficient as the other modes, the data throughput is much greater. 16APSK and 32APSK constellations have been optimized to operate over a non-linear transponder by placing the points on circles. Nevertheless their performances on a linear channel are comparable with those of 16QAM and 32QAM respectively. All the modes are also appropriate for operation in quasi-linear satellite channels, in multi-carrier Frequency Division Multiplex (FDM) type applications.

By selecting the modulation constellation and code rates, spectrum efficiencies from 0,5 to 4,5 bit/second/Hz are available and can be chosen dependant on the capabilities and restrictions of the satellite transponder used.

DVB-S2 also features the presence of a Physical Layer (PL) scrambler that is X-oring the I-Q modulator symbols (inclusive of the optional pilot symbols but excluding the PL header) with a complex binary randomization sequence of length truncated to the current PLFRAME duration. The complex randomization sequence has an original period of 262 143 symbols and is the one used in the terrestrial UMTS standard. It provides good auto and cross-correlation properties and allows to simply generate up to 262 142 distinct complex sequences. The main advantages of the physical layer randomization presence in DVB-S2 are:

- capability to uniquely "sign" individual carriers present in a multi-carrier multi-channel transponder;
- randomization of periodic pilot symbols pattern when pilot is time interleaved in the carrier;
- randomization of other satellite or same satellite other beams interference. It should be remarked that in case of interfering signals with lower baud rate than the useful carrier the physical layer descrambling present in the DVB-S2 demodulator will make interferer appearing as wideband interference thus reducing their degradation effect;
- the physical layer randomization also allows the application of repetition coding at the DVB-S2 modulator to further increase the C/(N+I) operating range of the system.

DVB-S2 has three roll-off factor choices to determine spectrum shape. These are $\alpha = 0,35$ as in DVB-S and two others, namely $\alpha = 0,25$, $\alpha = 0,20$ for tighter bandwidth shape restriction.

DVB-S2 is suitable for use on different satellite transponder bandwidths and frequency bands. The symbol rate is matched to given transponder characteristics, and, in the case of multiple carriers per transponder (FDM), to the frequency plan adopted.

Two levels of framing structures have been designed:

- the first at physical level, carrying few highly-protected signalling bits;
- the second at base-band level, carrying a variety of signalling bits, to allow the maximum flexibility on the input signal adaptation.

Physical Level framing

The first level of framing structure has been designed to provide robust synchronization and signalling at physical layer [i.12]. Thus a receiver may synchronize (carrier and phase recovery, frame synchronization) and detect the modulation and coding parameters before demodulation and FEC decoding. The DVB-S2 physical layer "train" is composed of a regular sequence of periodic "wagons" (physical layer frames, PL Frame): within a wagon, the modulation and coding scheme is homogeneous, but may change (Variable Coding and Modulation) in adjacent wagons. The PL framing structure is application independent (Constant Coding and Modulation or Variable Coding and Modulation).

Every PL Frame is composed of:

- a payload of 64 800 bits (normal FEC frame) or 16 200 bits (short FEC frame), generated by encoding the user bits according to the selected FEC scheme; thus the payload corresponds to a code block of the concatenated LDPC/BCH FEC;
- a PL Header, containing synchronization and signalling information: type of modulation and FEC rate, frame length, presence/absence of pilot symbols to facilitate synchronization.

The PL-Header is always composed of 90 symbols (using a fixed $\Pi/2$ binary modulation), and the payload is always composed of an integer multiple of 90 symbols (excluding pilot symbols). Since the PL Header is the first entity to be decoded by the receiver, it could not be protected by the powerful LDPC/BCH FEC scheme. On the other hand, it had to be perfectly decodable under the worst-case link conditions. Therefore designers selected a very low-rate 7/64 block code, suitable for soft-decision correlation decoding, and minimized the number of signalling bits to reduce decoding complexity and global efficiency loss. For example, assuming a 64 800 bit frame, the worst case efficiency of the PL Frame is 99,3 % (excluding pilot symbols).

Base-band Level framing

Another level of framing structure, the "baseband frame", allows a more complete signalling functionality to configure the receiver according to the application scenarios: single or multiple input streams, generic or transport stream, CCM (Constant Coding and Modulation) or ACM (Adaptive Coding and Modulation). Thanks to the LDPC/BCH protection and the wide length of the FEC frame, the Baseband (BB) Header may contain many signalling bits (80) without loosing neither transmission efficiency nor ruggedness against noise.

This BB-Header carries other important signalling information, such as: labelling the modulator input streams, describing the position and characteristics of user packets, indicating the presence of padding bits in the transmitted "baseband frame", signalling the activation of specific tools (Null-packet deletion function, Input Stream Synchronization function, as described in [i.12]), signalling the adopted modulation roll-off factor (see note 2).

NOTE 2: The roll-off factor needs not be signalled at physical layer, since (sub-optimum) reception is possible even assuming unknown roll-off factor.

4.3.1 The system block diagram

The DVB-S2 System is composed of a sequence of functional blocks as described in figure 2.

The block identified as "Mode Adaptation" is application dependent. Input sequences may be single or multiple Transport Streams (TS), single or multiple Generic Streams (packetized or continuous) such as Generic Stream Encapsulation (GSE) ETSI TS 102 606 [i.41] continuous streams: the block provides input stream interfacing, optional tools required for ACM (e.g. synchronization (see note 1) and null-packet deletion for Transport Streams (see note 2), described in clause 4.4.2.1), CRC coding (and replacement of SYNC bytes) for error detection in the receiver for packetized input streams. Furthermore, for multiple inputs, it provides merging of input streams in a single transmission signal and slicing in FEC code blocks, Data Fields. These latter are composed of DFL bits, where K_{BCH} -80 ≥ DFL ≥0, taken from a single input port, to be transmitted in a homogeneous transmission mode (FEC code and modulation). K_{BCH} is the BCH uncoded block length, which is dependent on the FECFRAME length (normal or short) and on the coding rate, and 80 bits is the BBHEADER length. The Base-Band Header is appended in front of the Data Field, to notify the receiver of the input stream format and Mode Adaptation type.

NOTE 1: Data processing in DVB-S2 may produce variable transmission delay. This block allows to guarantee constant-bit-rate and constant end-to-end transmission delay for packetized input stream [i.13].

NOTE 2: To reduce the information rate and increase the error protection in the modulator. The process allows null-packets re-insertion in the receiver in the exact place where they originally were [i.13].

NOTE 3: Input Stream Synchronizer, Null-Packet Deletion and CRC-8 encoder sub-systems are not relevant for GSE streams.

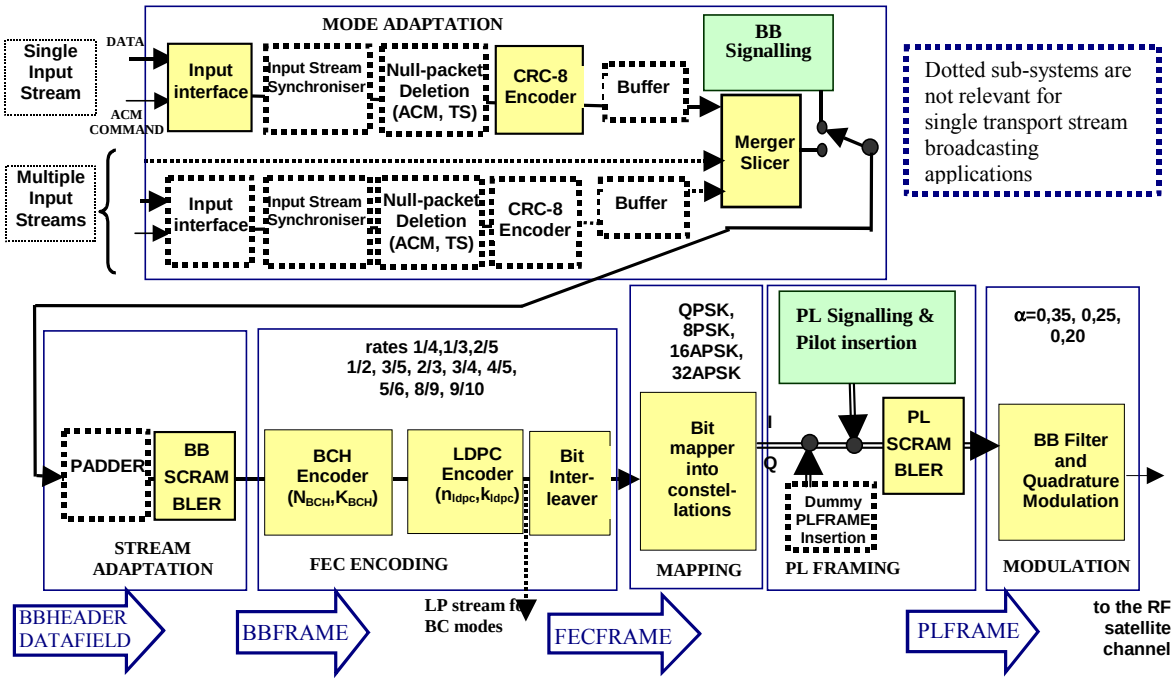

Figure 2: Functional block diagram of the DVB-S2 system

In case the user data available for transmission are not sufficient to completely fill a BBFRAME, padding is provided by the "Stream Adaptation" block to complete it. Base-band scrambling is also provided.

"FEC Encoding" carries out the concatenation of BCH outer code and LDPC inner codes. Depending on the application area, the FEC coded blocks (FEC frames) can have length 64 800 (normal frame) or 16 200 (short frame) bits. When VCM or ACM are used, FEC and modulation mode are constant within a frame but may be changed in different frames; furthermore, the transmitted signal can contain a mix of normal and short code blocks. Bit interleaving is then applied to FEC coded bits for 8PSK, 16APSK and 32APSK to separate bits mapped onto the same transmission signal.

"Mapping" into QPSK, 8PSK, 16APSK and 32APSK constellations is then applied to get a complex XFECFRAME, composed of 64 800/η_{MOD} or 16 200/η_{MOD} modulated symbols (η_{MOD} being the number of bits carried by a constellation symbol).

"Physical Layer Framing", synchronous with the FEC frames, provides optional dummy PL frame insertion (when no useful data is ready to be sent on the channel), PL header and optional pilot symbols insertion (2,4 % capacity loss) and scrambling for energy dispersal. Pilot symbols insertion occurs at regular intervals (36 pilot symbols each 1 440 data symbols), starting after each PLHEADER. This allows achieving the high channel estimation accuracy indicated by the standard and needed to track channel variation when ACM is utilized. The modulated symbols are inserted in a regular physical layer frame structure, composed of fixed length slots of 90 symbols. As the XFECFRAME length is dependent on both the frame type (short or normal) and the modulation order, it occupies a variable integer number of slots, which is larger the lower is the modulation order (see table 11 in ETSI EN 302 307-1 [i.2]). The PLFRAME is obtained by adding the PLHEADER, which occupies one extra slot and carries the information related to the frame type and to the physical layer mode. After decoding the PLHEADER, the receiver can derive, through the knowledge of the transmission parameters, the current frame length and thus the start of the following frame, even if the status of the channel does not allow for successful data decoding in the current frame.

Finally, "Modulation" applies Base-Band Filtering and Quadrature Modulation, to shape the signal spectrum and to generate the RF signal. Square-root raised cosine filtering is used at the transmit side, with choice on three roll-off factors: 0,35, 0,25 and 0,20.

4.3.2 Reference performance

4.3.2.0 General

The DVB-S2 system may be used in "single carrier per transponder" or in "multi-carriers per transponder" (FDM) configurations. In single carrier per transponder configurations, the transmission symbol rate R_s can be matched to given transponder bandwidth BW, to achieve the maximum transmission capacity compatible with the acceptable signal degradation due to transponder bandwidth limitations. To take into account possible thermal and ageing instabilities, reference can be made to the frequency response mask of the transponder. Group delay equalization at the transmitter may be used to increase the transmission capacity or to reduce degradation. Alternatively, if no group delay equalization at the transmitter is applied, a maximum acceptable characteristic group delay is suggested in figure 3.

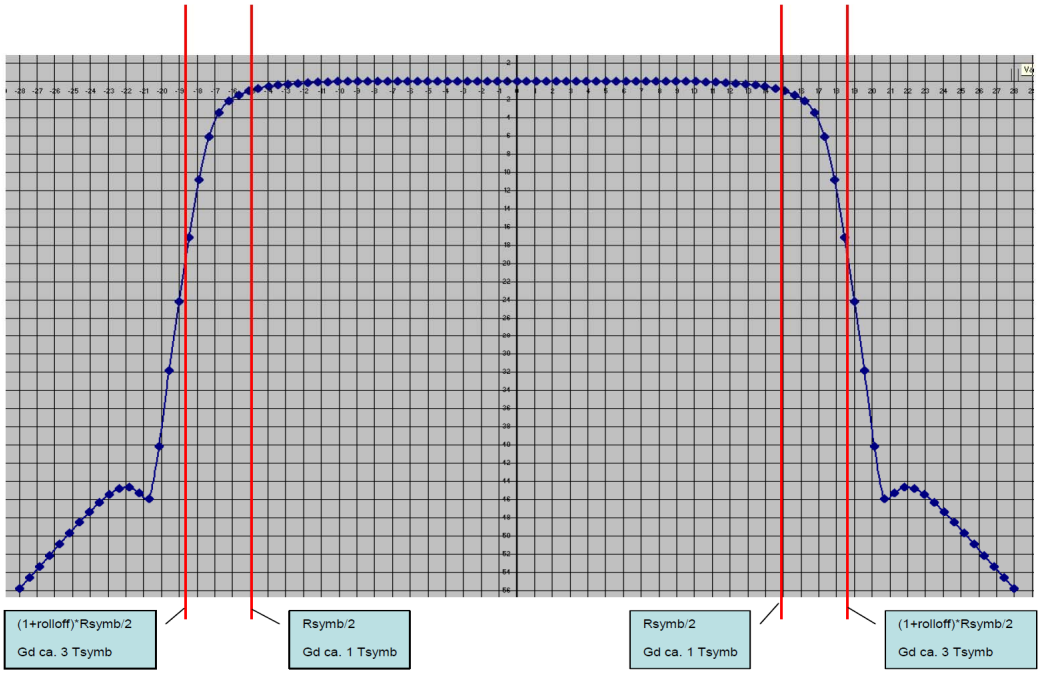

Figure 3

In the multi-carrier FDM configuration, R_s can be matched to the frequency slot B_S allocated to the service by the frequency plan, to optimize the transmission capacity while keeping the mutual interference between adjacent carriers at an acceptable level.

4.3.2.1 Single carrier per transponder configuration

4.3.2.1.0 Performance

Dependant on the selected code rate and modulation constellation the system can operate at carrier to noise ratios from -2,4 dB using QPSK 1/4 to 16 dB using 32APSK 9/10 (assuming AWGN channel and ideal demodulator) figure 4 shows the required C/N (Carrier-to-Noise power ratio measured in a bandwidth equal to the symbol rate) versus the spectrum efficiency (useful bit-rate for unit symbol rate R_S), obtained by computer simulations on the AWGN channel (ideal demodulator, no phase noise). These results have been obtained by computer simulations for a Packet Error Rate of 10^{-7}, both for DVB-S2 and DVB-S/DVB-DSNG, and correspond about to one erroneous Transport Stream Packet per transmission hour in a 5 Mbit/s video service (see note 1).

NOTE 1: It should be noted that this definition is slightly different from the Quasi Error Free target adopted in ETSI EN 300 421 [i.1]. Furthermore modem implementation margins reported in ETSI EN 300 421 [i.1] and ETSI EN 301 210 [i.4] are not included in figure 4.

On AWGN, the result is typically a 20 % to 35 % capacity increase over DVB-S and DVB-DSNG under the same transmission conditions or 2 dB to 2,5 dB more robust reception for the same spectrum efficiency.

Before Nyquist filtering in the modulator, the peak-to-average power ratio is 0 dB for QPSK and 8PSK, while it is in the range [1,05 ÷ 1,11] dB for 16APSK (the exact value can be calculated using expression $4\ \gamma^2/\ (3\ \gamma^2 + 1)$) and [1,97 ÷ 2,12] dB for 32APSK (the exact expression is $8\ \gamma_2{}^2/\ (4\ \gamma_2{}^2 + 3\gamma_1{}^2 + 1)$).

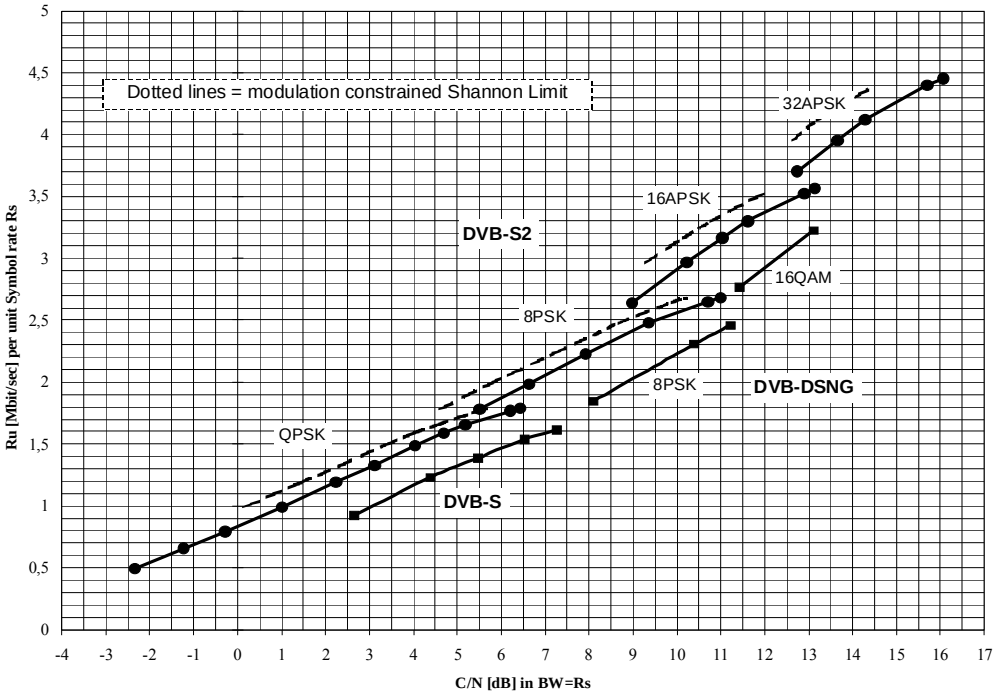

Figure 4: Required C/N versus spectrum efficiency, obtained by computer simulations on the AWGN channel (ideal demodulation) (C/N refers to average power)

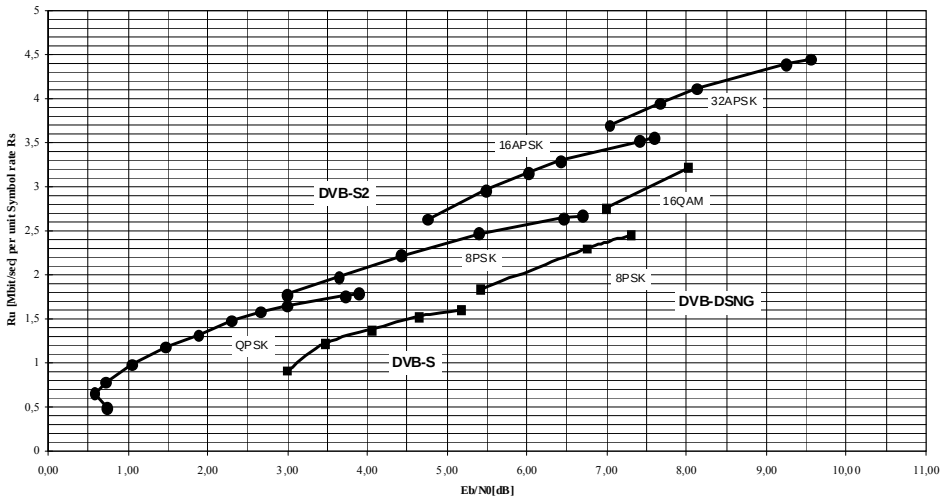

Figure 5: Required Eb/N0 versus spectrum efficiency, on the AWGN channel (ideal demodulation)

Figure 5 shows the efficiency plot versus Eb/N0, to allow comparing the different FEC schemes.

Figure 6 shows instead the DVB-S2 performance for constant satellite bandwidth $BW = R_S(1+\rho)$ on the AWGN channel assuming ideal demodulation. The figure does not take into account the performance degradation which is expected on the satellite channel due to the signal envelope, which increases with decreasing roll-off. For DVB-DSNG only the normative roll-off 0,35 is considered, even if DVB-DSNG also includes, optionally, 0,25.

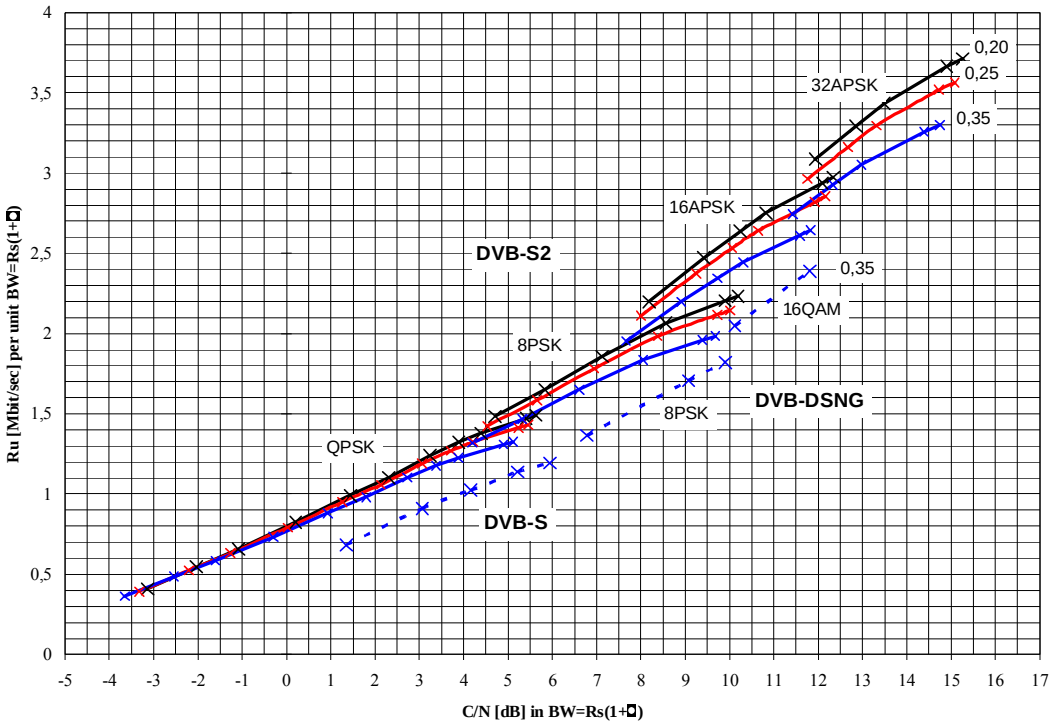

Figure 6: Required C/N versus spectrum efficiency for constant satellite bandwidth BW = $R_S(1+\alpha)$ on the AWGN channel (ideal demodulation) (C/N refers to average power)

Figure 7 gives examples of the useful bit rate capacity R_u achievable by the system versus the LDPC code rate, assuming unit symbol rate R_S. The symbol rate R_S corresponds to the -3 dB bandwidth of the modulated signal. $R_S(1+\alpha)$ corresponds to the theoretical total signal bandwidth after the modulator, with α representing the roll-off factor of the modulation. The figures refer to Constant Coding and Modulation, normal FEC frame length (64 800 bits), no padding field, no pilots (the pilots would reduce the efficiency by about 2,4 %). Typical BW/R_S or B_S/R_S ratio is $1+\alpha = 1,35$: this choice allows to obtain a negligible E_S/N_0 degradation due to transponder bandwidth limitations, and also to adjacent channel interference on a linear channel. The use of the narrower roll-off factors $\alpha = 0,25$ and $\alpha = 0,20$ may allow a transmission capacity increase but may also produce larger non-linear degradations by satellite for single carrier operation. BW/R_S factors less than $1+\alpha$ may also be adopted, but careful studies should be carried-out on a case-by-case basis to avoid unacceptable interference and distortion levels.

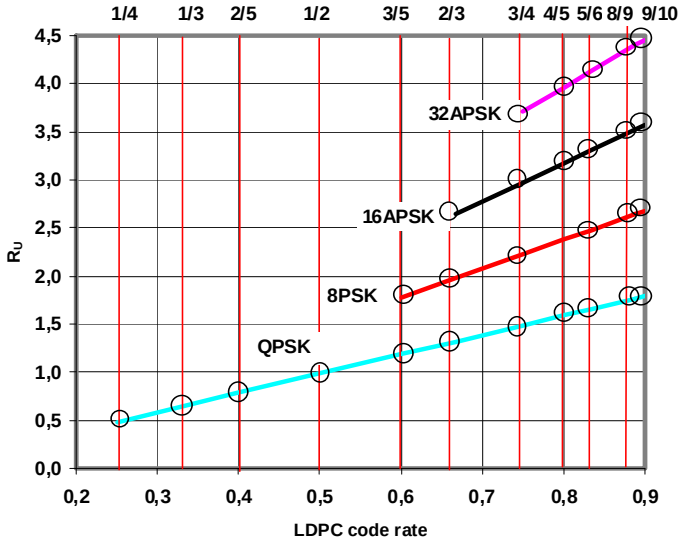

Figure 7: Examples of useful bit rates R_U versus LDPC code rate per unit symbol rate R_S

When DVB-S2 is transmitted by satellite, quasi-constant envelope modulations, such as QPSK and 8PSK, are power efficient in single carrier per transponder configuration, since they can operate on transponders driven near saturation. 16APSK and 32APSK, which are inherently more sensitive to non-linear distortions and would require quasi-linear transponders (i.e. with larger Output-Back-Off, OBO) may be greatly improved in terms of power efficiency by using non-linear compensation techniques in the up-link station [i.11]. A significant feature of DVB-S2 standard is to support high-order modulation such as 16APSK and 32 APSK. These modulation schemes, although specifically designed for non-linear channels, are particularly sensitive to the characteristics of the satellite transponders. Computer simulation studies, based on the use of the satellite transponder model of clause H.7, demonstrated that there are significant opportunities to further enhance the performance by pre-distortion of the transmitted signal and/or intersymbol interference suppression technique in the receiver.

In FDM configurations, where multiple carriers occupy the same transponder, this latter will be kept in the quasi-linear operating region (i.e. with large OBO) to avoid excessive inter-modulation interference between signals. In this case the AWGN performance figures may be adopted for link budget computations.

Table 1 shows, for the single carrier per transponder configuration, the simulated C/N degradation using the satellite channel models and phase noise mask given in ETSI EN 302 307-1 [i.2]. (non linearized TWTA, IMUX and OMUX filters, phase noise relevant to consumer LNBs), at the optimum operating TWTA point (see note 2). C_{SAT} is the un-modulated carrier power at HPA saturation, OBO is the measured power ratio (dB) between the un-modulated carrier at saturation and the modulated carrier (after OMUX). Phase noise degradation figures refer to a pilot-based carrier recovery system [i.11]. The figures show the large advantage offered by the use of dynamic pre-distortion for 16APSK and 32APSK. The large phase noise degradations quoted for APSK, and in particular for 32APSK, can be considered as pessimistic, since they refer to consumer-type LNBs, while for professional applications better front-ends may be adopted at negligible additional cost.

NOTE 2: The following parameters have been simulated [i.11]: R_s = 27,5 Mbaud, roll-off factor α= 30 % (not available in DVB-S2, but giving performance between roll-off 0,35 and 0,25).

Table 1: C_{SAT}/N loss [dB] on the satellite channel (simulation results, Single Carrier per Transponder, optimum TWTA operating point)

Transmission Mode	C_{SAT}/N loss [dB] without predistortion without Phase Noise	C_{SAT}/N loss [dB] with dynamic predistortion without Phase Noise	C_{SAT}/N loss [dB] with dynamic predistortion with Phase Noise
QPSK 1/2	0,62 (IBO = 0; OBO = 0,33)	0,5 (IBO = 0 dB; OBO = 0,38)	0,63
8PSK 2/3	0,95 (IBO = 0,5; OBO = 0,35)	0,6 (IBO = 0;OBO = 0,42)	0,85
16APSK 3/4	3,2 (IBO = 5; OBO = 1,7)	1,5 (IBO = 1; OBO = 1,1)	1,8
32APSK 4/5	6,2 (IBO = 9; OBO = 3,7)	2,8 (IBO = 3,6; OBO = 2,0)	3,5
NOTE: Operational constraints might require higher OBO.			

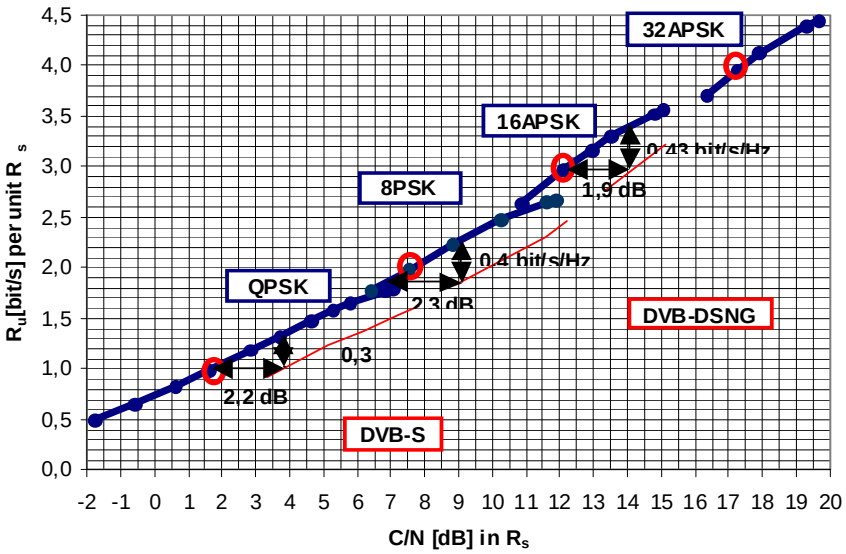

Figure 8: Examples of R_U versus required C/N by satellite, in single carrier per transponder configuration

Figure 8 shows, in the C/N - Spectral Efficiency plane, the overall performance of DVB-S2 by satellite, compared to DVB-S and DVB-DSNG (see note 3). The C/N gain of DVB-S2 versus DVB-S and DVB-DSNG, at a given spectral efficiency, remains substantially constant around 2 dB to 2,5 dB, confirming the results on AWGN. Similarly, the capacity gain at a given available C/N confirms to be in the range 0,3 to 0,4 bit/s/Hz (2,6 % pilot symbol loss is not indicated, since pilots are optional). Compared to AWGN simulations, satellite simulation curves for 16APSK and 32APSK are more aligned with QPSK and 8PSK curves, due to the amplitude limitation of the non-linear TWTA characteristics.

NOTE 3: The transmission modes indicated by circles are fully simulated [i.11], while the other configurations are extrapolated. The degradations of table 1 are added to the AWGN simulated figures, for the relevant constellation order, neglecting the effect of coding rates on degradations; M-QAM degradations is assimilated to M-APSK.

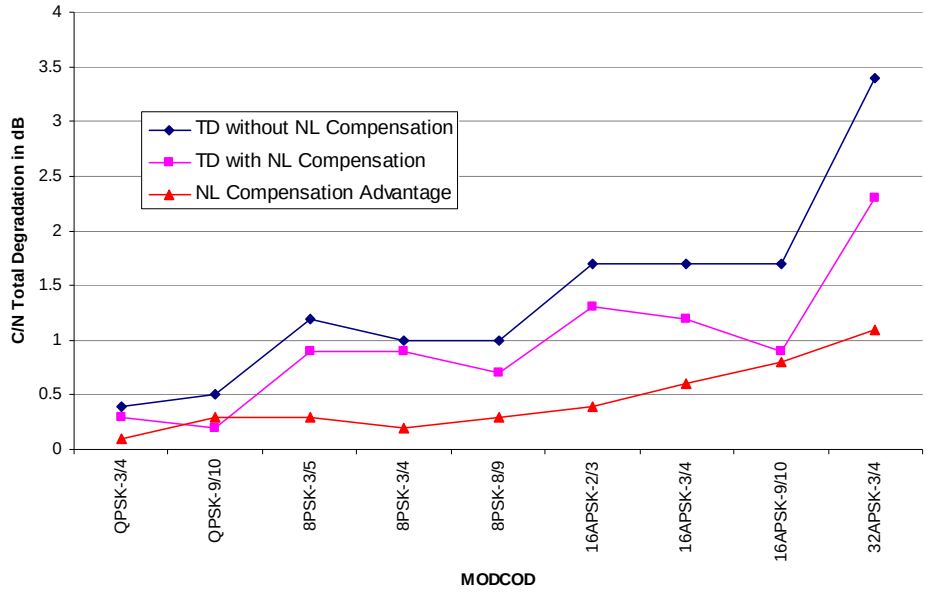

Figure 9: Performance degradation due to the satellite nonlinearity with and without pre-distortion

Figure 9 from [i.16] shows measured performance over the Telesat Anik F1R satellite in the case of a single carrier per transponder without and with dynamic pre-distortion on ground. For each MODCOD tested, the optimum TWTA operating point is found to minimize C/N total degradation, defined as the sum of non-linear degradation at QEF and output back-off. Symbol rate is 20 Mbaud for all MODCOD except for 32APSK where 10 Mbaud has been used for link budget closure reasons. Carrier roll-off is 25 %.The measurement results show that, as expected, the TWTA can be operated close to saturation for the quasi-constant envelope QPSK and 8PSK modulations (with constellation points located on a single circle). The resulting degradation is in the order of 0,5 to 1,0 dB in line with the simulation results presented in table 1. Also in line with table 1. simulation results, activating non-linear pre-distortion in the modulator gives a very small improvement for QPSK and 8PSK. Instead for 16APSK (dual ring constellation) and 32APSK (triple ring constellation) modulations, higher nonlinearity degradations are measured, up to 3,4 dB, for which non-linear pre-distortion is able to compensate up to 1,1 dB. The measured dynamic pre-distortion gain is less than what simulated in table 1. This may be due to the fact that the dynamic pre-distortion technique used during the test was based on one of the first 2008 commercial DVB-S2 modulator having such a feature. It can not be guarantee that the pre-distortion performance measured corresponds to the current state-of-the-art products.

4.3.2.1.1 Sensitivity to satellite power amplifier characteristics

The sensitivity to different satellite power amplifiers has been investigated by means of software simulations [i.34]. The same channel model and phase noise mask as in ETSI EN 302 307-1 [i.2] has been used. Three different amplifiers have been considered: the two models defined in ETSI EN 302 307-1 [i.2], linearized TWTA (LTWTA) and non-linearized TWTA (NL-TWTA), and a second linearized-TWTA (LTWTA2), whose characteristics are reported respectively in figures 10 and 11. Only the 16APSK modulation scheme with LDPC rate ¾ is considered for a 27,5 Mbaud link and roll-off factor 0,3.

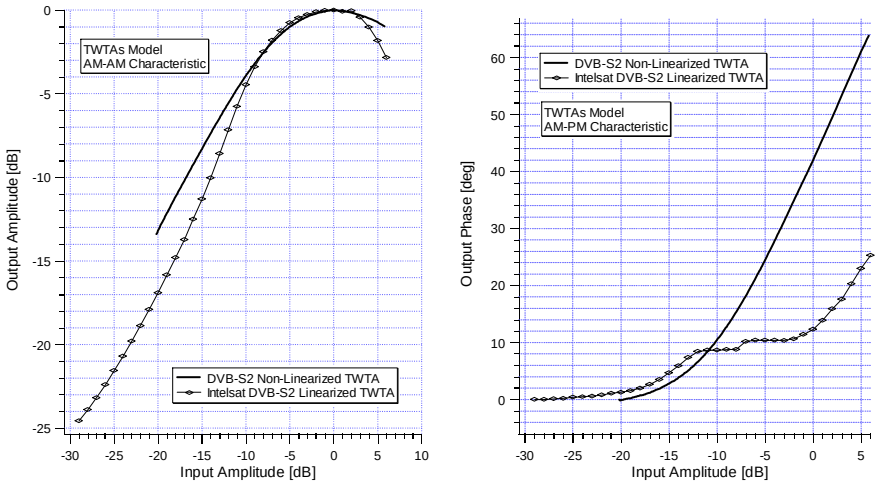

Figure 10: AM/AM and AM/PM characteristic of DVB-S2 linearized (LTWTA) and non linearized TWTA (NL-TWTA) models

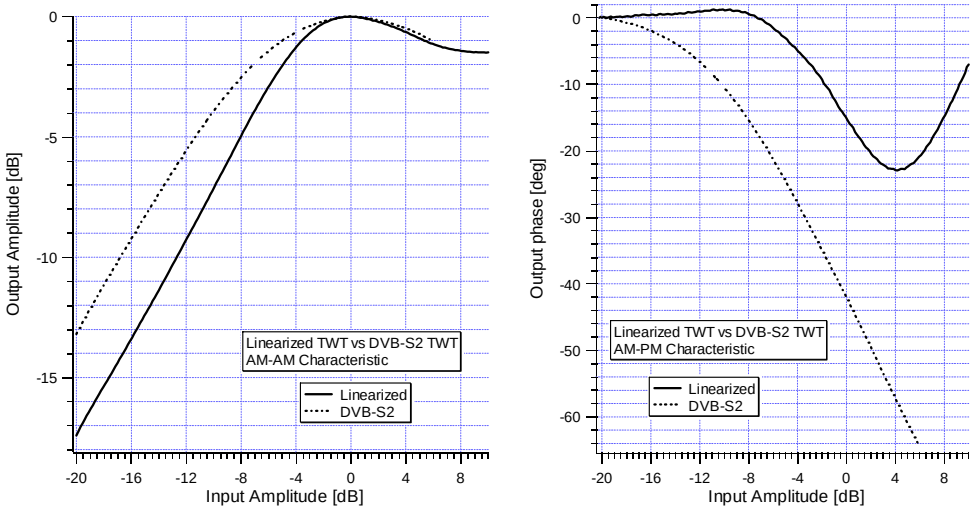

Figure 11: AM/AM and AM/PM Characteristic of linearized TWTA LTWTA2

Tables 2 and 3 report results for this configuration; in these tables, D represents the demodulator loss due to the non-linearity. Simulations findings indicate that linearized TWTAs work better than the non-linearized one. This is true both for the case when pre-distortion algorithm is used and for the case when the original constellation is transmitted. LTWTA2 provides the smallest demodulation loss (D) at the price of higher OBO. The total loss is slightly higher than for LTWTA, that has a less linear characteristic but lower OBO. Furthermore, using simple static constellation pre-distortion the L-TWTA can bring about 0,3 to 0,4 dB gain over classical TWTA, whereas without pre-distortion the gain goes up to 0,8 dB. The performance of NL-TWTA, when a pre-distorted constellation is used, is comparable to the one of the linearized TWTA without pre-distorted constellation. Since the AM/AM characteristic of the two amplifiers is very similar in the region of interest when IBO > 12 dB, the advantage appears to be related to the flatter AM/PM characteristic of the linearized amplifier.

Table 2: Summary of results for 1 carrier/HPA with no pre-distortion algorithm, 16APSK 3/4

HPA	Optimum IBO [dB]	OBO [dB]	D [dB]	C_{SAT}/N loss [dB]
NL-TWTA	4,5	1,5	1,7	3,2
LTWTA	4	1,3	1,1	**2,4**
LTWTA2	3	1,6	**0,85**	2,45

Table 3: Summary of results for 1 carrier/HPA with static pre-distortion algorithm, 16APSK 3/4

HPA	Optimum IBO [dB]	OBO [dB]	D [dB]	C_{SAT}/N loss [dB]
NL-TWTA	2	1	1,4	2,4
LTWTA	2	1,0	1,0	**2,0**
LTWTA2	2	1,35	**0,8**	2,15

The impact of the NL-TWTA and LTWTA have also been measured on a DVB-S2 test-bed [i.15], with an FPGA implementation of the demodulator, using a 10 Mbaud carrier with 25 % roll-off factor. Similar results to table 2 and table 3 simulation results have been obtained in real measurements without and with static pre-distortion. The main conclusion is that on-ground pre-compensation of TWTA non-linearities gives equivalent performances to linearized TWTA without pre-compensation in the case of 16APSK modulation. Also it can be concluded that simple static pre-distortion is of interest starting from 16APSK modulation.

4.3.2.1.2 Sensitivity to roll-off

Decreasing the roll-off factor causes an increase of the loss over non-linear channel due to the fact that the ISI becomes stronger. Simulations carried on with the same channel model and phase noise as for the previous case have shown however that the resulting effect is only marginal. A roll-off factor of 0,2 produces a loss of about 0,1 dB w.r.t. the case of roll-off 0,3 for all the modulation schemes, in case of adoption of static pre-distortion techniques. Similar results are expected when using dynamic pre-distortion.

4.3.2.1.3 Sensitivity to phase noise

The impact of phase noise has been measured on the laboratory test-bed described in [i.15], which demodulator algorithms for channel estimation are decribed in Annex C. These tests have been performed at 10 Mbaud with pilot symbols activated. Different phase noise masks have been synthesized (see figure 12) from the DVB-S2 Standard ETSI EN 302 307-1 [i.2] Annex H.8 and from a range a LNB products. E_s/N_0 degradation has been measured at QEF for the 28 MODCOD.

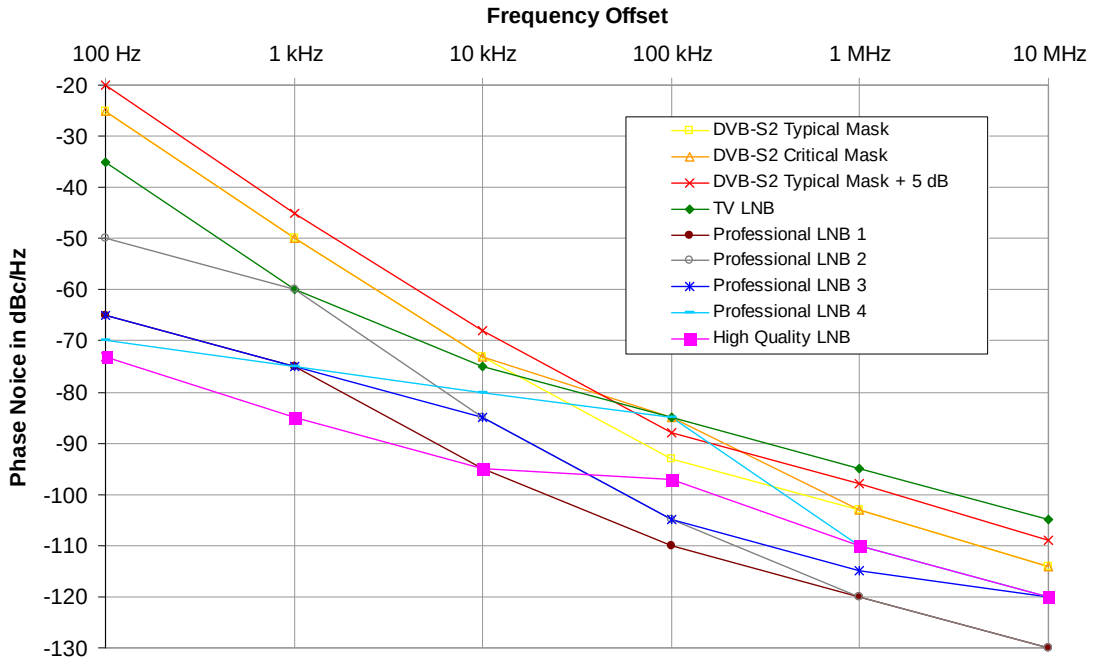

Figure 12: Synthesized phase noise

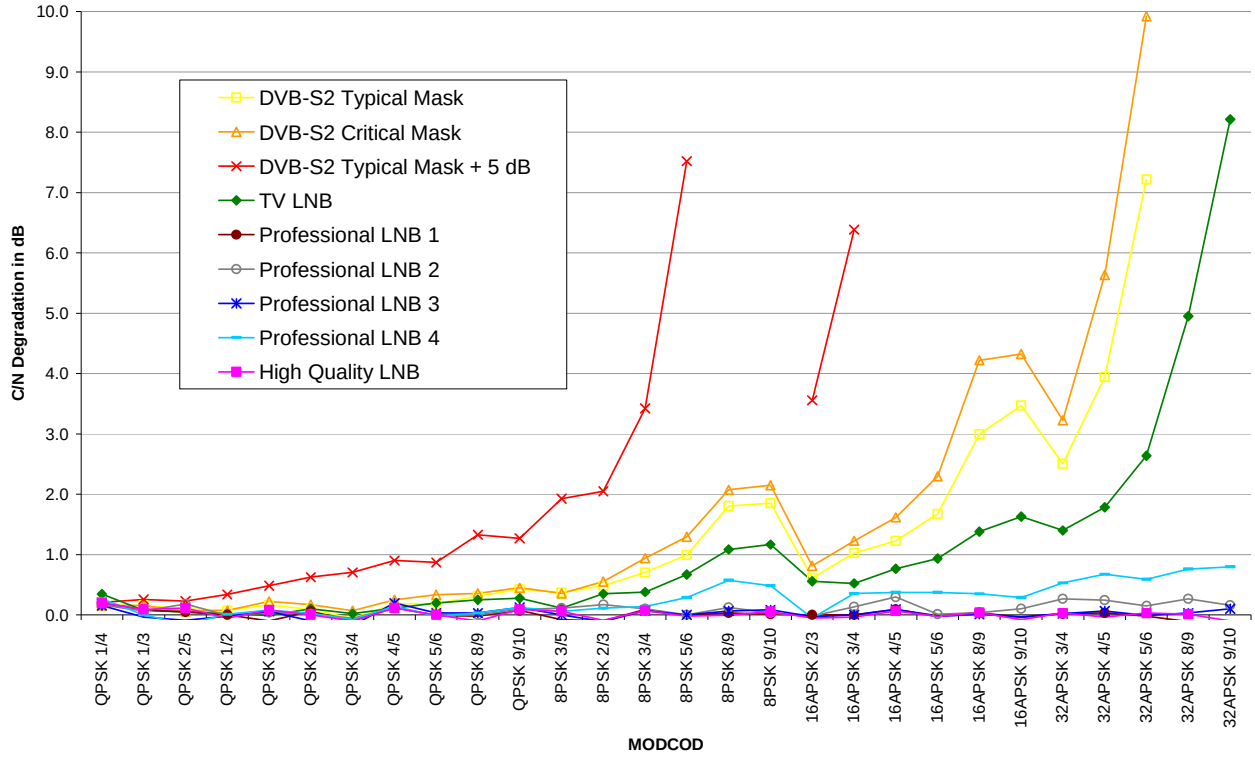

Figure 13: Performance degradation with phase noise

The following results are highlighted:

- The impact of phase noise of the link performance primarily depends on the robustness of the MODCOD. High order modulations are more sensitive to phase noise because of their constellation more pronounced sensitivity to recovered carrier phase errors (lower distance between ring constellation points). Similarly more degradation is measured when LDPC code rate increases (less redundant FEC bits available).

- For the DTH low-cost mass market LNB, degradation varies between 0 and 1,2 dB for QPSK and 8PSK modulations (normative modulations for broadcasting services), ranges from 0,5 to 1,6 dB for 16APSK (used by broadband multi-beam systems) and goes up to 8,2 dB for 32APSK rate 9/10 which is typically used for professional applications.

- Performance degradation with professional LNB and high quality LNB, representative of interactive, DSNG and professional services, is generally very limited, even for high order modulations.

It can be concluded that measured performances with different types of LNBs resulted to be better than with the typical phase noise masks from the DVB-S2 Standard Annex H.8, which can be considered as pessimistic.

4.3.2.1.4 Impact of demodulator digital equalization

Linear equalization is usually implemented in satellite receivers to diminish the effects of linear distortions coming from the satellite channel (typically filters group delay) and the ground radio frequency front-end possible mismatches. Figure 14 from ESA contract No. 19572 [i.16] shows how a commercial DVB-S2 demodulator acquisition threshold can be improved by using equalization techniques when transmitting a 20 Mbaud DVB-S2 carrier in a commercial 36 MHz transponder. This test was performed over satellite using a commercial demodulator. Receiver equalization can also be useful to limit *a posteriori* the received signal inter-symbol interference caused by the combination of TWTA non-linearity and bandlimiting filters. Although the gain measured in figure 14 is limited to about 0,4 dB, the gain is largely dependent on the specific application scenario and will increase when using higher baud rates compared to the transponder bandwidth. Furthermore, in practical home based DTH implementations the likelihood of mismatches between the LNB and the satellite receiver is not negligible.

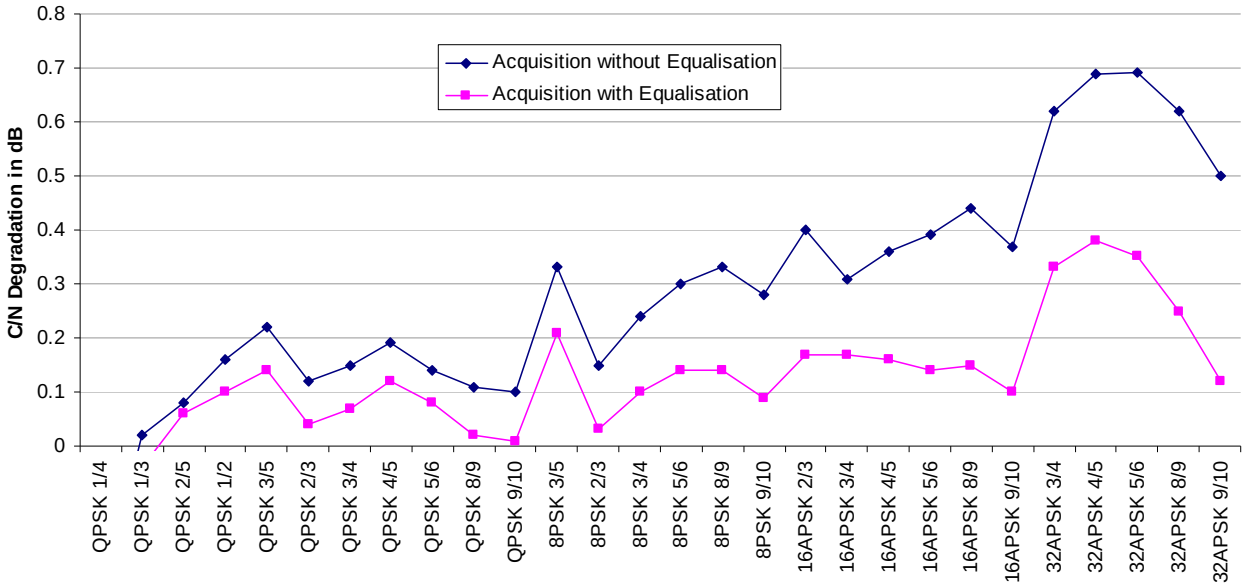

Figure 14: Demodulator acquisition with and without equalization (compared to QEF thresholds from standard)

4.3.2.2 Multiple carrier per transponder configuration

In [i.34], simulations of multi-carrier systems have been carried out on the same satellite channel model as in clause 4.3.2.1. 8PSK rate 2/3 and 16APSK rate 3/4 have been tested in this configuration. Results for 2 carrier/HPA are summarized in tables 4 to 7. From the tables is immediately clear that there is no great advantage in using a pre-distortion technique for none of the modulation schemes when 2 carriers travel along the same amplifier. As expected the conventional TWTA (NL-TWTA) behaves worse than the others. Recalling the characteristics of the two linearized tubes defined in clause 4.3.2.1 (figures 10 and 11), LTWTA2 is expected to behave better than LTWTA, since its AM/AM characteristic is more linear. Such a thesis does not match the results. Indeed, despite a slightly less demodulation loss (D column), the OBO of LTWTA2 is higher and makes the total loss higher. Therefore, once more, this indicates the importance of OBO factor for the total degradation of the whole system.

From the same results it appears that the use of pre-distortion techniques does no mitigate the total loss. It is then clear that when two or more carriers go through the same tube, the intermodulation products due to the non-linearities represent the main contribution to the global ISI. Therefore, neither a static pre-distortion technique nor one with memory can attenuate this contribution.

A positive outcome of using pre-distortion techniques is the reduced OBO that results in a slightly higher DC to RF conversion efficiency (see tables 6 and 7).

Table 4: Summary of results for 2 carriers/HPA with no pre-distortion algorithm for 8PSK 2/3

HPA	Optimum IBO [dB]	OBO [dB]	D [dB]	C_{SAT}/N loss [dB]
NL TWT	1,0	1,0	1,0	2,0
LTWTA	1,5	1,05	**0,7**	**1,75**
LTWTA2	0,0	1,25	0,8	2,05

Table 5: Summary of results for 2 carriers/HPA with Static pre-distortion algorithm for 8PSK 2/3

HPA	Optimum IBO [dB]	OBO [dB]	D [dB]	C_{SAT}/N loss [dB]
NL TWTA	1,0	1,0	1,0	2,0
LTWTA	1,5	1,05	**0,7**	**1,75**
LTWTA2	0,0	1,25	0,8	2,05

Table 6: Summary of results for 2 carriers/HPA with no pre-distortion algorithm for 16APSK 3/4

HPA	Optimum IBO [dB]	OBO [dB]	D [dB]	C_{SAT}/N loss [dB]
NL-TWTA	5,0	2,01	2,1	4,1
LTWTA	4,5	1,75	**1,35**	**3,1**
LTWTA2	3,0	2,0	1,5	3,5

Table 7: Summary of results for 2 carriers/HPA with Static pre-distortion algorithm for 16APSK 3/4

HPA	Optimum IBO [dB]	OBO [dB]	D [dB]	C_{SAT}/N loss [dB]
NL-TWTA	5,0	2,0	2,05	4,05
LTWTA	4,0	1,6	1,5	**3,1**
LTWTA2	3,0	2,0	**1,45**	3,45

Simulations for 5 carriers/HPA have been carried only for the LTWTA being the one that performs better in case of 2 carriers/HPA. Moreover since data pre-distortion does not provide any noticeable advantage, only the original constellation of 8PSK and 16APSK schemes has been used. Results are shown in table8.

Table 8: Summary of results for 5 carriers/HPA on LTWTA with no pre-distortion algorithm for 8PSK 2/3 and 16APSK 3/4

Modulation	Optimum IBO [dB]	OBO [dB]	D [dB]	C_{SAT}/N loss [dB]
8PSK 2/3	4,0	1.70	1,4	3,1
16APSK 3/4	6,5	2,8	1,6	4,4

4.4 Adaptive Coding and Modulation

4.4.0 Overview

The ETSI EN 302 307-1 DVB-S2 standard [i.2] has been conceived for a wide range of satellite broadband applications, including point-to-point applications like IP unicasting or DSNG, with the adoption of Adaptive Coding and Modulation (ACM), allowing different modulation formats and error protection levels (i.e. coding rates) to be used and changed on a frame-by-frame basis within the transmitted data stream. By means of a return channel, informing the transmitter of the actual receiving condition, the transmission parameters may be optimized for each individual user, dependant on path conditions.

ACM has been considered as a powerful tool to further increase system capacity, allowing for better utilization of transponder resources. As a consequence, in DVB-S2 standard ACM is included as normative for the interactive application area and optional for DSNG and professional services.

As IP traffic is driving interactive services and applications offered by broadband unicast systems, the new standard is intended to be IP friendly, by improving the efficiency of carriage of IP data. This goal has been coupled with the legacy induced by the current wide utilization of MPEG Transport Stream (MPEG-TS) packets for encapsulating IP datagrams ETSI EN 301 192 [i.5] as well as with the definition of a new adaption layer called GSE ETSI TS 102 606 [i.41] aimed at an efficient encapsulation of IP over generic streams and a more efficient system operation for interactive systems that utilize advanced physical layer techniques such as Adaptive Coding and Modulation (ACM) ETSI TS 102 771 [i.42].

The result is a highly flexible standard, which supports for interactive applications both (GSE) generic streams and MPEG-TS. One of the implications of such a high flexibility is the multiplicity of solutions allowed by DVB-S2 for implementing ACM in interactive systems. Finally, support of individual Quality of Service targets has been recommended for interactive applications.

4.4.1 ACM: the principles

Current point-to-point multi-beam satellite systems based on the DVB-S standard are designed for link closure in the worst-case propagation and location conditions. The standard, envisaged for broadcasting applications, considers a fixed coding rate and modulation format, which are selected according to the assumed coverage and availability requirements. This approach implies the occurrence of high margins in the majority of the cases, when interference and propagation conditions allow for higher Signal to Interference plus Noise Ratio (SNIR). Typical Ku-band broadcasting links are designed with a clear-sky margin of 4 dB to 6 dB and a service availability target of about 99 % of the worst month (or 99,6 % of the average year). Since the rain attenuation curves are very steep in the region 99 % to 99,9 % of the time, many dBs of the transmitted satellite power are useful, in a given receiving location, for only some ten minutes per year. Unfortunately, this waste of satellite power/capacity cannot be easily avoided so far for broadcasting services, where millions of users, spread over very large geographical areas, receive the same content at the same time. However, the DVB-S2 VCM mode allows to reduce the static link margins in broadcasting mode if a video quality reception is acceptable to the end user (see Recommendation ITU-T H.264 [i.43] and clause 5.2 for more details).

However, this design methodology devised for broadcasting systems is not optimal for unicast networks. In fact, the point-to-point nature of link connections allows exploiting spatial and temporal variability of end-user channel conditions for increasing average system throughput. This is achieved by adapting coding rate and modulation format (ACM) to best match the user SNIR, thus making the received data rate location and time dependent. Fixed link margins are therefore avoided and a remarkable improvement in system capacity is obtained thanks to better utilization of system power resources.

Assuming a fixed beam power allocation, the key parameters responsible for SNIR variability within the satellite coverage are the fading attenuation, the satellite antenna gain and the antenna C/I. The fading attenuation variation is due to both geographical dependency of rain statistics and to propagation channel time variations.

Examples of fading attenuations statistics and Satellite Terminal (ST) received power variations during heavy fading events can be found in [i.13]. In [i.17], figure 5, some examples of satellite antenna C/I distributions are shown, which have been obtained in a study case assuming European coverage. Because of the spread of the distributions, which is covering from 15 to 20 dB range depending on the selected frequency reuse factor, antenna C/I is an important source of SNIR variations within the coverage.

In annex D a methodology [i.17] is illustrated for deriving ACM systems capacity and assessing the advantage with respect to current DVB-S multimedia systems. Capacity and link availability figures have been derived following the proposed methodology for a study case of an ACM multi-beam Ka-band system covering Europe, showing an important gain with respect to non-adaptive systems.

One of the key factors, which can heavily affect capacity, is the granularity of physical layer schemes supported by the system. It is important to ensure a reasonably small step in E_s/N_0 and spectral efficiency between consecutive schemes in order to maximize the data rate provided to STs. In particular, it is of the highest importance for capacity purposes utilizing a sufficiently fine granularity in the SNIR range experienced in the coverage during clear sky conditions. On the contrary, larger SNIR intervals can be assumed between the more robust modes without major capacity penalty, due to their lower occurrence probability. This is confirmed by simulation results shown in annex D. In the DVB-S2 standard code rates have been designed in order to obtain a granularity of about 1 dB in C/N (see figure 4), covering the wide range from -2 dB up to +16 dB on the AWGN channel.

Figure 15 shows the scheme of an ACM satellite link, composed by the Gateway (GW), which includes the ACM DVB-S2 modulator, the Satellite, the Satellite receiving Terminal (ST) connected to the GW via a return channel. Although DVB-S2 standard is also applicable to regenerative satellite systems, here a transparent satellite system architecture is considered.

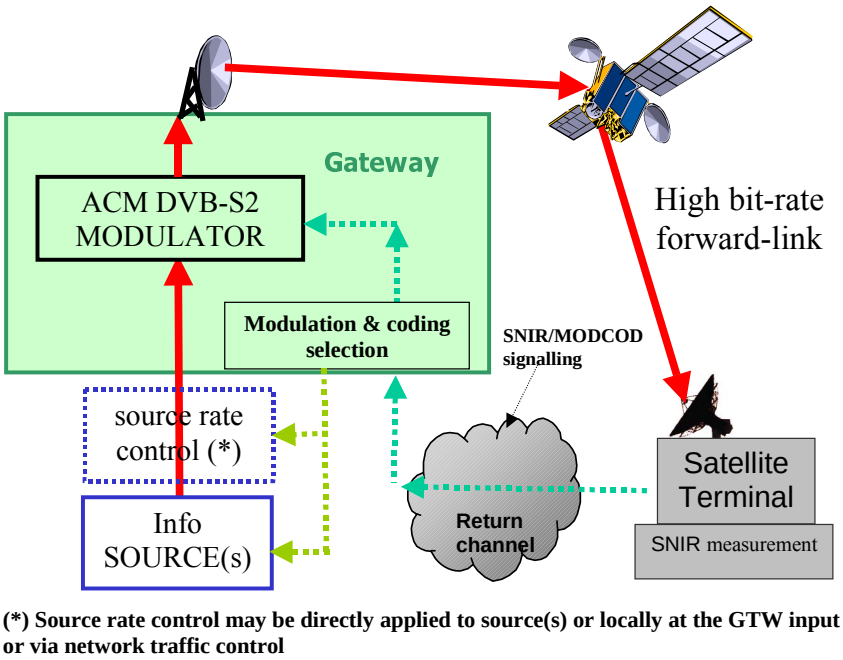

Figure 15: Block diagram of a DVB-S2 ACM link

The DVB-S2 ACM modulator operates at constant symbol rate, since the available transponder bandwidth is assumed constant. ACM is implemented by the DVB-S2 modulator by transmitting a TDM sequence of physical layer frames, each transporting a coded block and adopting a uniform modulation format. However, when ACM is implemented, coding scheme and modulation format may change frame-by-frame. Therefore service continuity is achieved, during rain fades, by reducing user bits while increasing at the same time FEC redundancy and/or modulation ruggedness.

Physical layer adaptivity which is discussed in Annex E and analyzed in detail in [i.14] is achieved as follows:

- Via a return channel, individual STs provide to the Gateway (GW) information on the channel status, by signalling the ST current SNIR or the most efficient modulation and coding scheme the ST can support.
  As periodic reports increase the signalling overhead on the return link, a preferable approach would be the ST sending a message whenever channel variations imply a change in the forward link spectral efficiency.

- The ST indications are taken into account by the GW in coding and modulating the data packets addressed to each ST. Therefore service continuity is achieved, during rain fades, by reducing user bits/frame while increasing at the same time FEC redundancy and/or modulation ruggedness. On the contrary, during the more frequent clear sky periods a much higher information rate/frame can be delivered to the ST thanks to a higher spectral efficient physical layer mode.

- In order to avoid information overflow during fades, a source bit rate control mechanism has to be implemented, adapting the offered traffic to the available channel capacity. This general principle can be implemented in different ways according to service requirements, system architecture and traffic statistics [i.13]. For example, when the source is co-located with the GW, its bit-rate may be directly controlled according to the SNIR reports. Instead, when information providers are remote, network traffic control policies may be implemented (e.g. TCP/IP protocol automatically reduces bit-rate when large reception delays are experienced), while low priority packet dropping may be an acceptable strategy to manage short traffic peaks under "best effort" service level requirement. When the aggregate channel capacity variations are small (e.g. because of the averaging effect on a large number of users, with different C/(N+I) conditions), and when capacity margins are allowed on the channel exploitation, user bit-rate control might even be avoided.
  The introduction of transmission buffers can be useful to absorb short traffic peaks, at the cost of an increase of the delays on data and, in some cases, on the ACM control loop.
  An alternative approach is to provide more time slots to the faded users to keep the offered bit rate constant. Being the spectral efficiency of faded users smaller than in the line of sight conditions this approach implies some capacity reduction but guarantees to maintain the user bit rate and thus the Q.o.S. for faded users. Normally the number of faded users is a small percentage of the overall population thus the capacity impact is limited if not negligible.

The GW can impose error protection applied to a given portion of user data according to two methods [i.13]:

- via the ACM command (see the system block diagram in figure 2);
- by splitting user data into various streams (one per required protection level), and feeding each of them to a different DVB-S2 modulator input. The modulator will apply a constant and suitable protection level to each input stream.

A crucial issue in ACM systems is the physical layer adaptation loop delay, as it is strictly linked to the system capability of tracking channel variations. The adaptation loop can be defined as the set of operations, which occur starting from channel estimation at the ST premises ending with reception of the information encoded/modulated according to the reported channel status. Whenever the user link is degraded in such a way that it requires a protection level higher than the estimated one, the received packet cannot be correctly decoded. On the contrary, if the channel conditions have improved so that a higher efficient physical layer mode could be supported, the result is a loss in efficiency due to the utilization of a not optimum physical layer scheme (i.e. carrying too much code redundancy). Therefore, the longer the loop delay the higher the impact physical layer adaptation has on user QoS, because of propagation channel dynamic. Maximum rain variation rates at Ka band have been estimated to be of about 0,5 dB to 1 dB per second, while faster SNIR variations are due to fading components with a high dynamic behaviour.

The loop delay is a sum of several contributions, including: the delay for transmission of the channel status reports, the return link propagation delay (depending on the selected return channel), the delay introduced within the GW (buffering, processing and transmission of data packets), and finally the fixed 250 ms propagation delay on the forward link. Different system architectures assuming different strategies for information processing and buffering at the GW side will lead in general to different QoS performance for the same channel variation rate.

A possible algorithm for channel estimation is the DA-SNORE [i.19], which, relying on pilot symbols, provides unbiased and accurate SNIR estimation for the E_s/N_0 range of interest. With the frame format assumptions of the DVB-S2 standard it can be shown that such algorithm leads to small channel estimation delays (in the order of 10 ms) for an error standard deviation of about 0,2 dB. Together with loop delay reduction, accurate channel estimations are critical for efficient physical layer adaptation. In case of DVB-S2, as the E_s/N_0 distance between physical layer schemes is in the order of 1 dB, an error standard deviation better than 0,3 dB is suggested to fully exploit system capabilities.

NOTE: Group-delay and non-linear distortions introduced by typical satellite transponders have non-negligible impacts on the channel estimation result and have a significant influence on the error standard deviation, rapidly exceeding 0,3 dB.

Depending on the channel estimation accuracy and on the system dynamicity, the number of physical layer configurations to be used by a certain ST can be optimized in order to ensure the desired QoS. However, as mentioned before, a reduction in the physical layer granularity has a direct impact on the throughput. In [i.14] the key parameters and trade-offs for efficient physical layer adaptation are shown. Besides, a methodology is illustrated, which allows, through physical layer thresholds optimization, meeting user Packet Error Rate (PER) requirements with a negligible impact on link efficiency.

4.4.2 Functional description of the DVB-S2 subsystem for ACM

4.4.2.0 General

With reference to the DVB-S2 modulator of figure 2, it may be noted that, unlike DVB-S, the second generation of the standard allows for several input stream formats, thus enhancing system flexibility. In addition to the widely used MPEG transport stream, generic streams, of constant (generic packetized streams) or variable (generic continuous streams) length packets, are encompassed by the standard. When this second configuration is selected, TS rules do not apply. Moreover, different encapsulation protocols with improved efficiency can be used as an alternative to the Multi Protocol Encapsulation (MPE) ETSI EN 301 192 [i.5], such as the Generic Stream Encapsulation (GSE) protocol ETSI TS 102 606 [i.41] for encapsulation over generic continuous streams. The data stream packets of both MPEG-TS and generic packetized streams are called User Packets (UPs). The input interface accepts both single and multiple streams. One additional input signal available in the standard is the "ACM command". This will be utilized in ACM systems in conjunction with a single input stream. It allows setting, by an external control unit, of the transmission parameters to be adopted by the DVB-S2 modulator for a specific portion of input data. The utilization of the ACM command interface allows for a system configuration, which is completely transparent to the physical layer scheme selection. This functionality is indeed performed by a unit external to the DVB-S2 modulator, which signals through the ACM command the transmission parameters associated to the data packets.

In interactive unicast networks, ACM functionality is normative and can be implemented either through a single generic stream with the utilization of the ACM command, or through multiple transport or generic streams. In order to better exemplify the DVB-S2 functionalities involved in the three different system configurations, in figure 16a, 16b and 16c the mode adaptation block diagram is shown respectively for the single GS, multiple TSs and multiple GSs case. In DSNG type of systems ACM can be implemented with a single transport stream or optionally with multiple transport streams. The different possible system configurations and their features will be illustrated in clause 6.1.

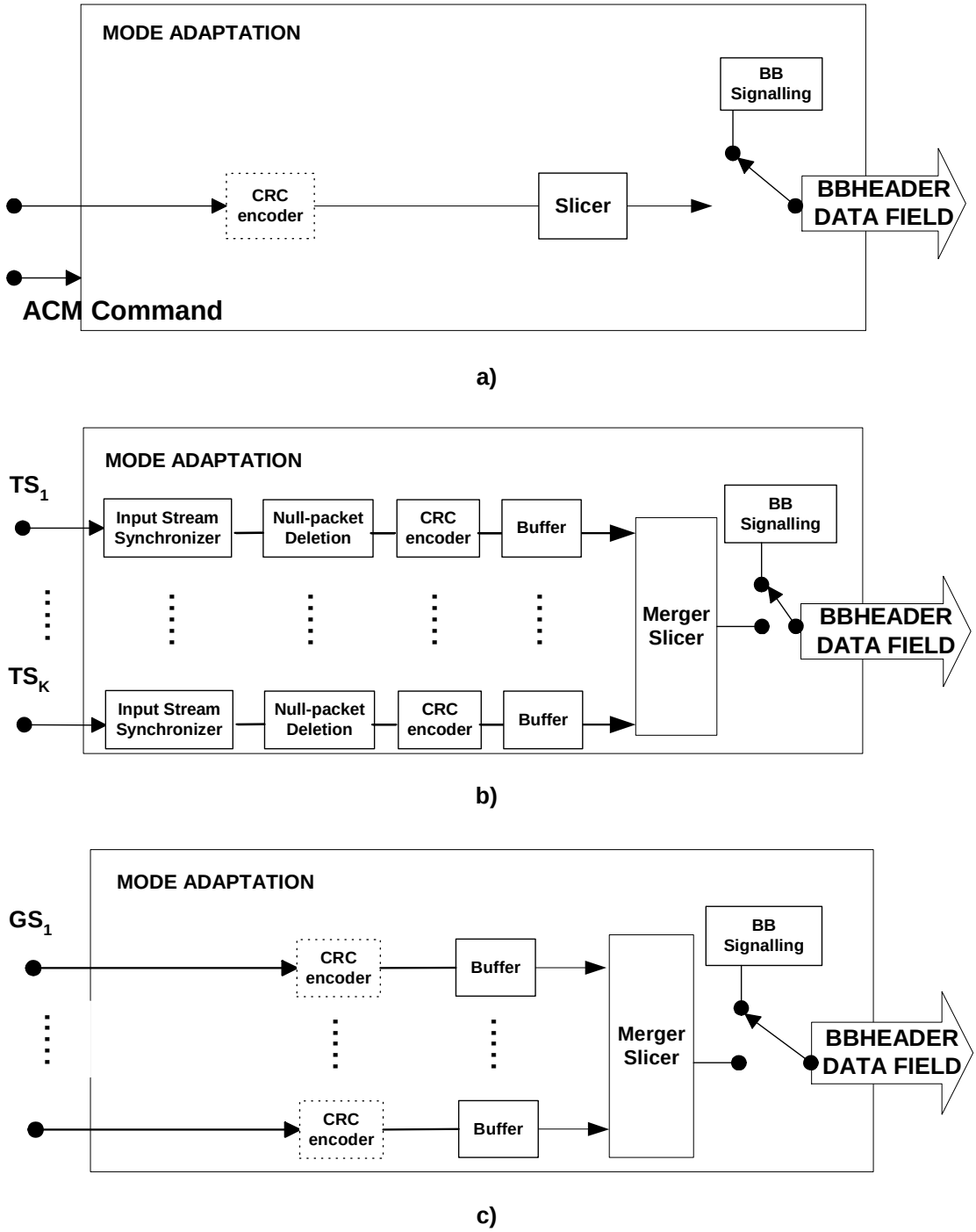

NOTE: The CRC encoder sub-system is not relevant for (GSE) generic continuous streams.

Figure 16: Mode adaptation subsystem in the system configuration: a) Single GS b) Multiple TS c) Multiple GS

The input interface is followed by two optional blocks, the Input Stream Synchronizer and the Null Packet Deletion. These two sub-systems are meant as tools to be utilized for implementing ACM over MPEG transport streams. The first aims at guaranteeing constant bit rate and end-to-end transmission delay, despite the variability introduced by data processing in the modulator and demodulator. The second identifies and removes null packets introduced by the transport stream multiplexer in order to reduce the transmitted information rate, by allowing for null packets reinsertion at the demodulator side. The two sub-systems will be further analysed and detailed in clause 4.4.2.1. CRC-8 encoding is applied to transport streams or generic streams with fixed length packets (i.e. packetized streams).

The input streams are then buffered, allowing a merger/slicer to read frame by frame the information necessary to fill the data field. In the case of a single stream, only the slicing functionality is required, while if multiple streams are present the merger/slicer is responsible for composing the data field by reading information bits from one of the input buffers. Hence, the merging of input streams does not take place within a single data field, but through reading different data fields from different inputs. Each data field needs to be homogeneous with respect to the physical layer mode, as it is indeed transmitted in one frame. The merging policy is application dependent. For unicast systems with multiple input streams the standard considers the possibility of performing a Round Robin polling with a time out for the user packets in each buffer. However, additional different policies can be implemented. When a data field is not available at any of the input buffers, a dummy frame is inserted and transmitted. The fixed length BBHEADER (80 bits) is finally inserted in front of the data field, describing its format.

While for broadcasting and DSNG applications the data field can be filled to its maximum capacity (K_{BCH} -80 bits), for unicast applications the data field may include an integer number of user packets. This allows for correct recovery of the user information when adaptive coding and modulation is utilized. As a consequence, padding is required to complete the constant length (K_{BCH}) BBFRAME. This also happens whenever UP available data are not sufficient to fill the BBFRAME. The stream adaptation subsystem is responsible for providing padding in case DFL < K_{BCH} -80, and scrambling the information at the encoder input. In clause 6.1.3 the impact of the introduced overhead on the overall encapsulation efficiency will be analysed.

Next, the BBFRAME is sent as input to the FEC encoder: in unicast systems, the output FECFRAME can have short (η_{LDPC} = 16 200 bits) or normal length (η_{LDPC} = 64 800 bits). Mapping is then applied to get a compleXFECFRAME: when ACM is used, coding rate and modulation format may be changed frame-by-frame.

PLFraming is then applied. It is worth noting that, as the PLFRAME length is dependent on both the frame type (short or normal) and the modulation order, it occupies a variable integer number of slots, which is larger the lower is the modulation order. After decoding the PLHEADER, the receiver can derive, through the knowledge of the physical layer mode, the current frame length and thus the start of the following frame, even if the status of the channel does not allow for successful data decoding in the current frame.

When ACM systems are considered, pilot symbols can be inserted in the physical layer frame structure for carrier synchronization and channel estimation purposes. In fact, phase recovery for 8PSK and higher modulation orders with the specified phase noise appears very difficult without any pilot. Besides, in ACM system, the key issue is that the receiver is in general able to decode only a part of the entire stream, and precisely only the frames where transmission parameters are compatible with user channel conditions. In this context, pilot symbols both allow for carrier recovery without knowledge of the frame data even in cases when some PLHEADERs are not correctly decoded. Pilot symbol insertion in DVB-S2 signal is optional, with possibility to carry out pilot switching on a frame-by-frame basis.

Finally, physical layer scrambling, baseband shaping and I-Q modulation are performed.

4.4.2.1 Specific subsystems for supporting ACM with MPEG-TS

Two subsystems have been introduced in the DVB-S2 standard in order to guarantee, even in ACM mode, constant transport stream bit rate and end-to-end delay, as required by MPEG-2 (see note).

NOTE: The PCR (Presentation Clock Reference) mechanism in MPEG exploits the recovered transport stream clock to reconstruct the clock for the decoded video signal.

The first problem encountered by DVB-S2 designers was that a transport stream is characterized by constant bit-rate, while ACM is by definition a variable bit-rate transmission, trading-off user bit-rate with FEC redundancy during rain fades. The introduction of the "null-packet deletion" block allowed to overcome this. The second problem was that, during rate adaptation, delay and rate variations may take place in the modem. This is taken into account by the "input stream synchronizer" block.

Null-packet Deletion

To understand MPEG transport over a DVB-S2 ACM physical layer, it is useful to remind some rules of MPEG Transport Streams:

- The TS packet length is fixed (188 bytes). The packet Header includes a PID field, with limited addressing capability.
- IP services are mapped into TS by gateways (GW), using the DSM-CC multi-protocol encapsulation (MPE) scheme. An IP packet may be split into different TS packets. The TS PID does not include the IP MAC address.
- Services multiplexed within a TS may be characterized by constant bit-rate (CBR) or variable bit-rate (VBR).
- Input services mapping into TS packets is random (i.e. there is no cyclic fixed allocation), but the packet position in the stream cannot be modified along the transmission chain, unless precise re-multiplexing rules are satisfied.
- The TS bit-rate (R_{TS}) is required to be constant (rate variations require a remultiplexer, updating PCR time stamps).
- The end-to-end transmission delay is required to be constant. Therefore, should a packet jitter be introduced on the channel, it has to be smoothed before the demultiplexer by a reception buffer of appropriate dimension.

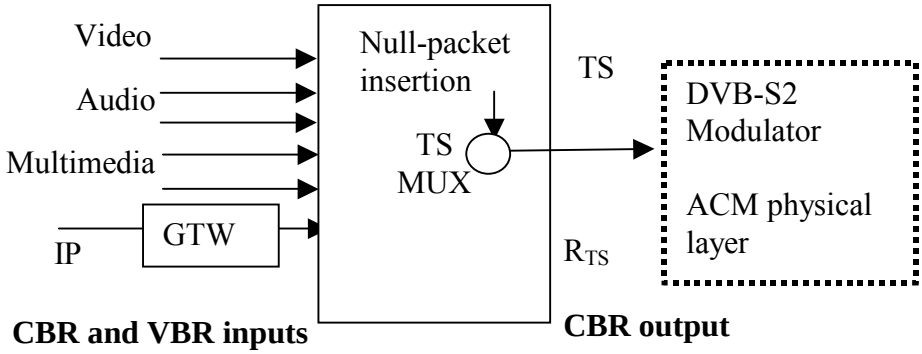

Figure 17: MPEG TS multiplexing scheme

To avoid data overflow in ACM, the useful bit rate generated by data sources (e.g. a video encoder) is controlled by a feed-back mechanism using the SNIR report from STs. When the user bit rate is modified at the input of a conventional MPEG-2 Transport Stream multiplexer, the output bit-rate R_{TS} is kept constant by adding "MPEG null-packets" (PID = $8\ 191_D$) (see figure 17), which do not carry any useful information. To map one/many constant bit-rate Transport-Stream(s) into a variable bit-rate ACM physical layer, the DVB-S2 modulator activates the subsystem called "Null-Packet deletion" (see figure 18). The function performed by this block is to discard all (or the majority of) the null packets, so that the output bit-rate is no longer constant, but corresponds to the useful source bit-rate. A signalling information (DNP, counting the deleted NPs) allows reinsertion, at the receiver side, of the deleted null-packets in the exact position where they were after the transmit multiplexer. Figure 18 describes the "null-packet deletion" process. For multiple transport stream operation, the null-packet deletion function operates independently over each TS, since the receiver is able to recognize packets belonging to each TS.

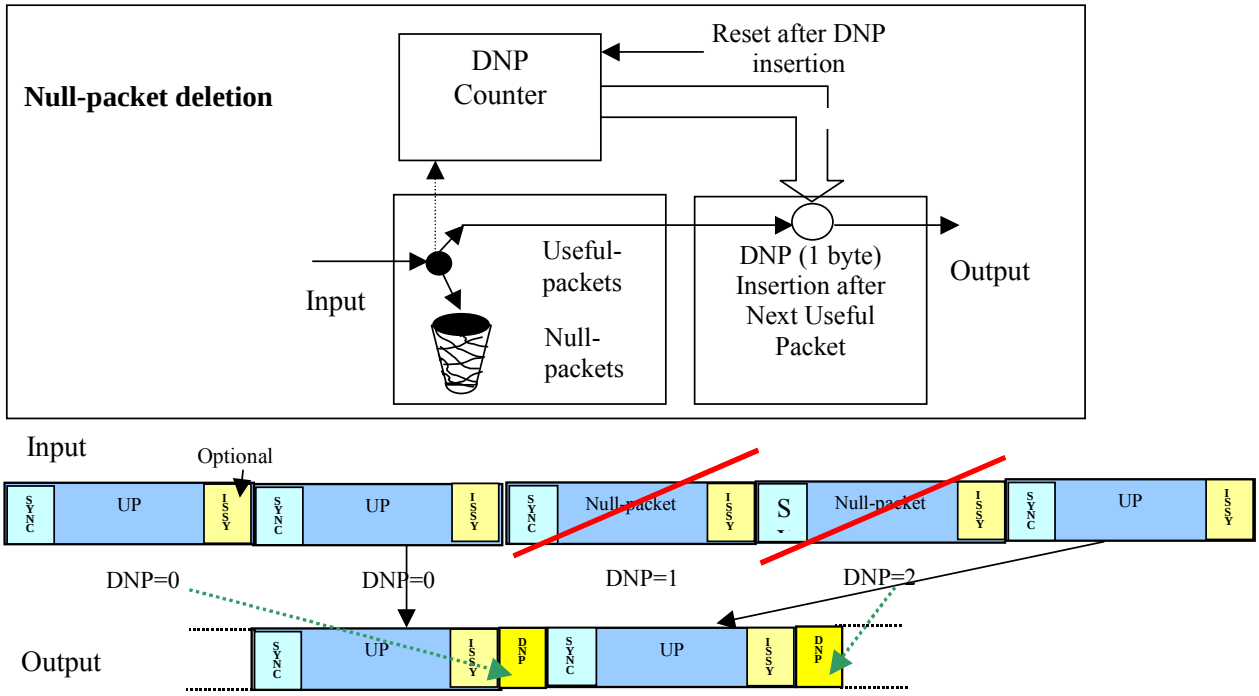

Figure 18: Null-packet deletion and DNP field (1 byte) insertion

Input Stream Synchronizer

In an ACM system, end-to-end Transport Stream delay variations ΔD_{TOT} may occur under dynamic bit-rate variations. For example, the following sources of delay variations may be listed:

- The ACM modulator and demodulator contain fixed length buffers (of typical capacity M [bit] of some LDPC code blocks). When a useful bit-rate variation $\Delta R = R_1 - R_2$ occurs (R in bit/s), these buffers are crossed at different speed, thus the delay dynamically varies in time, in a range of some tens milliseconds:

$$\Delta D = D_1 - D_2 = M\,[(1/R_1)-(1/R_2)] = (M\,\Delta R)/(R_1 R_2).$$

- In case of multiple input streams, the buffers in front of the merger (see figure 2) produce random delay jitter, depending on the merger priority strategy. Typical figures of such delay jitters are in the range of some tens to some hundreds milliseconds.

- Using DVB-S2 for video contribution purposes, the ACM bit-rate control-loop may drive the source bit-rate (e.g. VBR video encoder), but this latter may show a significant delay D_S (e.g. hundreds of milliseconds) in executing rate variation commands (see also clause 7.2.6 and figure 42). Therefore it may happen that the total control loop delay is too large to allow real time compensation of the fading variation. To increase the control speed, the rate control loop may be closed in parallel on the video encoder and on the DVB-S2 modulator (which may immediately react to the rate variation command). In this configuration, a large buffer of many Mbytes ($M = \Delta R\, D_S$) has to be inserted in the modulator after null-packet deletion, to avoid data overflow. This buffer generates transmission delay variations $\Delta D = (\Delta R/R_1)\, D_S$ during rate adaptation, which can be as large as some seconds.

In annex F two receiver schemes are proposed to regenerate the Transport Stream clock R'_{TS} under dynamic rate variations.

4.4.3 DVB-S2 performance in ACM mode

In annex D a method is described for capacity assessment in ACM systems. ACM technique allows to significantly increase the average system throughput and availability of satellite networks, thus making the system economically more attractive for interactive applications. The increase is mainly dependant on the adopted frequency band, target link and service area availability requirements and related system sizing options. Compared to CCM, an ACM-based system can provide:

- higher system throughput than the one supported by a CCM system, as an ACM system can take benefit from better link propagation and beam C/I conditions than the worst case link on which CCM physical layer is sized;
- higher availability (time-link and/or spatial) than the one supported by the CCM system as when deeper fading occurs the ACM system can use a more robust modulation and coding scheme. This is obtained through a very small reduction of the total system throughput as the number of users affected by these deep fade events is very limited. The highest link availability and service area supported by the system depends on the lowest modulation and coding scheme supported by the system;
- more optimization dimensions in the system design to cope with more pushed frequency reuse and more complex satellite antennas.

Examples reported in annex D indicate that ACM could allow a capacity increase up to 200 % with respect to CCM, dependent on the link parameters and system configurations.

4.5 System configurations

The DVB-S2 standard defines four application areas and profiles: Broadcast, Interactive, DSNG and professional.

Table 9 associates them to the system configurations and mechanisms specified in ETSI EN 302 307-1 [i.2], either defined as "Normative" or "Optional" or "Not Applicable". At least "Normative" subsystems and functionalities are implemented in the transmitting and receiving equipment to comply with ETSI EN 302 307-1 [i.2]. Configurations and mechanisms explicitly indicated as "Optional" within ETSI EN 302 307-1 [i.2] for a given application area, need not be implemented in the equipment to comply with ETSI EN 302 307-1 [i.2]. Nevertheless, when an "Optional" mode or mechanism is implemented, it has to comply with the specification as given in ETSI EN 302 307-1 [i.2].

Table 9: System Configurations and Application Areas

System configurations		Broadcast profile	Interactive profile	DSNG profile	Professional profile
QPSK	1/4,1/3, 2/5	O	N	N	N
	1/2, 3/5, 2/3, 3/4, 4/5, 5/6, 8/9, 9/10	N	N	N	N
8PSK	3/5, 2/3, 3/4, 5/6, 8/9, 9/10	N	N	N	N
16APSK	2/3, 3/4, 4/5, 5/6, 8/9, 9/10	O	N	N	N
32APSK	3/4, 4/5, 5/6, 8/9, 9/10	O	N	N	N
CCM		N	N (see note 1)	N	N
VCM		O	O	O	O
ACM		NA	N (see note 2)	O	O
FECFRAME (normal)	64 800 (bits)	N	N	N	N
FECFRAME (short)	16 200 (bits)	NA	N	O	N
Single Transport Stream		N	N (see note 1)	N	N
Multiple Transport Streams		O	O (see note 2)	O	O
Single Generic Stream		NA	O (see note 2)	NA	O
Multiple Generic Streams		NA	O (see note 2)	NA	O
Roll-off 0,35, 0,25 and 0,20		N	N	N	N
Input Stream Synchronizer		NA except (see note 3)	O (see note 3)	O (see note 3)	O (see note 3)
Null Packet Deletion		NA	O (see note 3)	O (see note 3)	O (see note 3)
Dummy Frame insertion		NA except (see note 3)	N	N	N
N = normative, O = optional, NA = not applicable					
NOTE 1: Interactive service receivers implement CCM and Single Transport Stream. NOTE 2: Interactive Service Receivers implement ACM at least in one of the two options: Multiple Transport Streams or Generic Stream (single/multiple input). NOTE 3: Normative for single/multiple TS input stream(s) combined with ACM/VCM or for multiple TS input streams combined with CCM.					

5 Broadcast applications

5.0 Introduction

In figure 19 a simplified block diagram of the DVB-S2 system for the broadcast profile is given for the single transport stream and CCM configuration, derived from figure 2.

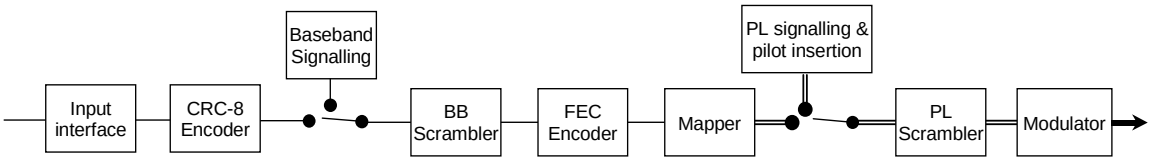

Figure 19: Simplified block diagram of the DVB-S2 system for the broadcast profile, single transport stream and CCM configuration

5.1 SDTV broadcasting

Table 10 shows comparisons between DVB-S2 and DVB-S broadcasting services via 36 MHz satellite transponders in Europe, using a 60 cm receiving antenna diameters. The example video coding bit-rates are: 4,4 Mbit/s using traditional MPEG-2 coding, or 2,2 Mbit/s using advanced video coding (AVC) systems the DVB Project is currently defining for future applications. The required C/N of the two systems, DVB-S and DVB-S2, have been balanced by exploiting different transmission modes and by fine tuning the DVB-S2 roll-off factor and symbol-rate. The results confirm the capacity gain of DVB-S2 versus DVB-S, exceeding 30 %. Furthermore, by combining DVB-S2 and AVC coding, an impressive number of 21 to 26 SDTV channels per transponder are obtained, thus dramatically reducing the per-channel cost of the satellite capacity.

Table 10: Example comparison between DVB-S and DVB-S2 for TV broadcasting

Satellite EIRP (dBW)	51		53,7	
System	DVB-S	DVB-S2	DVB-S	DVB-S2
Modulation and coding	QPSK 2/3	QPSK 3/4	QPSK 7/8	8PSK 2/3
Symbol-rate (Mbaud)	27,5 (α = 0,35)	30,9 (α = 0,20)	27,5 (α = 0,35)	29,7 (α = 0,25)
C/N (in 27,5 MHz) (dB)	5,1	5,1	7,8	7,8
Useful bit-rate (Mbit/s)	33,8	46 (gain = 36 %)	44,4	58,8 (gain = 32 %)
Number of SDTV programmes	7 MPEG-2 15 AVC	10 MPEG-2 21 AVC	10 MPEG-2 20 AVC	13 MPEG-2 26 AVC

5.2 SDTV and HDTV broadcasting with differentiated channel protection

The DVB-S2 system may deliver broadcasting services over multiple Transport Streams, providing differentiated error protection per multiplex (VCM mode) (see note). A typical application is broadcasting of a highly protected multiplex for SDTV, and of a less protected multiplex for HDTV. Figure 20 shows an example configuration at the transmitting side. Assuming to transmit 27,5 Mbaud and to use 8PSK 3/4 and QPSK 2/3, 40 Mbit/s would be available for two HDTV programmes and 12 Mbit/s for two-three SDTV programmes. The difference in C/N requirements would be around 5 dB.

NOTE: It should be noted that the DVB-S2 system is unable to differentiate error protection within the same TS MUX.

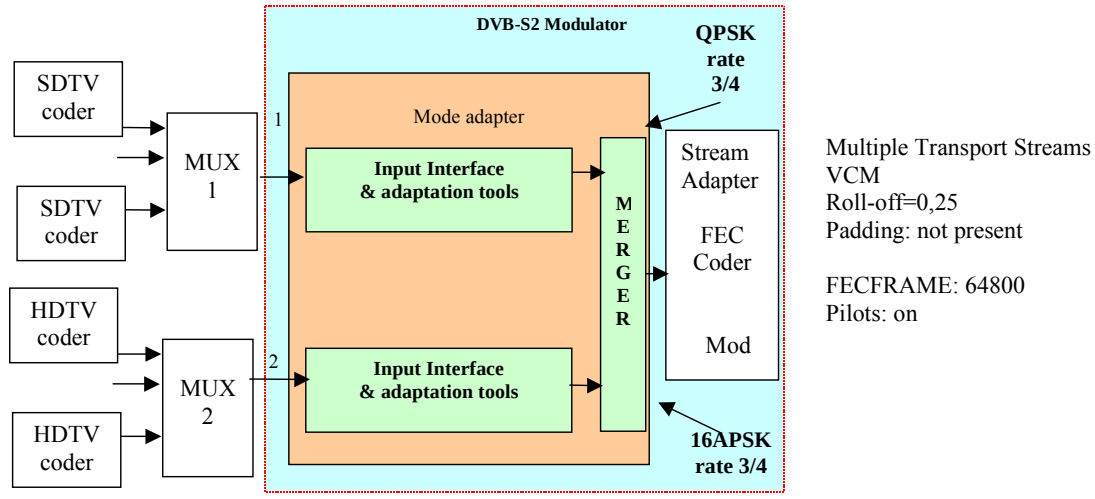

Figure 20: Example DVB-S2 configuration for TV and HDTV broadcasting using VCM

6 Interactive applications

6.0 Introduction

Interactive data services may take advantage of the possibility offered by DVB-S2 to change the modulation format and error protection level, by using the ACM functionality, thus allowing to differentiate service levels (priority in the delivery queues, minimum bit-rate, etc.). By means of a return channel informing the transmitter of the actual receiving conditions, the transmission parameters may be optimized for each individual user, dependant on path conditions.

Among the alternatives for the return path, DVB-RCS could be used. For DVB-S2 receiver to be used as forward link in conjunction with DVB-RCS2, the following requirements has to be guaranteed:

- The receiver has to output the full BBHdr and ideally CRC-8 valid indication.
- The receiver has to output the BCH valid indication.
- The receiver has to be able to filter out non-viable MODCODs.

6.1 IP Unicast Services

6.1.0 General

Figure 21 (derived from figure 15) shows a possible exchange of information (info request and info response) between the user, the Satellite Gateway and one of the information providers during an Internet navigation session by satellite (forward high capacity link) [i.13]. These interactive data services may take advantage of:

- non-uniform error protection (ACM);
- differentiated service levels (priority in the delivery queues).

IP unicast links using DVB-S2 ACM will adapt error protection on a user-per-user basis, where the number of users may be very large (e.g. up to hundreds of thousands). According to the negotiation between the Satellite Terminal (ST) and the "ACM routing manager", an "ACM router" may in principle separate IP packets per user, per required error protection and per service level. The aggregate input traffic on the various protection levels should not overload the available channel capacity; this applies to the average input traffic, while the peak traffic may temporarily exceed it, compatibly with the input buffering capacity and the service requirements on maximum delays. To fulfil this constraint when the total offered traffic becomes larger than the channel capacity, various strategies may be implemented: for example lower priority IP packets may be delayed (or even dropped) in favour of high priority packets, or the bit-rate delivered to users under poor reception conditions may be reduced. If the control-loop delays (including routing manager and ACM router) are too large to allow error free reception under fast-fading conditions, real time services (e.g. video/audio streaming) may be permanently allocated to a high protection branch, while lower priority services (e.g. best effort) may exploit the higher efficiency branches (i.e. lower cost) provided by ACM. In the ACM router, the polling strategy of the input buffers may be statically or dynamically profiled according to the traffic statistics, the propagation characteristics, and the traffic prioritization policy of the service operator.

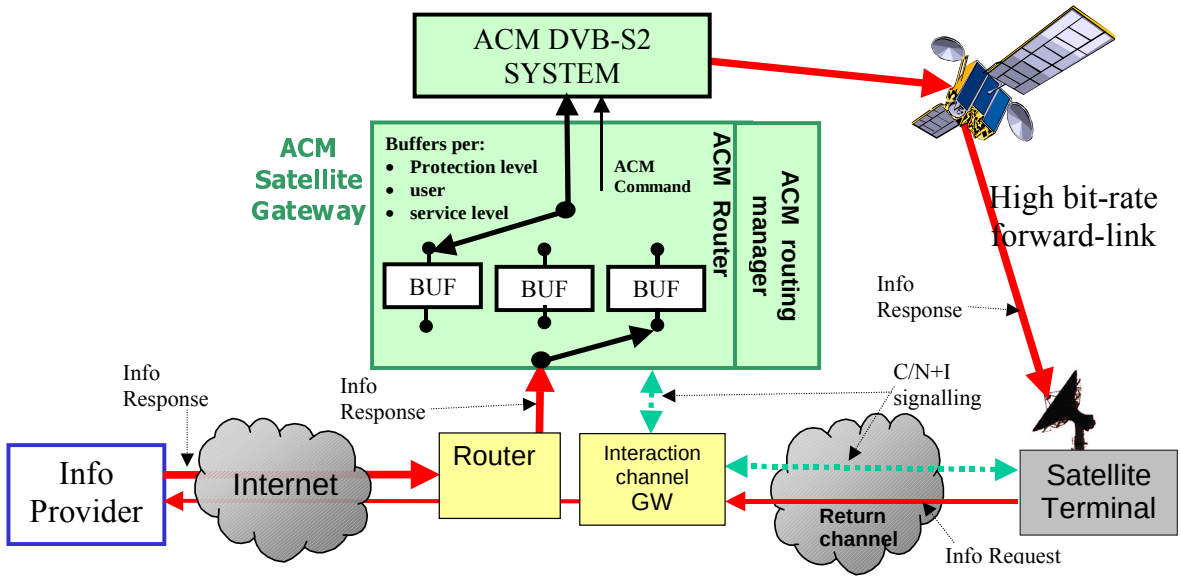

Figure 21: Example of IP services using a DVB-S2 ACM link

As illustrated in clause 4.4.2, the ACM router may interface with the DVB-S2 modulator via a Single Generic Stream input and the ACM Command input, or via Multiple (Transport or Generic) Stream inputs. The choice between the different options has a significant impact on the definition of the system architecture (intended as data processing, routing, buffering and transmission strategy) and consequently on the overall system performance in terms of efficiency, dynamicity, legacy constraints, user packet format, complexity. In the following two clauses, some examples of possible architectures for DVB-S2 unicast systems supporting ACM are shown and some considerations regarding their performance carried out.

6.1.1 Single Generic Stream and ACM command

According to this system configuration, the DVB-S2 ACM modulator receives two input signals. The first is the data stream, continuous or packetized. The second is the ACM command, carrying the MODCOD information used by the modulator for encoding and mapping each specific portion of the input data stream. This approach has the important implication that the scheduling function, which performs the selection and aggregation of the information to be transmitted in each frame, is located outside the DVB-S2 modulator subsystem. This strategy leads to a complete transparency of the modulator to layer 2 functions and therefore has the important advantage of an absolute flexibility in the choice of the scheduling algorithm.

It is worth noting that in ACM systems the choice of the physical layer mode to be used in each frame is necessarily linked to the scheduling process, as all the User Packets included in one frame are transmitted with the same physical layer parameters. From a different perspective, the data for filling a specific frame need to be selected taking into account the physical layer mode requested by the STs to whom they are addressed. This is the reason why the MODCOD information is generated at the same time of the user data selection and sent as an input to the DVB-S2 ACM modulator.

Figure 22 shows the block diagram of a possible architecture for buffering and processing the data prior to conveying them to the ACM modulator. The input data stream, composed of a sequence of User Packets, is routed according to the addressed user and his QoS requirements. Therefore, if L is the number of active users and N the possible QoS levels in the network, L × N is the maximum number of buffers needed to appropriately discriminate UPs. As active users are meant those STs, which have an open session. When no traffic is sent to an individual ST for a certain period of time, a time-out is exceeded and the user is not considered active any more. As a result, the associated buffers are de-allocated. In general, a user can simultaneously support applications requiring different QoS levels. However, as most of the users will probably support less than N simultaneous different applications with different QoS requirements, the number of allocated buffers is consequently reduced. In the simplified case where the service level agreement defines only one QoS level for each user, the number of buffers equals the number L of active users.

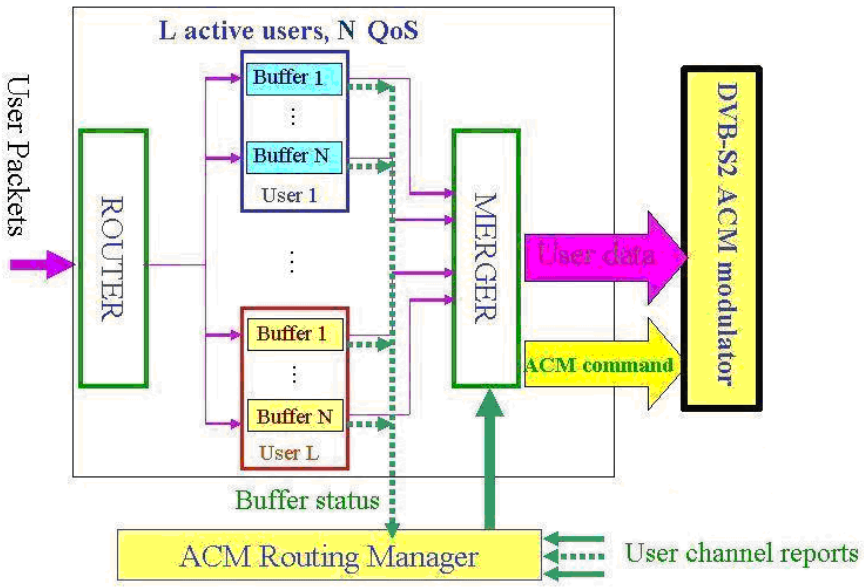

Figure 22: Block diagram of a possible system architecture with single generic stream input to the ACM DVB-S2 modulator

For each frame the merger selects from the input queues a number of packets, and combines them for building a set of information bits. Frame by frame successive data sets composed in this way are sent to the ACM modulator, together with the associated transmission parameters. When the number of bits in one set is not sufficient to completely fill the BBFRAME, the modulator will provide padding by automatically choosing the most suitable type of FECFRAME, with short or normal length.

The merger selection is driven by an ACM Routing Manager, which is responsible for packet scheduling. The scheduling policy is application dependent and needs to be designed for maximizing system efficiency while meeting QoS requirements. In order to achieve these goals, the ACM Routing Manager can take advantage of the channel status information reported by the STs, of the different priority levels and QoS requirements of the input queues, and finally of the information concerning the buffer occupation. In fact, the first type of information is needed in order to combine in one frame packets with the same transmission parameters; the second allows for meeting QoS requirements (maximum delay, minimum rate, etc.); the third can be used e.g. for satisfying QoS requirements without sacrificing efficiency (see clause 6.1.3) in presence of scarce traffic associated to a certain physical layer mode. In this case indeed, a smart scheduler policy could decide of merging these few packets with others more numerous requiring a lower efficient physical layer mode.

It is worth to mention that the high level of discrimination of the input flow (packets are routed according both to their QoS level and to the addressed user) increases the degree of choice in the packet selection process, allowing for a scheduler policy very flexible and effective. The above described queue organization thus makes easier support of individual ST QoS targets.

Furthermore, in the analysed system architecture the loop delay is minimized, thanks to the fact that the choice of the transmission parameters is made immediately before the encoding and mapping functions. The waiting time in the buffers before the scheduling process is not contributing to the loop delay, as a channel variation occurring when UPs are waiting in the queue does not lead to a wrong physical layer mode selection. On the other hand, no queues are present within the DVB-S2 modulator and the time interval comprised after the decision on the physical layer mode and before signal transmission is minimized. The complete separation between scheduler and modulator allows for a robust system, whose dynamicity is not affected by data buffering delay within the GW.

The system good performances in terms of flexibility, channel tracking capabilities and QoS satisfaction need nevertheless to be traded off against system architecture complexity. The quite large number of buffers, though of limited memory size requirements, and their dynamic allocation dependent on user traffic variations make implementation a challenging task. However, a functionally equivalent solution can be implemented with only N input buffers, in which the user packets are separated per QoS levels. As for each frame the ACM Routing Manager aggregates packets with the same requirements in terms of transmission parameters, there is a need for accessing all the buffers memory locations, instead of the first one only. Thus, the L × N FIFO buffers of figure 22 can be in principle replaced by N buffers of larger dimension, where all the packets in the buffers are made available to the merger for building the data field. This prevents the need for dynamic buffer allocation, thus simplifying implementation.

Other simplified yet high-performance scheduler implementations can be envisaged in the system implementation. Another example, for a single GSE generic stream configuration, is presented in clause 6.3 of ETSI TS 102 771 [i.42]. What has to be avoided is to devise architectures whereby the STs affected by the less favourable link conditions are significantly impacting the delay in packet delivery to other users [i.13].

6.1.2 Multiple (Generic or Transport) Streams

Figure 23 shows the block diagram of the DVB-S2 ACM system according to the system configuration where the DVB-S2 modulator interfaces with a number of input data streams. As regarding the data stream format, two solutions are possible:

- IP datagrams can be encapsulated in Transport Streams (Multi-Protocol Encapsulation - MPE), according to ETSI EN 301 192 [i.5];
- IP datagrams can be fragmented and encapsulated in variable or fixed length layer-2 packets, or directly mapped in the transmitted TDM stream. GSE, MPE or other encapsulation protocols can be assumed.

As explained in clause 4.5.2, the merger within the DVB-S2 modulator reads the data fields from one of its inputs. Since physical layer mode homogeneity is required for the data field, each data stream within the modulator needs to be associated with a certain physical layer mode. For this reason, the ACM router splits the users' packets per service level (priority) and per required protection level, and sends them to the multiple DVB-S2 input interfaces, each stream being permanently associated to a given protection level. Therefore, each input stream merges the traffic of all the users needing a specific protection level, and its useful bit-rate may (slowly) change in time according to the traffic characteristics.

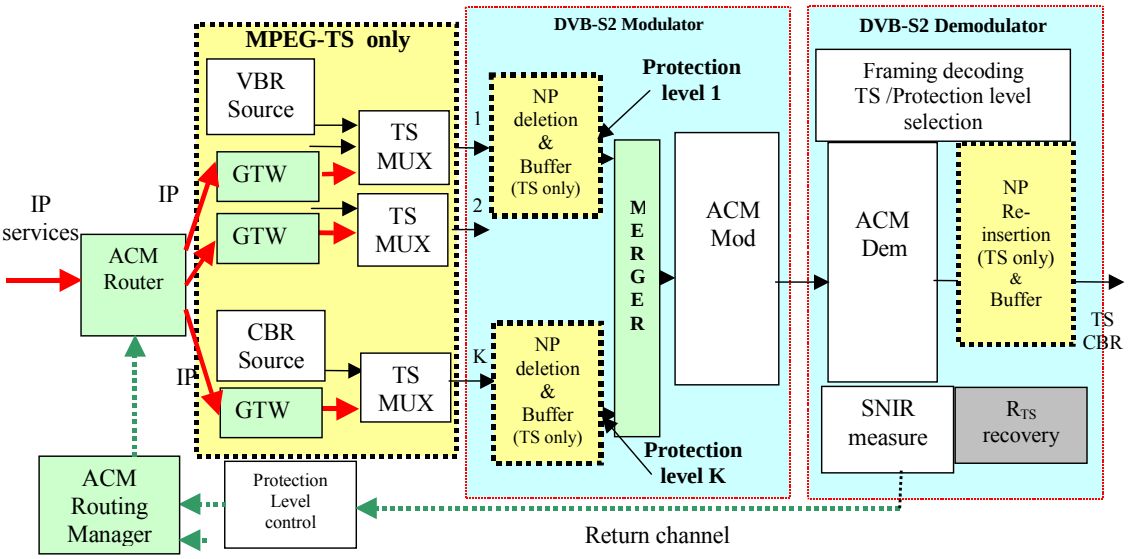

NOTE: For Generic input Streams, GWs, TS Muxes and null-packet deletion are not required..

Figure 23: IP Unicasting and ACM: Multiple input streams - uniform protection per stream

Dotted boxes in figure 23 address the specific case of IP services encapsulated in Transport Streams (Multi-Protocol Encapsulation - MPE), according to ETSI EN 301 192 [i.5]. In this case, K MPE gateways (GW_i) are associated to K TS multiplexers, to feed K DVB-S2 input streams (one per active protection level). Null-packet deletion, applied to each branch, reduces the transmitted bit-rate. The decoded TS, after null packets re-insertion, is a valid TS (the input stream synchronizer may optionally be activated). To fully exploit the potential ACM advantages, the additional control-loop delays introduced by the TS-specific equipment (Gateways, TS Muxes) should be minimized.

The Merger/Slicer in figure 23 cyclically polls the input buffers, and conveys to the ACM modulator a block of users' data ready to fill (or partially fill) a Data Field. A timeout may be defined in order to avoid long delays in each merger/slicer buffer. During traffic peaks, overloading the physical channel, a simple Round Robin policy may not fulfil the requirements of suitable distribution of the available throughput among users. Therefore, alternative policies to profile the Round Robin priority may be adopted.

It is important to note that the queuing time spent in the Merger/Slicer inputs buffers contributes to the overall ACM control-loop delay. In fact, channel variations occurring within the time interval between physical layer mode decision and signal transmission can lead to the utilization of a sub-optimum physical layer mode or to unsuccessful decoding of UPs. To the purpose of minimizing such waiting time, a time out can be introduced. Moreover, other approaches can be followed, such as appropriately limiting the dimension of the Merger/Slicer input buffers according to the system requirements. By limiting the input buffer size to a small number of data fields, the queuing time would be consequently reduced. However, an additional buffer is needed before the ACM router to absorb traffic peaks, whose size to be designed taking into account the IP traffic flow at the GW input. Figure 24 shows the block diagram of a possible system architecture, which follows the approach described above. If N possible QoS levels are assumed in the network, the input data packets are first split according to their QoS requirements. As an individual ST can support simultaneously several services with different requirements, its packets can be routed to different buffers. The ACM router, driven by the ACM Routing Manager, reads the UPs in the input FIFO queues and separates them according to the channel status indications sent by the STs via the return channel. As for the architecture described in the previous clause, the ACM routing manager policy may also take advantage of the information concerning buffer occupation in order to increase traffic aggregation and thus maximizing efficiency.

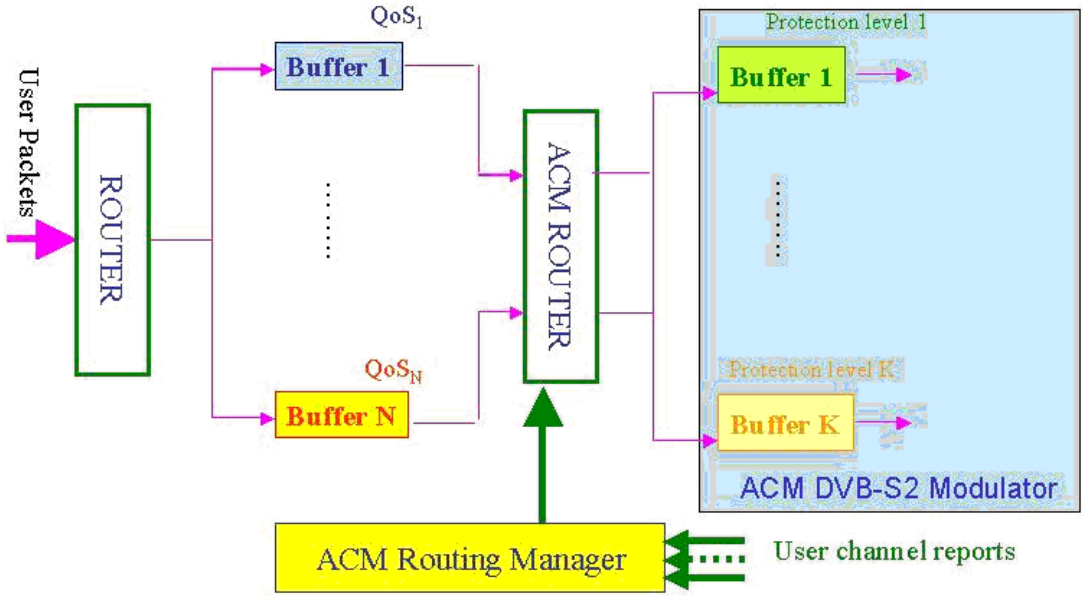

Figure 24: Block diagram of a possible system architecture with multiple DVB-S2 input streams (one per protection level)

In the multiple input streams configuration, unlike the single input stream configuration, the scheduling functions are not completely decoupled with respect to the DVB-S2 modulator. On the contrary, part of the scheduling functionalities is associated to the merging operation, and part takes place outside the DVB-S2 modulator and can be therefore system and application dependent. The overall system performance is thus driven both by the merger policy (cyclic polling in the reference case) and by the routing/scheduling algorithms applied outside the modulator.

In the system architecture case presented here the buffer organization is definitely less complex than the one described in the previous clause. However, simple FIFO queues, where UPs are aggregated without any differentiation, coupled with a Round Robin merging policy, can present some performance limitations when adaptive systems are considered. The impact on throughput and packet delay of this system architecture is analysed in depth in clause 6.1.4.

6.1.3 Encapsulation efficiency of ACM modes

The Internet Protocol (IP) interconnects multiple networks attached to the Internet and the DVB-S2 network can be seen as another upcoming access network offering adaptive physical layer. When an IP packet enters/exits a particular access network, it can be encapsulated into a local packet or capsule, having only meaning within the local network and adding some additional overhead. The capsule of DVB-S2 is called BBFRAME (in information bits) or FECFRAME (in encoded bits). The layered architecture of the DVB-S2 interface is presented in figure 25.

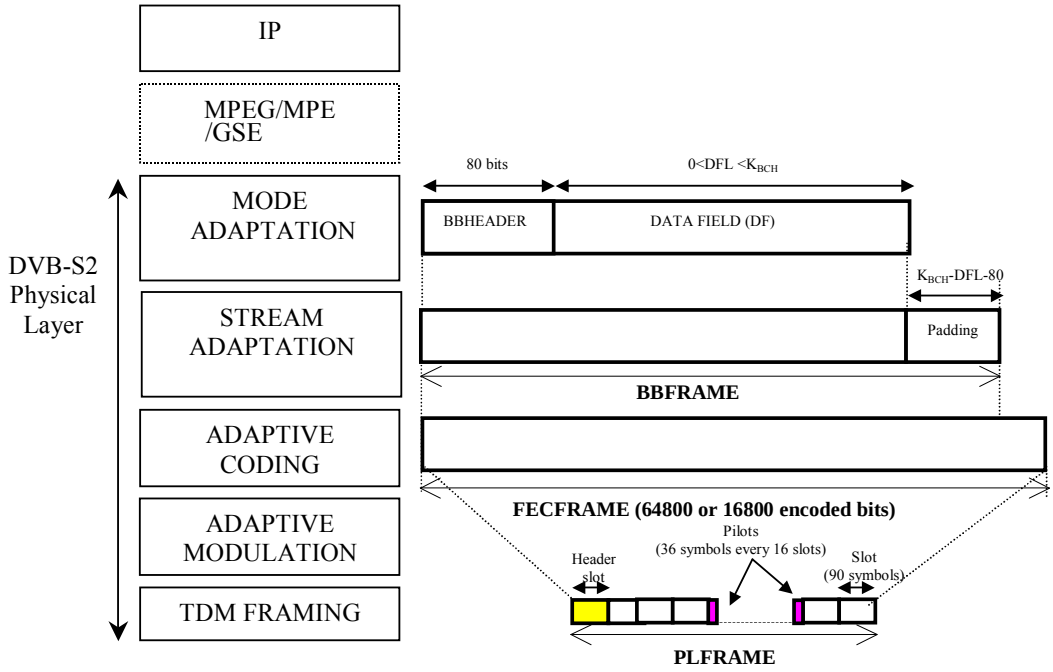

Figure 25: Air interface architecture of the DVB-S2 using ACM

From the layered air interface architecture of figure 25, following the detailed description of [i.13], the overall encapsulation efficiency for the MPEG encapsulation may be computed as a function of the spectral efficiency η and of the IP packet length L, according to the following expression:

$$\psi_{DVB-S2}(\eta, L) = \psi_{MPEG}(L)\psi_{MS}(\eta, L)\psi_{\text{framing}}(\eta) \quad (1)$$

While DVB-S was only based on MPEG transport streams, DVB-S2 allows a second flavour, the so-called generic stream either packetized (fixed packet length) or continuous (variable packet length). The efficiency of the MPEG encapsulation, $\psi_{MPEG}(L)$, equates one if IP packets are encapsulated directly on the DVB-S2 (note however that any other encapsulation is possible). $\psi_{MS}(\eta, L)$ includes both the encapsulation efficiency of DVB-S2 Mode adaptation and of the Stream adaptation, while $\psi_{\text{framing}}(\eta)$ includes the effects of the physical layer frames.

IP over MPEG encapsulation is currently performed via the Multi Protocol Encapsulation MPE, which allows concatenating IP packets ETSI EN 301 192 [i.5]. Figure 26 shows the MPEG encapsulation efficiency as a function of the IP packet length: when the IP packet length is significantly shorter than the TS packet length (188 bytes) the encapsulation efficiency is low, and this is even more evident when concatenation of packets is not allowed (i.e. only one IP packet per TS packet).

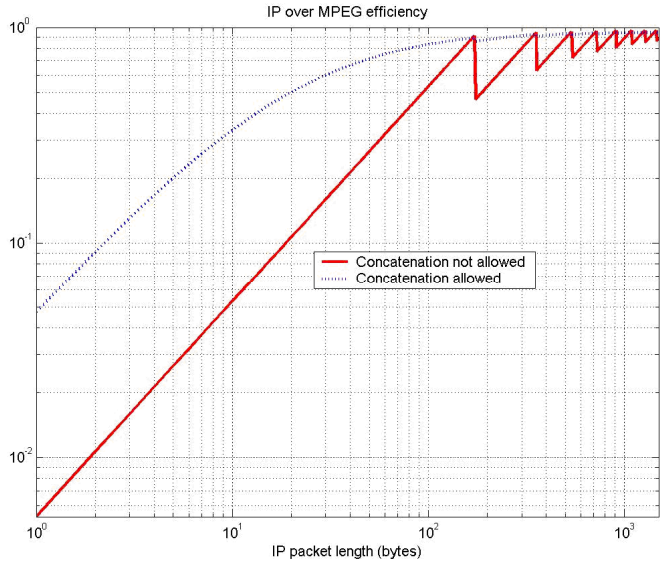

Figure 26: IP over MPEG encapsulation efficiency

Figure 27 shows $\psi_{MS}(\eta, L)$ when only one single IP packet is directly encapsulated (without MPEG-MPE). The large size of the DVB-S2 capsules in case of normal FECFRAME configuration (around 8 000 bytes after FEC coding, including a BBHeader, showing a very high efficiency, larger than 99 %) is the result of pursuing a synergy between broadcast and unicast systems (see note 1). As shown in figure 27, in order to achieve a large protocol efficiency at DVB-S2 Mode and Stream Adapter level, the encapsulation process should multiplex many IP packets from different users in the same FECFRAME, to avoid padding losses. When MPEG MPE encapsulation is adopted, the MPEG packet length is fixed (188 bytes) and rather short, therefore the above mentioned need to concatenate multiple packets in each FECFRAME is confirmed.

NOTE 1: Broadcast systems requires BER < 10 - 11, where large code blocks offer better C/N performance.

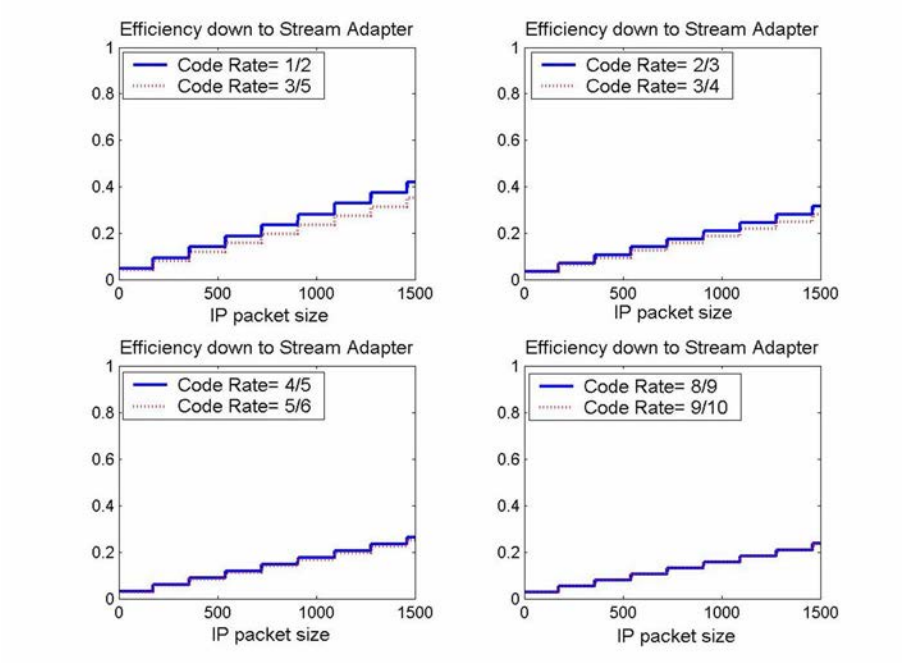

NOTE: Encapsulation efficiency ($\psi_{MS}(\eta, L)$) for a single IP packet: large efficiency may be achieved only for multiple IP packets encapsulation.

Figure 27: Mode and Stream adaptation layers

The framing efficiency $\psi_{fra\min g}(\eta)$ is fixed by the standard and is very high (above 97 %) for all the physical layer configurations.

In order not to make assumptions on buffer statistics, a straightforward way to calculate preliminary figures on encapsulation efficiency is as a function of the percentage of actual payload (Data Field Length) being encapsulated.

Table 11 shows the total encapsulation efficiency assuming different percentages of payload and is clear that the system is highly efficient only when buffers are constantly full (i.e. the padding field is small). Moreover a 10 % of efficiency is lost when MPEG encapsulation is used even assuming continuous filling (IP packet concatenation).

Table 11: Total DVB-S2 encapsulation efficiency as a function of percentages of available payload

	IP directly				MPEG/MPE				MPEG			
	Full	**80 %**	**50 %**	**20 %**	**Full**	**80 %**	**50 %**	**20 %**	**Full**	**80 %**	**50 %**	**20 %**
NORMAL FECFRAME 64 800 bits	0,97	0,78	0,479	0,19	0,88	0,71	0,44	0,18	0,78	0,62	0,39	0,16
SHORT FECFRAME 16 800 bits	0,96	0,77	0,48	0,19	0,87	0,70	0,44	0,18	0,77	0,61	0,38	0,15

Regarding the effect of the statistical distribution of the IP packet length L on the encapsulation efficiency, from [i.13] it can be inferred that its effect is limited to the case of MPEG MPE (see note 2). This also means that buffer utilization statistics will influence system efficiency more than packet size. As it is shown in [i.13], assuming buffers are always full, the encapsulation efficiency for the streaming video case is 86 % and 70 % (case of 64 800 coded bits) depending on whether IP concatenation is allowed in MPE or not, respectively. Therefore, when using MPEG encapsulation, the aggregate efficiency may be further reduced due to the IP packet size distribution.

NOTE 2: The Mode and Stream adaptation encapsulation may multiplex many input packets in a BBFrame, thus avoiding large padding sequences.

An appropriate design and dimensioning of the system should yield little encapsulation losses most of the time. Actual figures of encapsulation losses in presence of bursty traffic and time-varying channel conditions should be computed through simulations involving realistic models of traffic [i.18] and of DVB-S2 physical layer TDM composition.

A performances analysis of the overall encapsulation efficiency for GSE over DVB-S2 generic streams, taking into account the different components of DVB-S2 systems in ACM mode, is provided in Annex A of ETSI TS 102 771 [i.42]. This analysis also includes a comparison of GSE and MPE/MPEG-TS encapsulation efficiency.

6.1.4 Scheduling issues

The example scheduler architectures considered in clauses 6.1.1 and 6.1.2 are summarized in figures 22 and 24. Both of them, in principle, assume FIFO buffering (of un-specified depth) at any queuing entity, and both allow for any type of encapsulation. Figure 22 refers to a single input stream plus the ACM command, thus avoiding DVB-S2 modulator scheduling functionality. Figure 24 refers to multiple Input Streams (one per each of the K protection levels), where scheduling functionality is included in the DVB-S2 modulator (merger/slicer function). The baseline scheduling policy (so-called "merging policy") is a cyclic polling of input buffers (Round Robin, RR) plus a timeout, as explained in clauses 6.1.1 and 6.1.2. The use of Normal and Short FECFRAME is allowed. The scheduling relevant to service level (N buffers, one per each QoS) is performed by the ACM router, outside the DVB-S2 system.

In order to perform a preliminary analysis, the following simplistic design decisions were taken according to figure 24:

- Single QoS services (best effort) and fixed user packets length.
- Total number of physical layers and FIFO buffers K = 24, out of the 28 allowed by DVB-S2.
- Depth of the K buffers: equal to two times DFL (see note 1) (DFL depends on modulation and coding scheme).
- Slicing/merging policy: simple Round Robin plus timeout, no padding, only Normal FECFRAME.

NOTE 1: To be noted that the K FIFO buffers are included in the ACM control loop, therefore their depth should be minimized.

A more complete analysis, including the effect on performance of user packet length, is described in [i.18].

In order to set up a simulation framework, a jointly event and time driven simulator has been developed based on the block diagram of figure 28. A multi-beam system has been implemented in order to simulate the location-and-time dependant SNIR. The RF interference from the neighbouring beams is assumed to be constant in time but location-dependent. The model allows arbitrary number of beams and arbitrary antenna pattern and frequency reuse pattern. Each beam is split in a number of uncorrelated fading regions [typically 4 for a ~0,67° beam aperture].

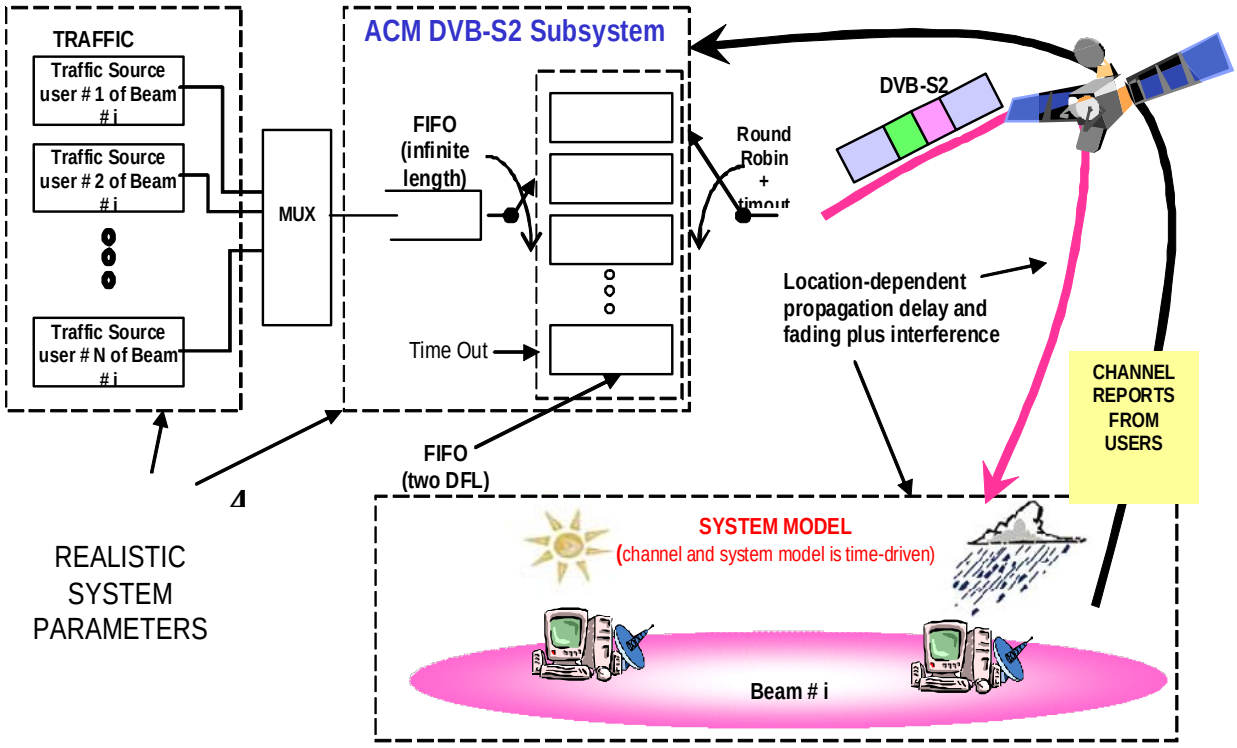

Figure 28: Block diagram of the jointly time and event driven simulator

Assuming a total number of U users within the beam, the corresponding SNIR levels at location of user u_i (including time and location variations) are computed, and the spectral efficiencies η_i (useful bits per unit transmission bandwidth by satellite) are derived from the DVB-S2 characteristics (according to the DVB-S2 specification ETSI EN 302 307-1 [i.2], clause H.1).

A "SNIR report" is sent back to the GW any time a change in the physical layer is detected. One of the key parameters under analysis is the end-to-end delay experienced by user data packets in the forward link path. This can be derived as $T_{loop} = T_{prop} + T_q$, where T_{prop}, propagation time, is around 240 ms to 250 ms, depending on the latitude and longitude of the user location, and T_q is the waiting time at the queues encountered across the system.

Traffic injected into the system is event-driven and exponential inter arrival times are considered. Also the whole packet scheduling procedure is event-driven.

In [i.13], a study-case simulation is illustrated, verifying the behaviour of the ACM subsystem in case the unique FIFO architecture is implemented. The load of the simulated DVB-S2 system should be either limited below 90 % or controlled by some admission control mechanism. FIFO queuing places an extremely low computational load and implementation complexity compared with more elaborate policies.

Their behaviour is easily predictable, since maximum delay is determined by the maximum depth of the queue. However, a unique FIFO queuing also poses the following limitations:

- routers may not organize/access buffered packets, e.g. according to a particular physical layer;
- the queuing delay equally impacts all flows without discrimination. In the ACM case, "congestion" due to the bit rate reduction of "bad" users (low SNIR) will affect "good" users (high SNIR);
- during congestions, non-TCP flows are favoured over TCP flows, since TCP-based applications adaptively reduce their transmission rate;
- a very bursty flow may consume the entire buffer space causing all others not to be serviced for a while. A worst-case would occur if a bursty flow occurs on a faded channel.In the case of ACM using multiple TS or generic streams, assuming a per-physical layer buffering, the simple Round Robin polling strategy adopted as baseline in the specification can dynamically distribute the capacity between the various protection levels when the average traffic load is below the maximum capacity. Instead, during overload periods, it implies a pre-defined (overall and per protection level) capacity allocation profile (see note 2), and predefined delay characteristics penalizing both "good" and "bad" users. It should be noted that "bad" users consume a significant amount of the overall system "transmission time" resources, while achieving a reduced throughput (due to the low code rate). Therefore the baseline Round Robin policy is a sort of "simple solution" not specifically designed to facilitate good-users or to maximize the overall system throughput during channel fades. In order to allow optimizations according to specific service requirements, the DVB-S2 specification opens the door to additional merging/slicing policies, for example weighted Round Robin strategies (see note 3) profiled by the service operator.

NOTE 2: One data field contains KBCH bits and is transmitted in a time interval inversely proportional to the modulation capacity: for example rate ¼ users receive at half bit rate than rate ½ users assuming the same modulation, but QPSK users are allocated double "transmission time resources" than 16APSK users.

NOTE 3: For example, the merger may read k_i consecutive data fields from the *i*-th protection branch, where k_i may be profiled by the service operator.

6.2 Independent frames structure for Packetized streams with VCM/ACM

6.2.1 Independent framing issues (applicable to MPEG-TS)

Packetized streams are composed by user packets (UP) of constant length UPL bits (the maximum UPL value is 64K, therefore constant length packets exceeding 64kbit are treated as continuous streams). UPs are processed by CRC-8 encoder, whose output replaces the SYNC byte of the following UP. In ACM or VCM applications, MODCOD may change on a frame by frame basis, therefore some PL frames may use MODCOD configurations that some receivers cannot demodulate. This case is represented in figure 29, where PL frame n is not demodulated by receiver # 2, so part of the packets at PL frame boundaries is lost and the streams merged at the two receivers differ.

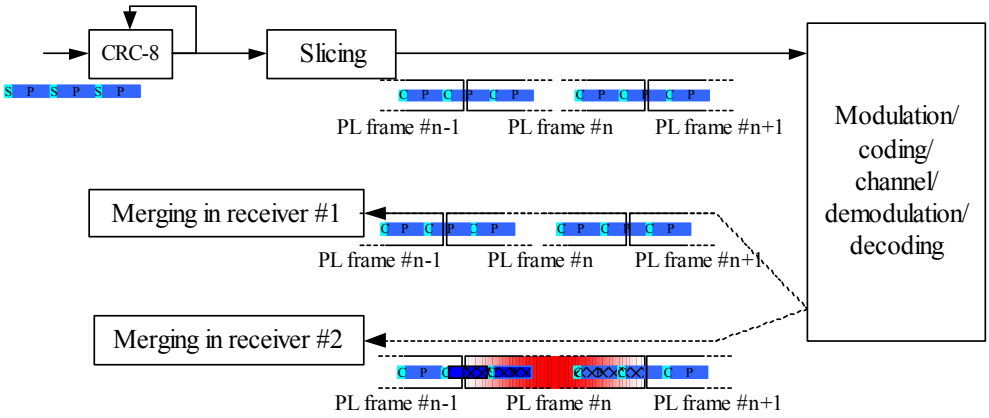

Figure 29: Example of different reconstructions for VCM mode

As, at the output of CRC-8 encoder, packets contain CRC computed on the data part of the previous packet and current packet payload, if SYNCD = 0 it is also possible that the receiver can decode the payload, but not the corresponding CRC, part of next PL frame.

The example cases reported imply that care should be taken in defining the slicing process in order to generate PL frames with independent contents, so that the streams can be rebuilt correctly at the receiver. In addition, the slicing process should minimize the overhead and therefore avoid solutions like re-inserting null packets (this solution remains available if needed). ETSI EN 302 307-1 [i.2] leaves maximum flexibility in the definition of the slicing process, allowing to transport packetized streams with independent contents of the PL frames, thus avoiding the occurrence of the above mentioned cases. In the following clause an example slicing method is described, applicable to ACM/VCM packetized streams, to exclude possible reception problems.

6.2.2 Example slicing process

The principle is to put in a PL frame only the data that can use the associated MODCOD and the corresponding CRC values. As the CRC-8 value of each UP is appended at the beginning of next packet, this results in splitting packets at the boundaries of the PL frame between the CRC value and next payload data. Padding will then be inserted to fill PL frames (grey blocks in figure 30).

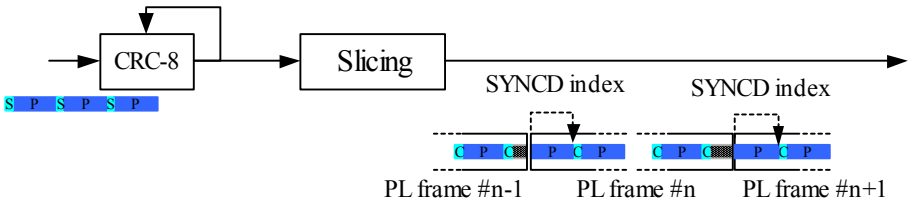

Figure 30: Slicing process with padding and SYNCD index value

Using this scheme, the overhead induced by padding is smaller than the one obtained by reinserting null packets.

It is important to notice that this means, for a receiver decoding only frames n-1 and n+1, a specific interpretation of SYNCD value when a PL frame is recovered and the previous one not. With reference to figure 30:

- if SYNCD value is equal to UPL-8 (UP length field of BB header), then a full UP is available before SYNCD pointer (because CRC is always 8 bits) and its associated CRC is also available; therefore it has to be used by the merging process;
- otherwise, data before SYNCD pointer value are linked to previous PL frame and are therefore not exploitable, so they have to be discarded by the merging process.

In a symmetrical way, a CRC closing the PL frame is exploited to check the correctness of the preceding UP, even if the rest of the packet in the following PL frame cannot be decoded.

6.2.3 Specific cases

It is possible to imagine cases of consecutive PL frames having different values of UPL that could, in some occasions, generate a wrong interpretation of the packets sequence when adopting the slicing procedure of clause 6.2.2, because UPL refers to the size of packets in the current PL frame as the continued part of payload data could, theoretically, use a different size in the previous frame. Those cases may be avoided by using a simple rule:

- The merging process in the receiver assumes continuity of the BB frames that it is able to decode correctly (see note) and that belong to the same packetized input stream ID. In particular, when SYNCD ≠ 0 then the UPL parameter applied to parse the first SYNCD bits of the data field is the UPL of the previous correctly decoded frame within the same transport stream ID.

NOTE: Correctly decoded BB frames are determined by the CRC-8 check for the BB header, optionally combined with further error detection offered by BCH decoding of the frame.

The proper solution for transporting user packets with heterogeneous packet sizes is by using generic continuous streams with appropriate encapsulation protocol, e.g. GSE.

7 Contribution services, data content distribution/trunking and other professional applications

7.1 Distribution of multiple MPEG multiplexes to Digital Terrestrial TV Transmitters

Digital Terrestrial Television (DTT) is being introduced in many countries in the world. One of the possible solutions to distribute the MPEG streams to the digital terrestrial transmitters is via satellite. Current systems are based on DVB-S, allowing the transmission of a single MPEG multiplex per signal. The result is that, for the distribution of *n* MPEG multiplexes, *n* carriers per transponder should be transmitted, requiring a large HPA OBO. Alternatively, *n* transponders can be used, or remultiplexing performed at each transmitting site. The adoption of DVB-S2 could allow the distribution of multiple MPEG multiplexes using a single carrier per transponder configuration, thus optimizing the power efficiency by saturating the satellite HPA. For example, assuming the availability of a BW = 36 MHz transponder, a symbol rate of 30 Mbaud may be transmitted using $\alpha = 0{,}20$. Thus to transmit two DTT MUXes at 24 Mbit/s each, a spectrum efficiency of 1,6 [bit/s/Hz] is required, corresponding to QPSK rate 5/6. The required C/N is around 6 dB. Figure 31 shows an example configuration at the transmitting side.

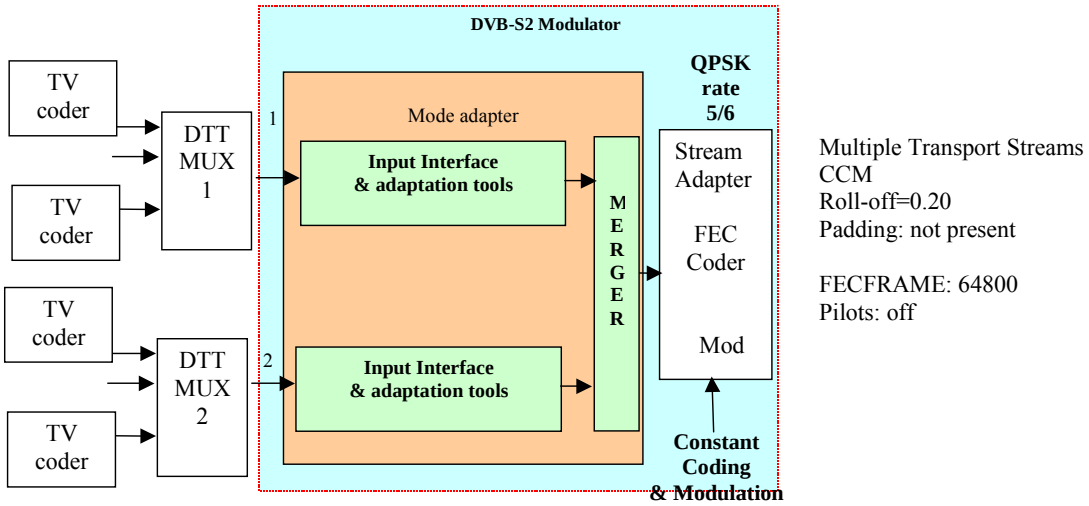

Figure 31: Example of DVB-S2 configuration for multiple DTT multiplexes distribution

The target link availability (99,9 % a.y.) could be achieved with a 3 m up-link antenna (EIRP of 64 dBW), near-saturated transponder in clear sky, and 1,2 m receiving antennas at the terrestrial transmitters sites. Using DVB-DSNG with 8PSK 2/3 and allocating two FDM carriers in 36 MHz at a symbol rate of 13,3 Mbaud, the required C/N would be of 9 dB in the receiver bandwidth. To guarantee 99,9 % average year link availability the transmitted up-link EIRP could be set to 75 dBW, the transponder gain setting adjusted to achieve OBO = 5,5 dB per carrier in clear sky and the receiving antenna size could not be less than 2 m [i.31]. Therefore DVB-S2 would allow significantly smaller receiving antennas (nearly halved diameters) and cheaper up-link stations.

7.2 DSNG and other professional applications

7.2.0 Introduction

For professional applications, DVB-S2 offers many advantages over DVB-S. Its bandwidth efficiency increase in Constant Coding and Modulation mode can be exploited in different ways:

- narrower frequency slots for the same service bit rate;
- higher service bit rates for the same frequency plan;
- increased availability;
- reduced uplink power need.

The transport stream multiplexing feature could be used in several ways:

- simultaneous uplink of multiple sources, e.g. multiple camera viewpoints, without MPEG multiplexer;
- multiplexing of service channels (for example voice or IP return).

The Variable Coding and Modulation mode allows unequal protection of the components of a transport multiplex, e.g. different protection of primary and secondary camera.

Adaptive Coding and Modulation (ACM) allows to dynamically adapt the service bit rate to variations in the link margin without glitches in the service, ideally keeping the link margin constant and small. In general this requires:

- link margin measurement and feedback to the DSNG uplink location;
- coordinated operation of variable rate encoders and DVB-S2 uplink equipment.

Simplified ACM scenarios are also possible. For example the feedback and the action taken could be binary, e.g. feedback = "link margin sufficient/critical" and action = "insert or drop the secondary camera - no change in service bit rate per camera".

7.2.1 DSNG bit rates and symbol rates

The introduction of DVB-S2 coincides with advances in compression technology (MPEG-4) and with the introduction of high resolution broadcast (HDTV). As outlined in ETSI TR 101 221 [i.7] the required bit rate also depends on the video content, video post-processing needs and on the number of code/decode steps before the program reaches the viewer. MPEG-2 bit rates are listed in ETSI TR 101 221 [i.7]. Advanced video coding techniques currently allows delivery of SDTV programs at bit rates of 1 Mbit/s to 3 Mbit/s and of HDTV programs at 6 to 12 Mbit/s. Multiple sources can be multiplexed to higher aggregate bit rates, either using MPEG multiplexing or by direct use of the multiplexing features of DVB-S2. Therefore there is a need to address 1 Mbit/s to 3 Mbit/s transmissions. In the following clauses, examples are given for extreme bit rates: 1 Mbit/s, associated to DVB-S2 mode 16APSK 4/5 and an approximate symbol rate of 300 ksymbol/s and 30 Mbit/s, associated to DVB-S2 mode QPSK 1/2 and an approximate symbol rate of 30 Msymbol/s.

7.2.2 Phase noise recommendation

The system phase noise mask of table 12 is recommended for DSNG applications. The recommendation is within reach of C-band and Ku-band phase locked block converter technology. Note that at low frequency offsets, it is much more severe than the simulation mask for broadcast in ETSI EN 302 307-1 [i.2] clause H.8.

Table 12: DSNG Phase Noise Recommendation

@	System phase noise	Possible split of system phase noise	
		DSNG TX	DTV RX STATION
10 Hz	-30 dBc/Hz	-32 dBc/Hz	-35 dBc/Hz
100 Hz	-58 dBc/Hz	-60 dBc/Hz	-63 dBc/Hz
b1 kHz	-68 dBc/Hz	-70 dBc/Hz	-73 dBc/Hz
10 kHz	-78 dBc/Hz	-80 dBc/Hz	-83 dBc/Hz
100 kHz	-87 dBc/Hz	-90 dBc/Hz	-90 dBc/Hz
1MHz	-93 dBc/Hz	-96 dBc/Hz	-96 dBc/Hz
10 MHz	-105 dBc/Hz	-108 dBc/Hz	-108 dBc/Hz

7.2.3 Receiver filter mask

In ETSI EN 302 307-1 [i.2], no mask is provided for the Nyquist receiver (RX) filter. However, in multi-carrier per transponder applications, the RX filter will influence the allowed channel spacing. It is recommended to use a RX filter design mask identical to the transmission (TX) filter mask, i.e. as provided in ETSI EN 302 307-1 [i.2], table A.1.

7.2.4 DSNG carrier spacing

Following the notation of ETSI TR 101 221 [i.7], the normalized carrier spacing is expressed as BS/R_s where BS is the frequency slot bandwidth and R_s is the symbol rate. When the TX and RX filters are ideal and the TX frequency reference is very accurate there is zero adjacent channel interference (ACI) for $BS/R_s > 1+\alpha$. In ETSI TR 101 221 [i.7] a carrier spacing of $BS/Rs > 1+\alpha$ was therefore adopted as a general rule and it was indicated that lower values should be applied only with caution after a case-by-case study. This is further analyzed below for DVB-S2 carriers.

The degradation due to adjacent channels depends on the $C_0/(N_0+I_0)$ failure point of the DVB-S2 mode (MODCOD) and on the relative level of the interfering adjacent carriers. These effects are illustrated in figure 32, and a recommendation for carrier spacing is given in table 13. In deriving figure 32 and table 13, it was assumed that:

- TX and RX filters satisfy the normative/recommended upper masks;
- all carriers have the same symbol rate and roll-off factor;
- the $C_0/(N_0+I_0)$ failure point is 2 dB above the value listed in ETSI EN 302 307-1 [i.2], table 13 (pessimistic assumption as safety margin);
- the TX HPA is operated in linear mode with 40 dB regrowth rejection (typically corresponding to 7 dB to 11 dB HPA OBO);
- the transmit frequency uncertainty is less than 0,5 % of the symbol rate.

It is seen that the value $BS/R_s > 1+\alpha$ is about right for 16APSK 4/5 with two adjacent carriers at +8 dB, but that significantly lower carrier spacings are possible in many cases. Additional cases are summarized in table 13. Situations where the carrier under test and the adjacent carriers do not have identical symbol rate and roll-off factor should be analyzed separately.

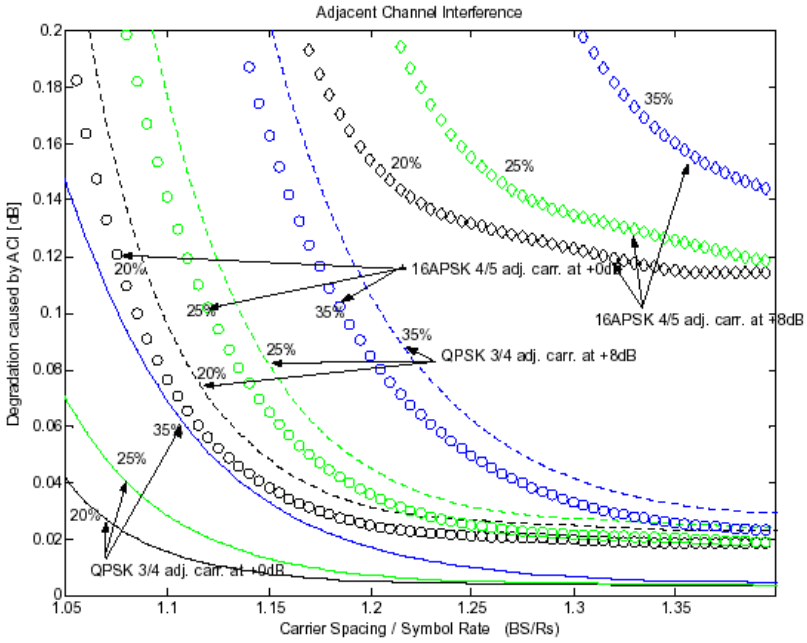

NOTE: Curves are shown for all roll-off factors and for an interfering carrier level +0 dB and +8 dB above the carrier under test. Use this figure with caution if the assumptions listed in the main text are not satisfied.

Figure 32: Expected degradation caused by adjacent channel interference for QPSK 3/4 and 16APSK 4/5 modes and assuming two adjacent carriers using the same symbol rate and the same roll-off factor

Table 13: Typical minimum carrier spacing BS/Rs

Mode of carrier under test	Roll-off factor	Adjacent carrier level +4 dB each	Adjacent carrier level +8 dB each
QPSK 3/4: Failure point assumed $C_0/(N_0+I_0)$ = 4 dB+2 dB	α = 0,20	1,10 (see note 2)	1,11
	α = 0,25	1,10 (see note 2)	1,14
	α = 0,35	1,14 (see note 2)	1,22
8PSK 3/4: Failure point assumed $C_0/(N_0+I_0)$ = 8 dB+2 dB	α = 0,20	1,11	1,17
	α = 0,25	1,14	1,21
	α = 0,35	1,22	1,30
16APSK 4/5 Failure point assumed $C_0/(N_0+I_0)$ = 11 dB+2 dB	α = 0,20	1,15	1,20
	α = 0,25	1,19	1,25
	α = 0,35	1,27	1,35
NOTE 1: Use this table with caution if the assumptions listed in the main text are not satisfied. NOTE 2: Values below 1,10 were not allowed in the table.			

7.2.5 Link budget examples for DSNG

7.2.5.0 Generic Hypothesis

In order to illustrate some potential examples of the use of the system, link budget analysis have been carried out assuming the following hypothesis:

- It is considered a full 36 MHz transponder loaded with 4 equals digital carriers each one in a 9 MHz bandwidth slot.
- A symbol rate of 7,20 Mbaud in 9 MHz (BW/R_s = 1,25) is considered. In table 14 the useful bit rate at the DVB-S2 modulator input for some transmission modes is summarized.

Table 14: Useful bit rate (Mbit/s) for a symbol rate of 7,2 Msymb/s

QPSK					8PSK			16APSK		
1/2	2/3	3/4	5/6	8/9	2/3	3/4	5/6	3/4	4/5	5/6
7,12	9,52	10,71	11,91	12,72	14,26	16,04	17,85	21,36	22,79	23,76

The satellite TWTA overall operating point is related to typical multicarrier per transponder operation in a non linearized transponder: total IBO = 8 dB, total OBO = 3,4 dB.

Satellite resources per carrier are, assuming that the percentage of the power consumption per carrier is the same as the percentage of bandwidth consumption per carrier:

- Power resources per carrier = 1/4 of the total power taking into account the overall operating point.
- Bandwidth resources per carrier = 1/4 of the total transponder bandwidth (i.e. 9 MHz).
- Quality of the links: PER equal to 10^{-7}.
- E_s/N_0 performance as summarizes in table D.2 (clause D.3).

Transmit DSNG transportable earth station characteristics:

- Location: at beam edge.
- Antenna diameter Φ = 0,9, 1,2 and 1,8 m.
- 65 % antenna efficiency, 0,3 dB coupling losses, 0,5 dB pointing losses.
- Equipped with a TWT amplifier of 250 W.
- Maximum operational EIRP (for 3 dB OBO) = 67 dBW for 1,8 m, 63 dBW for 1,2 m and 60 dBW for 0,9 m).

Receive earth station characteristics for DSNG transmissions:

- Location: at beam edge.
- Antenna Diameter Φ = 2,4 m (G/T = 25 dB/K); 4,5 m (G/T = 30 dB/K) and 8,1 m (G/T = 35 dB/K).
- 65 % antenna efficiency, 0,3 coupling losses, 0,5 pointing losses, 1,2 dB noise figure.

Satellite characteristics:

- G/T = 5,5 dB/K at beam centre (-0,5 dB/K at beam edge).
- EIRP (at saturation) = 50 dBW at beam centre (42 dBW at beam edge).
- IPFD = -85,5 dBW/m^2 (Nominal gain - NG) at beam centre (-79, dBW/m^2 at beam edge). A low gain setting of the IPFD = -82,5 dBW/m^2 is also considered.

Other assumptions are:

- Reference satellite orbital location: 0ºE.
- Uplink frequency: 14,25 GHz.
- Downlink frequency:11,75 GHz.
- Sea level height for the transmit and receive earth stations: 100 m.
- Atmospheric absorption: 0,3 dB for uplink and 0,2 dB for the downlink.
- Worst case polarization (Linear horizontal).

In figure 33 an example link budget is given.

HISPASAT-LINK BUDGET
DIGITAL SERVICES

	Clear Sky	Uplink Rain	Downlink Rain
GENERAL DATA			
Transponder bandwidth(MHz)	36		
Allocated bandwidth (-3dB) (KHz)	9000		
Velocidad de símbolo	7200		
Roll-off	1,25		
Modulation	QPSK		
Useful Information rate (Kb/s)	7157		
FEC (LDPC)	1/2	BCH	0,994074074
Occupied bandwidth (-3dB) (KHz)	7200,00		
BER	PER 10^-7		
Eb/No (dB)	1,90	See DVB-S2 Perf.	
Linealizer (0=NO, 1=YES)	0		
Nº de portadoras en el transpondedor	4,00		
Total IBO (dB)	8,00		
Total OBO (dB)	3,40		
C/I intermodulation	17,97		
Occupation factor	1,25		
Availability (%)	99,90		
Satellite longitude	0		
UPLINK			
E/S Tx Name	Rome		
E/S Tx Longitude (degrees E)	12,50		
E/S Tx Latitude (degrees N)	41,88		
E/S Tx Altitude (m)	100,00		
Rainfall Inten. 0,01% average year (mm/h)	41,00		
Uplink Frecuency (GHz)	14,25		
EIRP E/T Tx.(dBW)	**63,80**		

E/S Tx example	
HPA (W)	700,00
HPA-antenna (dB) losses	4,00
Antenna gain (dB)	39,35
Antena Eff (<1)	0,65
Antenna diameter (m)	0,77

Antenna Power Limits Violation?

Polarization discrim (dB)	30,00		
Polarization accuracy (º)	1,00		
% unavailability		0,09900	
Rain atten.		7,60	
Atmosp. Atten. loss (dB)	0,30		
Pointing error loss (dB)	0,50		
Free sky losses (dB)	207,07		
S.F.D. (dBW/m2)	-99,55	-107,15	
Saturation S.F.D. Beam Centre (dBW/m2)	-85,50		
Back-off Input (dB)	14,05	21,65	
Geogr. correction (dB)	0,00		
G/T satellite at Beam Centre (dB/K)	5,5		
C/N up (dB)	21,45	13,85	
C/I cochannel up(dB)	24,84	17,24	
C/I Out of band emissions (dB)	25,00	17,40	
C/(N+I) uplink (dB)	18,66	11,06	

	Clear Sky	Uplink Rain	Downlink Rain
DOWNLINK			
E/S Rx Name	Madrid		
E/S Rx Longitude (degrees E)	-3,69		
E/S Rx Latitude (degrees N)	40,41		
E/S Rx Altitude (m)	100,00		
Rainfall Inten. 0,01% average year (mm/h)	18,70		
Downlink Frecuency (GHz)	11,75		
EIRP satellite in the beam center (dBW)	50,00		
Back-off output (dB)	9,45	17,05	
Geogr. correction (dB)	0,00		
% unavailability			0,00100
Rain Atten.			9,81
Atmosp. Atten. loss (dB)	0,20		
Pointing error losses (dB)	0,50		
Free sky losses (dB)	205,34		
G/T E/T Rx. (dB/K)	**25,00**		21,06

E/T Rx Example	
Ant. Gain(dB)	47,59
Antenna Effciency (<1)	0,65
Antenna-receiver losses (dB)	0,50
Tlna (ºK)	90,00
Ta (ºK)	45,00
Tsyst. (ºK)	161,64
Antenna diameter (m)	2,41

Polarization discrim.(dB)	30,00		
Polarization accuracy (º)	1,00		
C/N downlink (dB)	19,54	11,93	5,78
C/I cochannel down(dB)	24,84	24,84	24,84
C/I adjacent channel(dB)	21,90	21,90	21,90
C/(N+I) downlink (dB)	14,34	7,81	5,38

GLOBAL RESULTS

Total C/(N+I) (dB)	12,97	6,13	5,18
C/I other ineterferences (dB)	11,87	11,87	11,87
C/(N+I with other interf.) Total (dB)	9,38	5,10	4,33
Additional margin (dB)	0,50	0,50	0,50
Eb/No available (dB)	8,91	4,63	3,86
Eb/No required (dB)	1,90	1,90	1,90
Margin (dB)	7,01	2,73	1,96

Figure 33: Example DSNG link budget

7.2.5.1 DSNG Examples

Clear Sky Margin

Figures 34, 35 and 36 summarize the results in terms of clear sky margins obtained for the DSNG links using the above hypothesis for the transponder nominal gain operation.

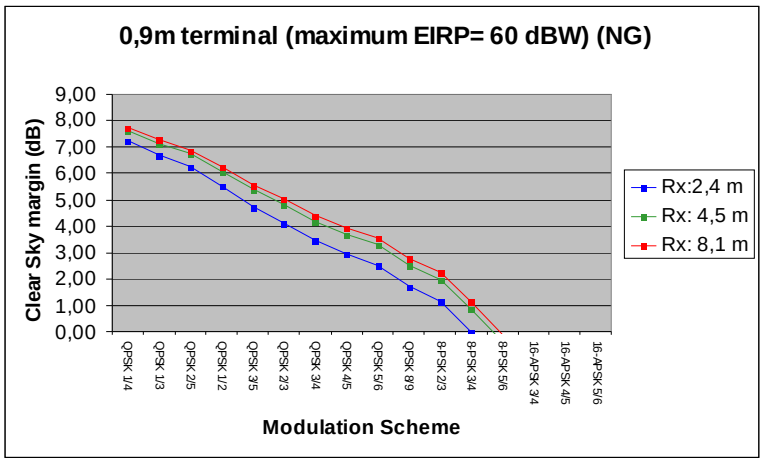

Figure 34

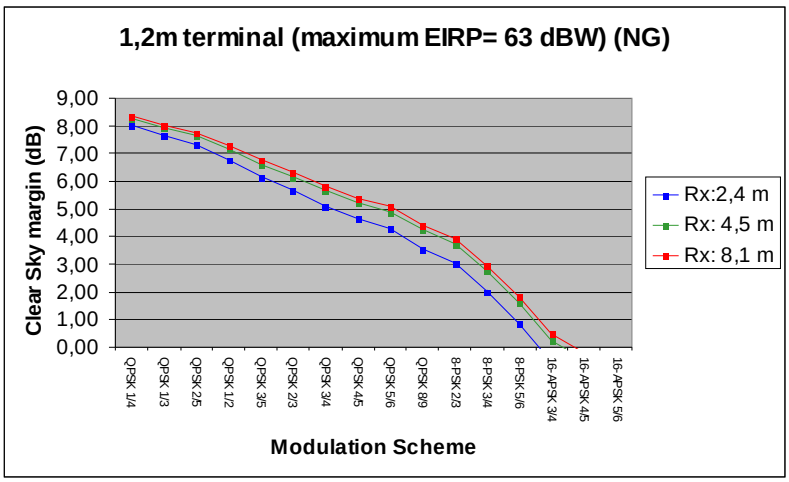

Figure 35

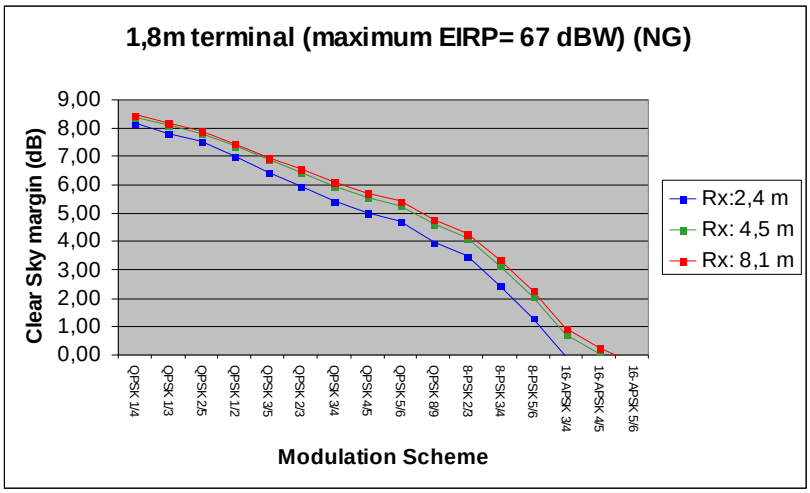

Figure 36

Figures 37, 38 and 39 provide the results for the computations in transponder low gain setting.

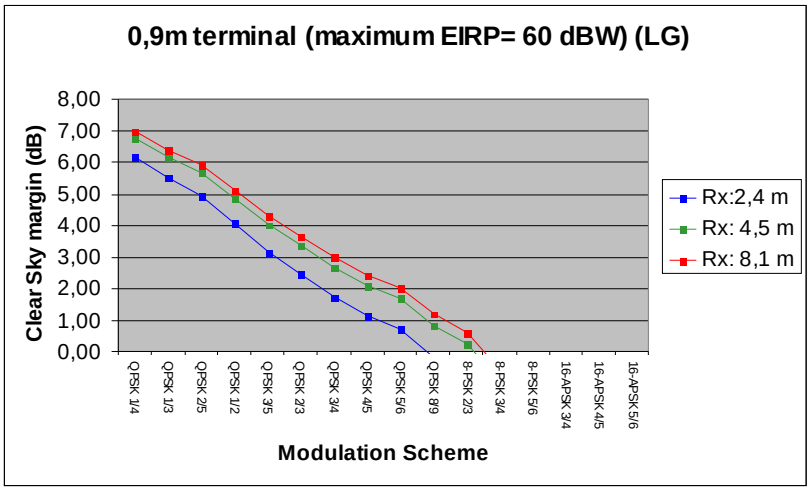

Figure 37

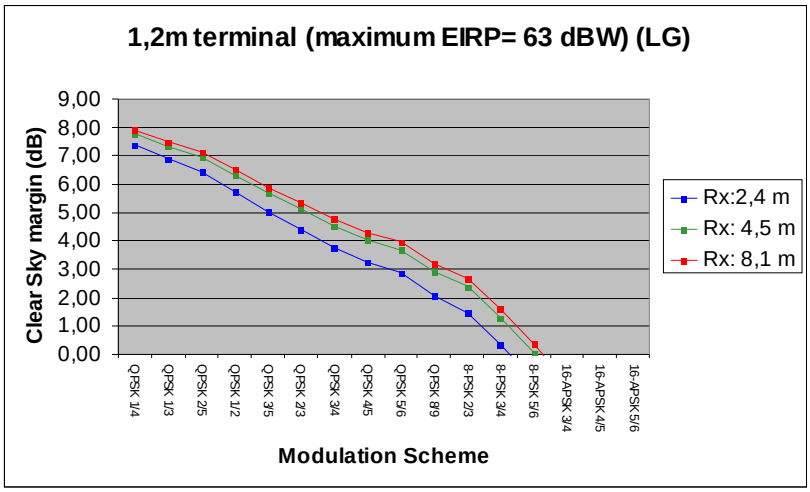

Figure 38

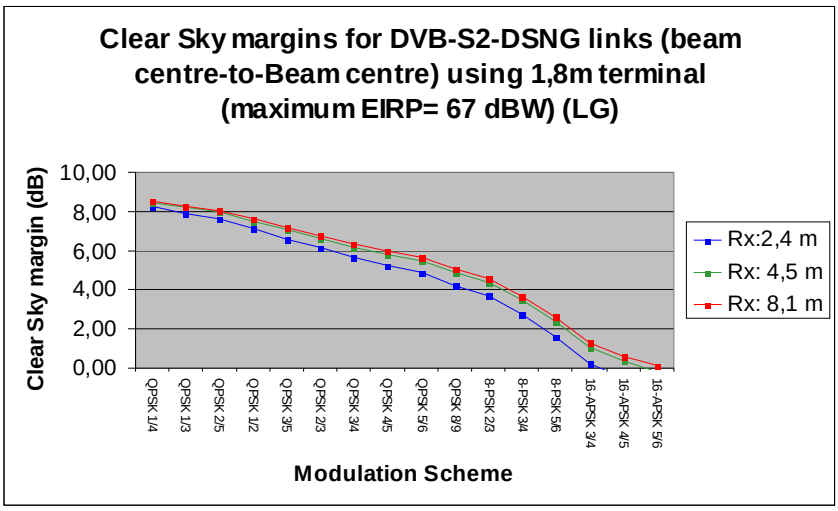

Figure 39

Link availability

In figures 40 and 41 it is summarized the availability (% of the averaged year) in terms of the required margin (dB) for Ku band (14/12 GHz), following the Recommendation ITU-R P.618-11 [i.46], P.837-6 [i.47] and P.839-4 [i.48], for a number of cities.

ITU rain characteristics for the examples are summarized in table 15.

Table 15: ITU rain characteristics

City	Country	I0,001 mm/h (P.837-3)	ho (m) P.839-3	Sea level height (m)
Miami	USA	95,8	4 209	0
La Paz	Bolivia	84,7	4 829	2 761
Sao Paulo	Brazil	68,1	4 181	708
Rome	Italy	41,0	2 685	73
Paris	France	25,4	2 226	92
Madrid	Spain	18,7	2 647	786

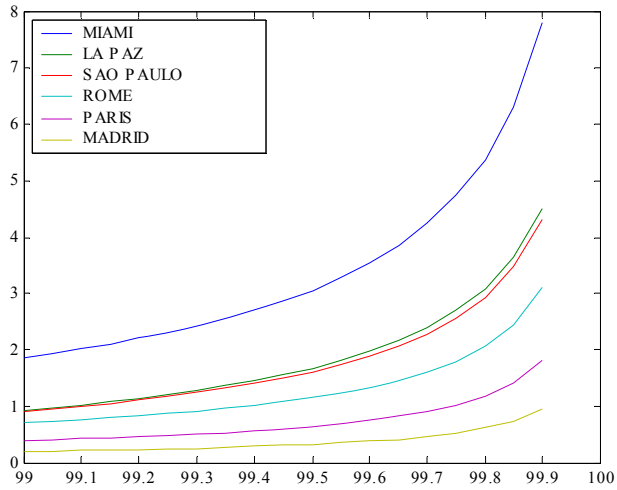

Figure 40: Attenuation (dB) versus availability (% a.y.) @ 14 GHz

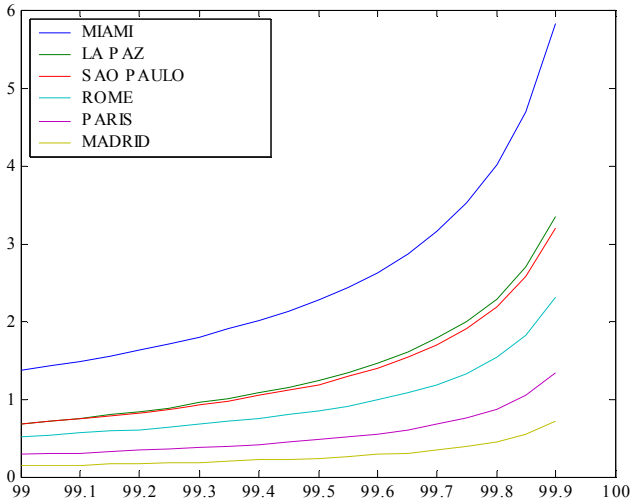

Figure 41: Attenuation (dB) versus availability (% a.y.) @ 12 GHz

Overall Availability Considerations

For a given service an overall availability is usually requested. Considering a 99,5 % availability for a link, for example from Rome (up-link) to Paris (down-link), the global availability can be computed as follows.

It can be assumed that the rain does not occur simultaneously in both places (up and down-link). The total unavailability (0,5 %) can be equally divided: 0,25 % in uplink and 0,25 % for the downlink. The margin required to assure this availability (99,75 %) could be estimated following the above graphics: about 2 dB for Rome in the up-link (14 GHz) figure 40, and 0,6 dB for Paris in the down-link (12 GHz) (figure 41).

Following this example, to assure an overall availability of 99,5 %, a clear sky margin of about 2,6 dB should be required.

In the DSNG examples, for 0,9 m DSNG transmitting antenna and 2,4 m receiving antenna in NG (see figure 34 for the 99,5 %), a maximum useful rate of 11,91 Mbit/s (QPSK 5/6) can be transmitted (2,6 dB clear sky margin operation). Taking advantage of the new DVB-S2 features, under clear sky conditions the margin can be used to increase the useful data rate up to 16,04 Mbit/s with 8PSK 3/4.

7.2.6 DSNG transmitting station identification

The proliferation of SNG stations and, in particular, the fact that operators sometimes do not strictly adhere to standard operating regulations, has created the problem of how to identify the interference origin. This happens also for fixed earth stations, that, having to be repositioned when working with several satellites, are very often not correctly aligned.

Solutions to this problem are nowadays mostly based on operational rules (by recommending mandatory procedures when operating satellite stations). A technical device which gives information about the transmitting station identification is necessary to facilitate application of the operational rules. The DVB-S2 specification allows to use the physical level scrambling sequence as signature sequence for identification of the interfering signal. The number of possible codes offered by this process seems to be largely sufficient.

The operational requirements on:

- A registration procedure has to be established. The elements to be registered are (i) a country code and (ii) identification of the owner of the station. A similar procedure already exists in the DVB structure.
- The identification code has to be set up by the supplier of the equipment and access to the identification code has to be protected. This will guarantee the system against tampering to disable or modify the identification maliciously.
- The identification process for a previously unknown carrier should be as rapid as possible.
- Transmission on the satellite could be of very short duration; "a few minutes" can be taken as a typical minimum value.

In addition to this, it would be useful if information about the geographical location of the station could be included in the stream. Inclusion of this information has to be fully automatic in order to avoid error and falsification. The knowledge of geographical location information is essential, in any case, to permit correct setting up of the station antenna.

7.2.7 DSNG Services using ACM

In point-to-point ACM links, where a single TS is sent to a unique receiving station (e.g. DSNG), the TS packets protection has to follow the C/(N+I) variations on the satellite channel in the receiving location. When propagation conditions change (see figure 42, yellow arrow), the PL frames F_i switch from protection mode M_j to protection mode M_k to guarantee the service continuity. Constant Transport Stream bit-rate and end-to-end delay, as required by MPEG, may be guaranteed by using DVB-S2 stream adaptation tools which are described in detail in clause 4.4.2.1.

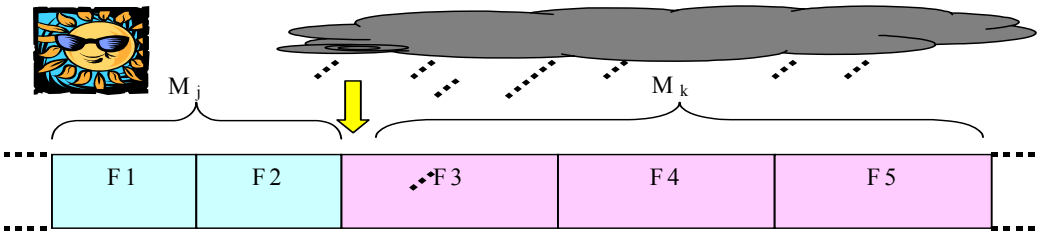

Figure 42: PLFRAMEs changing protection during a rain fading

The DVB-S2 system may operate as follows (see figure 43):

1) The bit-rate control unit keeps the video encoder bit-rate at the maximum level compatible with the actual C/(N+I) channel conditions. In parallel, it may set the DVB-S2 modulator transmission mode via the "ACM Command" input port.

2) The variable bit-rate (VBR) source encoder outputs a constant bit-rate transport stream, where rate variations of the useful bit-rate are compensated by the insertion of MPEG null-packets.

3) The Null Packets (NP) are deleted in the Mode Adapter, so that the actual bit-rate on the channel corresponds to the source bit-rate [i.13]. The deleted NPs are signalled in the DNP byte.

4) The receiver re-inserts Null Packets exactly in the original position, and the Transport Stream clock is regenerated using the Input Stream Clock Reference (see clause 4.4.2.1).

With reference to figure 43, during a deep fading the bit rate control unit may impose a rate reduction first on the source encoder, and only after the command has been executed (e.g. after 100 ms to 500 ms), to the DVB-S2 modulator (via ACM Command). A drawback of this configuration is that the video encoder and MUX delays (D5 and D6 in figure 43) are included in the control loop, with the risk of service outage under deep fading conditions. To overcome this additional delay the ACM Command can be instantly delivered also to the modulator, but to avoid packet losses large buffers have to be inserted in the DVB-S2 modulator and demodulator (see clause 6.1.1).

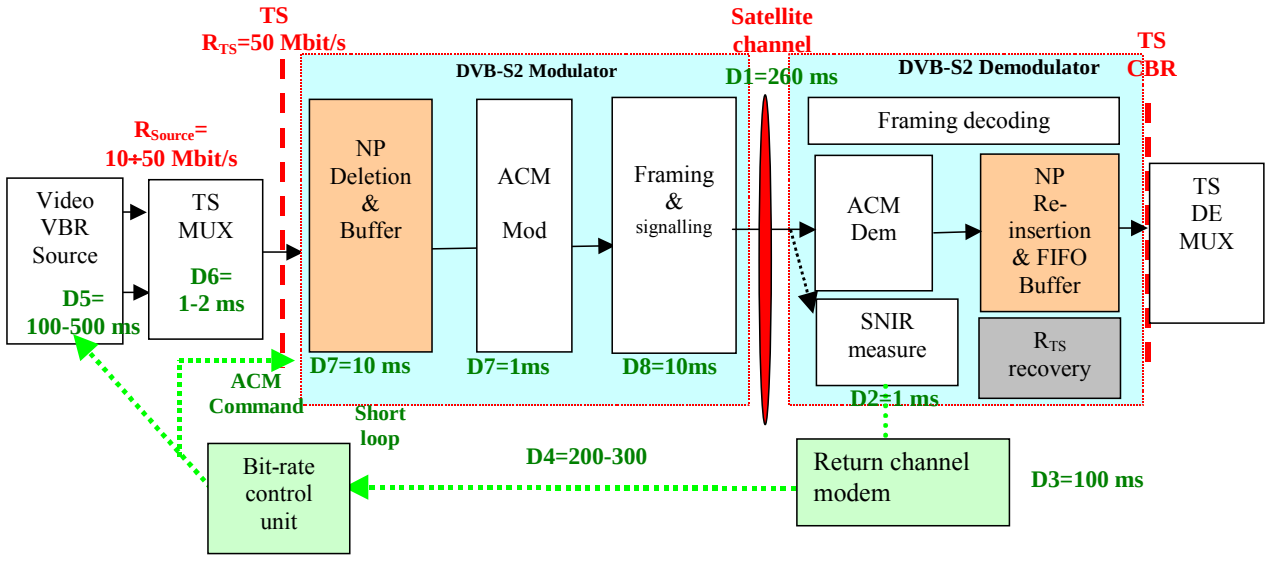

Figure 43: Single TS - uniform protection for long periods: transmission and receiving schemes

8 Transmission on wideband satellite transponders using time-slicing

See annex G.

Annex A:
Low Density Parity Check Codes

A.0 General description

LDPC codes [i.9], [i.20], [i.21] are linear block codes with sparse parity check matrices $H_{(N-K)\times N}$, where each block of *K* information bits is encoded to a codeword of size *N*.

As an example, an LDPC code of codeword size *N* = 8 and rate 1/2 can be specified by the following parity check matrix.

$$H = \begin{array}{c} \begin{matrix} n_1 & n_2 & n_3 & n_4 & n_5 & n_6 & n_7 & n_8 \end{matrix} \\ \begin{bmatrix} 1 & 0 & 0 & 1 & 1 & 0 & 0 & 1 \\ 0 & 1 & 1 & 0 & 1 & 0 & 1 & 0 \\ 1 & 0 & 1 & 0 & 0 & 1 & 0 & 1 \\ 0 & 1 & 0 & 1 & 0 & 1 & 1 & 0 \end{bmatrix} \end{array} \begin{matrix} m_1 \\ m_2 \\ m_3 \\ m_4 \end{matrix}$$

The same code can be equivalently represented by the bipartite graph in figure A.1 which connects each check equation (check node) to its participating bits (bit nodes).

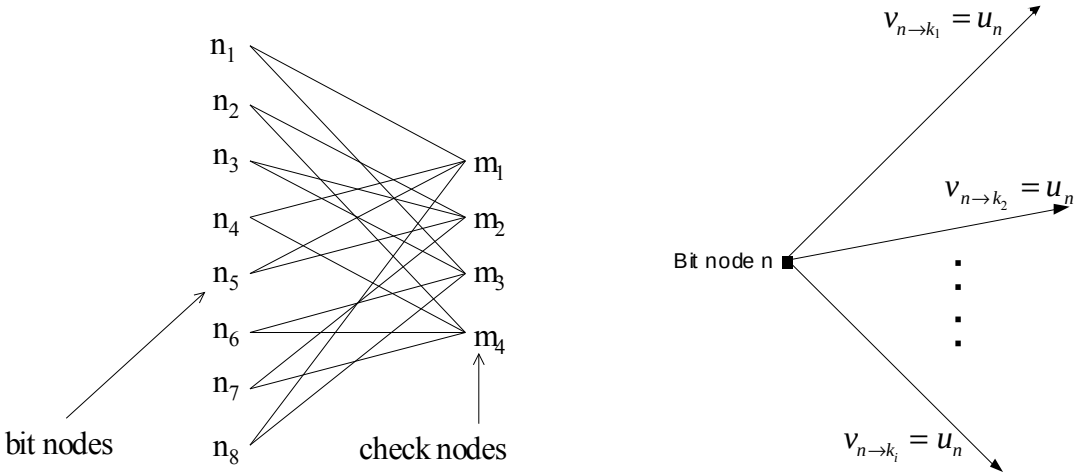

A.1 (a) A.1 (b)

Figure A.1: (a) Bipartite graph of an LDPC code; (b) Initialization of outgoing messages from bit nodes

The purpose of the decoder is to determine the transmitted values of the bits. Bit nodes and check nodes communicate with each other to accomplish that. The decoding starts by assigning the received channel value of every bit to all the outgoing edges from the corresponding bit node to its adjacent check nodes. Upon receiving that, the check nodes make use of the parity check equations to update the bit node information and send it back. Each bit node then performs a soft majority vote among the information reaching from its adjacent check nodes. At this point, if the hard decisions on the bits satisfy all of the parity check equations, it means a valid codeword has been found and the process stops. Otherwise bit nodes go on sending the result of their soft majority votes to the check nodes.

The decoding algorithm is described in the following, and a detailed explanation can be found in [i.10]. The number of edges adjacent to a node is called the degree of that node.

- Initialization:

$$v_{n\to k_i} = u_n, \quad n = 0,1,...,N-1, \quad i = 1,2,...,\deg(bit\ node\ n)$$

Here $v_{n\to k_i}$ denotes the message that goes from bit node *n* to its adjacent check node k_i, $u_n$denotes the channel value for the bit *n* and *N* is the codeword size. The initialization process is also shown in Figure G.1.

- Check node update:

Let us denote the incoming messages to the check node *k* from its d_c adjacent bit nodes by $v_{n_1\to k}, v_{n_2\to k}, ..., v_{n_{dc}\to k}$ (see figure A.2(a)). Our aim is to compute the outgoing messages from the check node *k* back to d_c adjacent bit nodes. Let us denote these messages by $w_{k\to n_1}, w_{k\to n_2}, ..., w_{k\to n_{dc}}$.

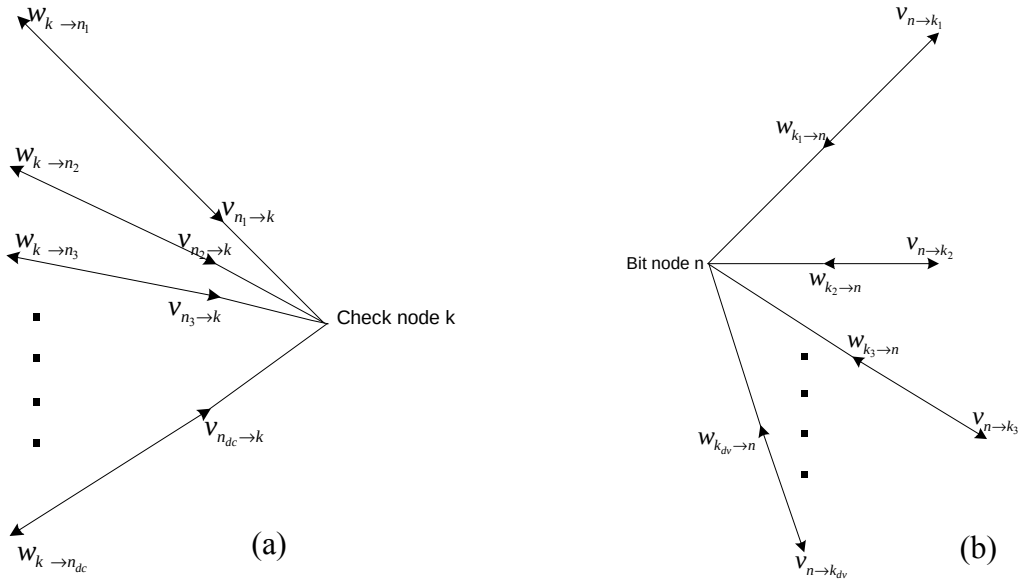

Figure A.2: Message update at check nodes (a), and at bit nodes (b)

$$w_{k\to n_i} = g(v_{n_1\to k}, v_{n_2\to k}, ..., v_{n_{i-1}\to k}, v_{n_{i+1}\to k}, ..., v_{n_{dc}\to k})$$

where $g(a,b) = sign(a)\times sign(b)\times\{\min(|a|,|b|)\} + LUT_g(a,b)$;

and $LUT_g(a,b) = \log(1+e^{-|a+b|}) - \log(1+e^{-|a-b|})$.

- Bit Node Update:

Let us denote the incoming messages to the bit node *n* from its d_v adjacent check nodes by $w_{k_1\to n}, w_{k_2\to n}, ..., w_{k_{dv}\to n}$ (see figure A.2(b)). Our aim is to compute the outgoing messages from the bit node *n* back to d_v adjacent check nodes. Let us denote these messages by $v_{n\to k_1}, v_{n\to k_2}, ..., v_{n\to k_{dv}}$.

They are computed as follows: $v_{n\to k_i} = u_n + \sum_{j\neq i} w_{k_j\to n}$.

- Hard Decision Making:

After the bit node updates, hard decision can be made for each bit *n* by looking at the sign of $v_{n\to k_i} + w_{k_i\to n}$ for any k_i. If the hard decisions satisfy all the parity check equations, it means a valid codeword has been found, therefore the process stops. Otherwise another check node/bit node update is performed.

If no convergence is achieved after a pre-determined number of iterations, the current output is given out. As SNR increases, the decoder converges with fewer iterations.

A.1 Structure of Parity Check Matrices of Standardized LDPC Codes

LDPC codes can be specified through their parity check matrices. However, in general, generator matrices are needed for encoding. Of course, for any linear code once the parity check matrix is known, a generator matrix can be derived using for instance Gaussian elimination method. But, even though parity check matrices of LDPC codes are sparse, the resulting generator matrix would no longer be sparse leading to storage and encoding complexity problems, since the standardized LDPC codes are tens of thousands of bits long. Therefore, to facilitate the description of the codes and for easy encoding, certain structure has been imposed on the parity check matrices H of the DVB-S2 codes. Even though there are methods that partially solve the problem [i.22], restricting a sub-matrix of the parity check matrix to be lower triangular eliminates the need to derive a generator matrix and leads to linear encoding complexity. More specifically, the parity check matrix of the DVB-S2 codes was restricted to the form $H_{(N-K)\times N} = [A_{(N-K)\times K}\ B_{(N-K)\times(N-K)}]$ where B is staircase lower triangular as in figure A.2.

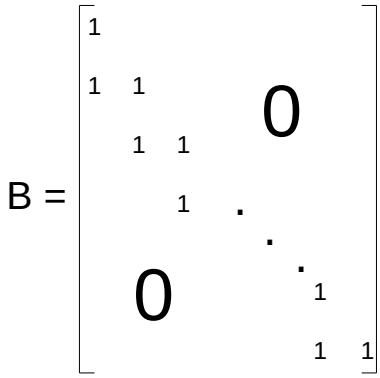

Figure A.3: Submatrix of Parity Check Matrix

Then any information block $\boldsymbol{i} = (i_0, i_1, ..., i_{k-1})$ is encoded to a codeword $\boldsymbol{c} = (i_0, i_1, ..., i_{k-1}, p_0, p_1, ... p_{n-k-1})$ using $H\mathbf{c}^{\mathbf{T}} = \mathbf{0}$, and recursively solving for parity bits.

$a_{00}i_0 + a_{01}i_1 + ... + a_{0,k-1}i_{k-1} + p_0 = 0 \Rightarrow$ Solve p_0

$a_{10}i_0 + a_{11}i_1 + ... + a_{1,k-1}i_{k-1} + p_0 + p_1 = 0 \Rightarrow$ Solve p_1

: : :

$a_{N-K-1,0}i_0 + a_{N-K-1,1}i_1 + ... + a_{N-K-1,k-1}i_{k-1} + p_{N-K-2} + p_{N-K-1} = 0 \Rightarrow$ Solve p_{N-K-1}

The matrix A is sparse; as a result encoding has linear complexity with respect to the block length.

Simulations show that the above lower-triangular restriction on the parity check matrix lead to negligible (within 0,1 dB) performance loss with respect to a general parity check matrix for the cases of relevant interest.

Furthermore to reduce the storage requirement of the matrix description by a factor of *M*, the following restriction on the *A* submatrix of parity check matrix design has been applied.

For a group of M bit nodes, if the check nodes connected to the first bit node of degree, say d_v, are numbered as $a_1, a_2, ..., a_{d_v}$ then the check nodes connected to i^{th} bit node $(i \le M)$ are numbered as:
$\{a_1 + (i-1)q\} \bmod (N-K), \{a_2 + (i-1)q\} \bmod (N-K), ..., \{a_{d_v} + (i-1)q\} \bmod (N-K)$ where $N-K$ = total number of check nodes and $q = \dfrac{N-K}{M}$.

For the following groups of M bit nodes, the check nodes connected to the first bit node of the group are in general randomly chosen so that the resulting LDPC code is cycle-4 free and occurrence of cycle-6 is minimized. From the above description, it is clear that adjacent check nodes of only one bit node need to be specified in a group of M. In DVB-S2, M is equal to 360.

A.2 Description of Standardized LDPC Codes

In DVB-S2, a wide range of bandwidth efficiency from 0,5 bits/symbol up to 4,5 bits/symbol is covered by defining ten different code rates 1/4, 1/3, 2/5,1/2, 3/5, 2/3, 3/4, 4/5, 5/6, 8/9 and 9/10 with four different modulation schemes QPSK, 8PSK, 16APSK and 32APSK. These codes are optimized for broadcast modes. For each code rate, a parity check matrix is specified by listing adjacent check nodes for the first bit node in a group of $M = 360$. The coded block length is $N = 64\,800$ bits for all rates for broadcast mode. To improve the performance, irregular LDPC codes are used where degrees of bit nodes are varying [i.23]. The list of bit node degrees and the total number of nodes with those degrees are shown in table A.1 for all the code rates of this length.

Table A.1: Number of Bit Nodes of Various Degrees for N = 64 800 codes

Code Rate	13	12	11	8	4	3	2	1
1/4		5 400				10 800	48 599	1
1/3		7 200				14 400	43 199	1
1/2				12 960		19 440	32 399	1
3/5		12 960				25 920	25 919	1
2/3	4 320					38 880	21 599	1
3/4		5 400				43 200	16 199	1
4/5			6 480			45 360	12 959	1
5/6	5 400					48 600	10 799	1
8/9					7 200	50 400	7 199	1
9/10					6 480	51 840	6 479	1

For non-broadcast applications, a set of codes with N = 16 800 has also been generated with the same value of M, i.e. M = 360. table A.2 shows the list of bit node degrees and the total number of node with those degrees. The q value for the 64 800 bit codes and the 16 200 bit codes are listed in tables A.3 and A.4, respectively. Constellation labellings for all the modulations specified are shown in figure 1.

Table A.2: Number of Bit Nodes of Various Degrees for N = 16 200 codes

Code Rate	13	12	11	8	4	3	2	1
1/5		360				2 880	12 959	1
1/3		1 800				3 600	10 799	1
2/5		2 160				4 320	9 719	1
4/9				1 800		5 400	7 999	1
3/5		3 240				6 480	6 479	1
2/3	1 080					9 720	5 399	1
11/15		360				11 520	4 319	1
7/9						12 600	3 599	1
37/45	360					12 960	2 879	1
8/9					1 800	12 600	1 799	1

Table A.3: q Values for Codes with N = 64 800 bits

Code Rate	q
1/4	135
1/3	120
2/5	108
1/2	90
3/5	72
2/3	60
3/4	45
4/5	36
5/6	30
8/9	20
9/10	18

Table A.4: q Values for Codes with N = 16 200 bits

Code Rate	q
1/4	36
1/3	30
2/5	27
1/2	25
3/5	18
2/3	15
3/4	12
4/5	10
5/6	8
8/9	5

A.3 Performance Results

Even though the above design restricts the parity check matrix to be structured, the performance is still very good due to the careful choice of check node/bit node connections. Performance of various code rates with different constellations on AWGN channel is depicted in figure A.3 for N = 64 800, for QPSK, 8PSK, 16APSK and 32APSK modulation. Each LDPC frame is divided to form multiple MPEG packets, 188 bytes each. Since the error rate requirements of DVB-S2 are rather stringent (10^{-7} packet error rate), an outer BCH code with the same block length as LDPC frame and an error correction capability of up to 12 bits is employed, as defined in ETSI EN 302 307-1 [i.2].

Performance of the N = 16 200 bit codes for QPSK modulation is shown in figure A.4. Typically, these codes are about 0,25 dB to 0,3 dB worse than the N = 64 800 bit codes.

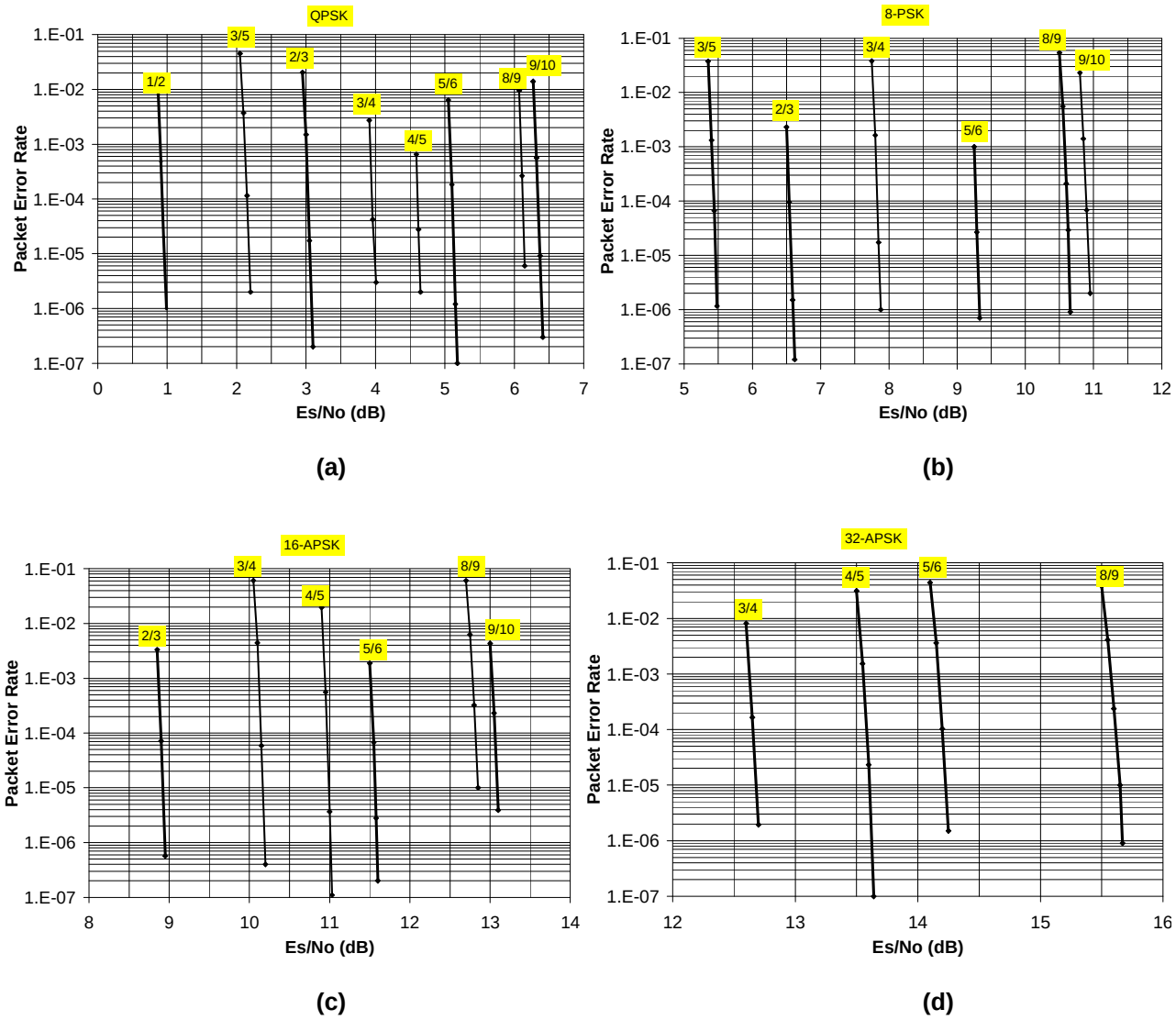

Figure A.4: Performance of LDPC+BCH Codes over AWGN Channel, *N* = 64 800 bits, (a) QPSK, (b) 8PSK, (c) 16APSK, (d) 32APSK

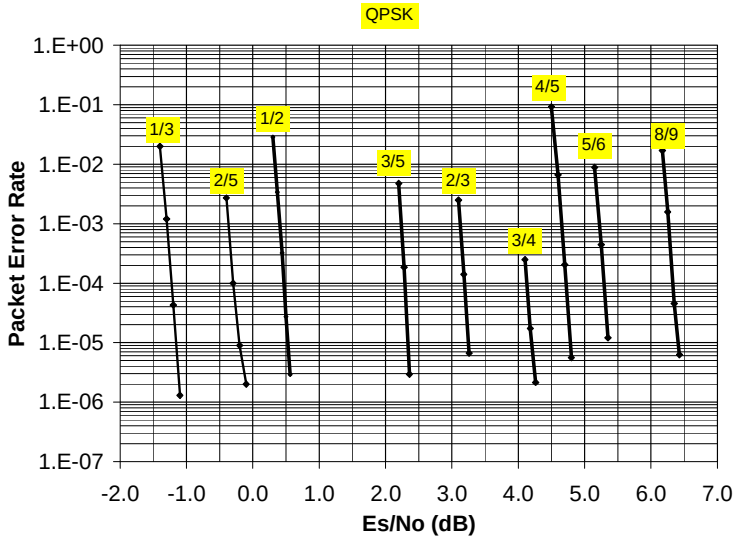

Figure A.5: Performance of LDPC+BCH Codes over AWGN Channel, N = 16 200 bits

Annex B:
DVB-S2 Physical Layer Frame and pilot structure

B.0 Introduction

Frame synchronization is needed to indicate the start of each FEC block for the decoder. It also provides the necessary information for the receiver to apply the appropriate demodulator and decoder to demodulate and decode the transmitted information. Given that some overhead is necessary for frame synchronization, it is also designed such that it can be used to reduce initial frequency and phase uncertainty of the modulated signal. The frame synchronization is designed to provide reliable operation in the worst case E_s/N_0 with minimum overhead. It is also used to minimize the demodulator implementation loss in the presence of consumer quality low-noise-block (LNB) phase noise. In fact, phase noise is particularly detrimental to demodulator performance for higher-order modulation such as 8PSK, 16APSK, and 32APSK. To preserve the near Shannon limit performance of the DVB-S2 FEC, pilot symbols may be added to assist the demodulator to minimize probability of cycle-slips and to provide more accurate phase estimates. These pilot symbols are also designed to use a minimum overhead of the overall bandwidth, and can be turned on or off as desired. The frame synchronization structure and the pilot structure are described in this annex. The frame and carrier synchronization algorithms that make use of this framing structure are described in annex C.

B.1 Structured PLS code for Frame Synchronization

Figure B.1 illustrates the general structure of DVB-S2 physical layer frames. Each LDPC coded block is preceded by the Start of Frame (SOF) and the Physical Layer Signalling (PLS) code (PLSCODE). SOF is a known 26-symbol pattern. PLSCODE is a 64-bit linear binary code, which conveys 7 bits of information with a minimum distance 32, i.e. a [64, 7, 32] code. In total, SOF and PLSCODE occupy one slot (90 symbols).

Figure B.1: Frame structure of DVB-S2

Independent from the modulation scheme of the LDPC coded block that follows, these fields are modulated by π/2-BPSK modulation to reduce the envelope fluctuation in comparison with the classic BPSK scheme. π/2-BPSK rotates the signal constellation 90 degrees every symbol. The 7 bits carried by the PLSCODE inform the receivers about the modulation scheme, code rate, pilot configuration, and length of the LDPC coded data. In the broadcasting mode, the length of LDPC codes is 64 800 coded bits regardless of code rates and modulation schemes. In the Adaptive Coding and Modulation (ACM) mode, LDPC codes of length 16 200 can also be used. Once frame and phase synchronization are acquired, the probability of incorrectly decoding the PLSCODE is negligible. As long as the PLSCODE is correctly decoded, the next SOF can be located and the frame synchronization can be maintained. In the broadcast mode, since modulation and coding scheme will not change on a frame-by-frame basis, maintaining frame synchronization does not require the correct decoding of PLSCODE. Instead, frame synchronization can be maintained as long as the symbol timing loop is in lock. In both cases, the frame synchronization can be maintained after it is initially acquired. Therefore, the discussions will be focused on the initial frame synchronization.

Extensive analysis showed that SOF by itself is too short to provide reliable and rapid frame synchronization. Given that PLSCODE uses a rather low rate code, it is natural to consider embedding certain structures into this code to aid the initial frame synchronization. There are many ways to construct a [64,7,32] linear block code. For instance, it can be constructed as an extended BCH code, the dual of an extended Hamming code, an extended maximum length code, or a first-order Reed-Muller code [i.35]. In the DVB-S2 standard, a construction is used that is particularly useful for rapid frame synchronization and efficient maximum likelihood (ML) decoding.

The construction utilizes the first-order Reed-Muller code of parameters [32,6,16]. A generator matrix for [32,6,16] Reed-Muller code is shown as follows:

01010101010101010101010101010101
00110011001100110011001100110011
00001111000011110000111100001111

00000000111111110000000011111111
00000000000000001111111111111111
11111111111111111111111111111111

The generator matrix can be constructed recursively by the well-known $|\boldsymbol{u}|\boldsymbol{u}+\boldsymbol{v}|$ construction. This notation indicates how to use two codes of length n to construct a code of length $2n$, i.e. $\boldsymbol{u}$ and $\boldsymbol{v}$ are drawn from each of the component codes respectively. In the case of a first order Reed-Muller code, $\boldsymbol{v}$ uses the trivial linear code **0** and **1,** the all-zero and all-one vectors of length n, as codewords, and **u** belongs to a first-order Reed-Muller code of length n.

The formulation of a PLSCODE codeword is shown in figure B.2. For 7 information bits, the first six bits are encoded by the [32,6,16] first-order Reed-Muller code to obtain a binary vector **Y**. The vector **Y** is further duplicated into two identical vectors.

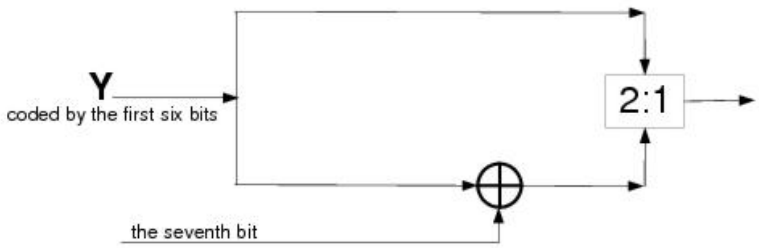

Figure B.2: Construction of PLSCODE

Every bit at the lower branch is binary summed with the seventh information bit. The upper and the lower branches are multiplexed bit by bit to form a vector of length 64. In other words, let $\mathbf{Y} = (y_0, y_1, \cdots, y_{31})$ be a codeword of the first-order Reed-Muller code [32,6,16]. Then two code words of the [64,7,32] code can be generated as $(y_0, y_0, y_1, y_1, \ldots, y_{31}, y_{31})$ and $(y_0, \bar{y}_0, y_1, \bar{y}_1, \ldots, y_{31}, \bar{y}_{31})$ respectively, where $\bar{y}$ represents the binary complement of y. Instead of bit by bit multiplexing the upper and lower vector, if the two vectors were cascaded together, it would have resulted in the $|u|u+v|$ construction of the first-order Reed-Muller code of parameters [64,7,32]. This shows that the PLSCODE constructed in such a way is actually an interleaved first-order Reed-Muller code of parameters [64,7,32], which is known to achieve the best minimum distance for a binary [64,7] code, therefore, the code as constructed in figure B.2 is an optimal binary [64,7] code.

A very useful property of the code for frame synchronization is that:

$$y_{2i} \oplus y_{2i+1} = \begin{cases} 0 & \text{if} \quad y_{2i+1} = y_{2i} \\ 1 & \text{if} \quad y_{2i+1} = \bar{y}_{2i} \end{cases} \quad \text{for } i = 0, 1, \ldots, 31.$$

Therefore, if a 64-bit codeword is taken and 32 pair-wise differences are formed between the adjacent bits, the same result will obtained for all 32 pairs. The reliability of the difference can be improbe by averaging all 32 values. If the modulation is BPSK, the pair-wise difference can average to a value equal to Δ or $\Delta+180°$. The seventh information can be easily detected and Δ, since the pair wise difference represents frequency offset, and if the frequency offset is small. For $\pi/2$-BPSK modulation, a constant $\pi/2$ shift need to be subtracted out from each pair-wise difference, the result is the same.

As DVB-S2 requires the receivers to acquire with an initial frequency offset up to 5 MHz, i.e. as large as 25 % of the symbol rate for a typical 20 Msymbol/s data stream, the carrier phase can rotate up to 90° in one symbol interval. There are only two options in such a scenario: frequency offset resistant non-coherent differential detection or searching through multiple hypotheses. The latter is clearly less preferred since it takes much longer time to acquire, up to 2 seconds (based on earlier analysis carried out during the standard development). That is too long during initial installation, when antenna pointing often requires an indication of proper reception of the signal. The differential detection scheme described above using information embedded in the PLSCODE is therefore preferred. In fact, as long as the difference, not necessarily a constant, is known *a priori,* receivers can take advantage of it. For this reason, it is possible to further scramble the codeword of PLSCODE to improve the autocorrelation property. The specific sequence used for the scrambling is as follows:

01110001100111011000001111001001010100110100001000101101111111010.

The scrambling sequence is essentially just an extended m-sequence.

In annex C, the algorithms for rapid frame synchronization by utilizing SOF and PLSCODE are described.

B.2 Pilot Structure

The design goal of DVB-S2 carrier recovery scheme is to deliver channel outputs reliably to the LDPC decoder at very low SNR with small synchronization overhead. The design objectives include:

- Negligible LDPC decoding performance loss due to carrier synchronization impairment (less than 0,1 dB to 0,3 dB for most modes).
- Capability of working at extremely low SNR, as low as E_s/N_0 = -2,0 dB.
- Capability of acquiring large carrier frequency offset (up to 5 MHz) with a 30 KHz/s ramp.
- Robustness to LNB phase noise characteristics specified by DVB-S, which works at higher SNR and allows more implementation margin.
- Rapid initial acquisition.
- Simple implementation.

The DVB-S2 phase noise specification is rather challenging due to the desire to reuse the millions of LNBs and antennas that have already been deployed for DVB-S reception. The major challenge for carrier recovery is to handle severe phase noise and large frequency offset at low SNR. Unlike DVB-S, that supports only QPSK modulation, DVB-S2 supports several modulation schemes, such as QPSK, 8PSK, 16APSK, and 32APSK. In order to expedite carrier recovery, the standard allows two operating modes for each modulation type: pilot-less and piloted, where pilot symbols are inserted to aid carrier synchronization. The system operators have the option to choose either operating mode. The receivers are informed of the pilot configuration from the PLSCODE residing in the PLHEADER. Thorough investigations on real mass market demodulators show that the following modes benefit in performance from pilot assistance for carrier recovery: QPSK ¼, 1/3 and 2/5, 8PSK rate 3/5, 2/3, ¾ and 5/6, 16APSK rate 2/3, 3/4, 5/6 and 8/9, and all code rate for 32APSK. Clearly, for most high rate codes, their operating SNRs are sufficiently high such that traditional decision-directed second order phase locked loop (PLL) should suffice. Therefore, when implementation complexity is concerned, a generic carrier recovery strategy that is suitable for all the modulation schemes with/without pilots is desired.

Based on these observations, the standard adopted the following *aggregated pilot* structure. Each LDPC coded frame is preceded by a one-slot (90-symbol) PLHEADER containing the SOF and PLSCODE. Afterward, 36 pilot symbols follow every 16-slot coded data symbols. If the pilot symbols coincide with the PLHEADER of the following frame, they will not be inserted. In [i.12], it is shown that this pilot structure is a good balance between the synchronization overhead and performance of 8PSK rate 2/3 modulation. Figure B.3 shows an example of the pilot structure, for 8PSK modulation.

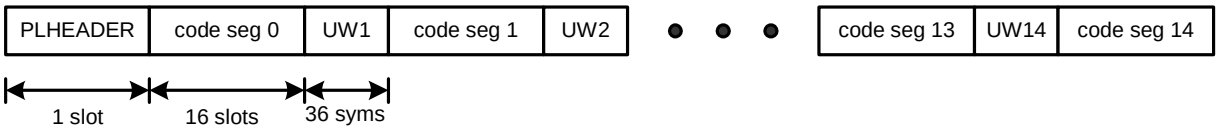

Figure B.3: Pilot structure for 8PSK modulation, where UWs (unique words) refer to pilot symbols

Annex C:
Modem algorithms design and performance over typical satellite channels

C.0 Architecture of the DVB-S2 demodulator

The DVB-S2 standard has been designed having in mind the peculiarities of the satellite channel, in particular the on-board satellite linear and non-linear distortions, the link fading impairments and the carrier phase noise dominated by the user terminal RF front-end. The adoption of high order modulation formats (up to 32-ary QAM) makes the potential channel impairments much more important than those encountered by the classical QPSK modulation format adopted by the former DVB-S standard ETSI EN 300 421 [i.1]. In the following of the annex a design of the main modulation and demodulation units of a modem compliant with the new DVB-S2 standard is proposed, to minimize the end-to-end link losses for the reference satellite channel and receiver characteristics defined in ETSI EN 302 307-1 [i.2]. The downlink satellite channel impairments (signal fading due to rain, scintillations, atmospheric gas absorption, etc.) have been modelled as a constant signal attenuation, taken into account within the signal E_s/N_0 at the demodulator input. The other impairments that are modelled within the downlink channel mostly pertain to the terminal receiver, like clock and carrier frequency errors as well as carrier phase noise. Clock frequency errors are due to long term instabilities of the terminal oscillator which provides the terminal demodulator sampling clock, while Doppler effects due to the GEO satellite movements are usually negligible. The precision of the oscillator depends on its quality (i.e. its cost) but usually it can be considered to be limited to a maximum of 10 p.p.m. Carrier frequency errors can be attributed to several factors, but the main contributors are the terminal LNB oscillator instabilities and Doppler effects. Within DVB-S2 a maximum carrier frequency error of 5 MHz has been specified for consumer-type of terminal receivers. However, the residual differential frequency errors when tuning to a different downlink carrier can be considered much smaller, i.e. in the order of max 100 kHz. The main contributor to the carrier phase noise is the terminal LNB RF oscillator, especially in low cost equipments. The terminal tuner contribution can also be not negligible. The worst case PSD (Power Spectral Density) of the combined phase noise contribution of terminal satellite receivers' tuners and LNB's is specified in ETSI EN 302 307-1 [i.2].

The architecture of a demodulator compliant with the DVB-S2 standard comprises of an RF/IF part whose architecture depends on the RF frequency band used by the application (Ku vs. Ka) as well as to whether low cost user equipments or professional equipments are used. Also, a number of choices can be made on the down-conversion strategy. For example, in low cost DTH terminals usually the RF received signal is first down-converted to a intermediate frequency by a LNB (Low Noise Block) that is placed in the proximity of the antenna feeder, then the signal is further down-shifted in frequency by a tuner, which usually, in low rate equipments, directly converts the signal to complex-baseband. A couple of well-matched A/D converters sample the signal and feed the digital demodulator section of the receiver. The block diagram of the digital demodulator is shown in figure C.1. It is assumed that the signal from the RF/IF front end is down-converted to baseband and so that the two I-Q components are made available to the digital demodulator input, sampled at a rate high enough to avoid signal aliasing.

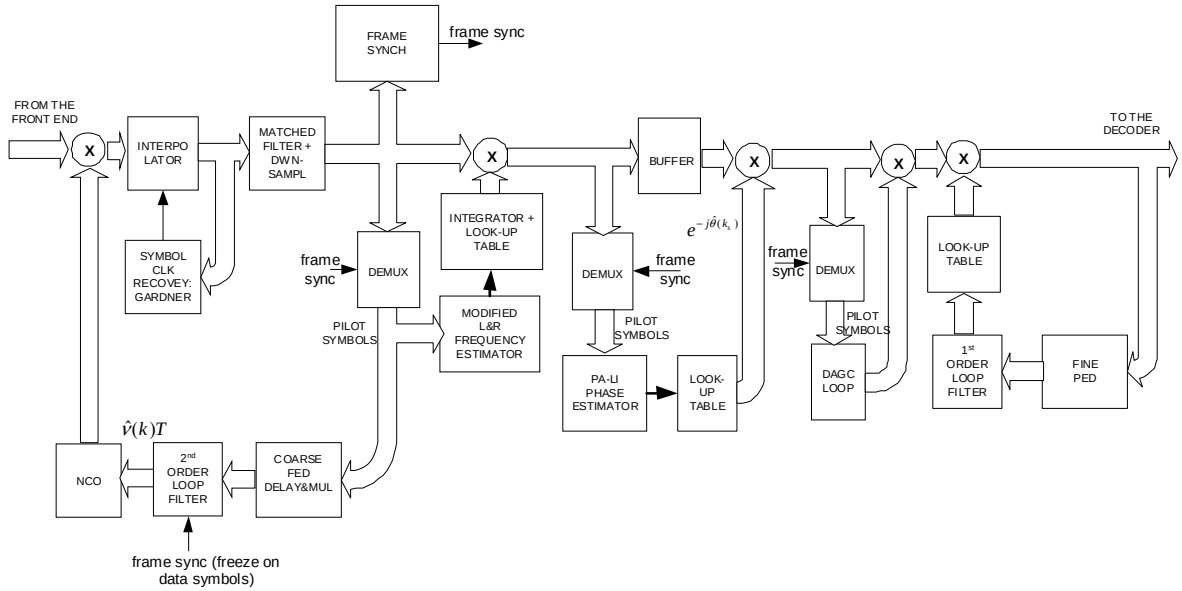

Figure C.1: Block diagram of the DVB-S2 digital demodulator

A number of synchronization sub-systems are present in the demodulator in order to coherently demodulate the received signal. They will be described in details in the next clauses but here a general overview is given. The first correction the signal receives is about the carrier frequency. The coarse frequency correction unit provides a first correction with an all-digital second-order frequency loop. The target is for a lock-in range of up to 5 MHz, which corresponds to half the minimum hypothesized symbol rate of 10 Mbaud. Then, the next block deals with clock recovery whose timing adjustment is carried out through a digital interpolator. Typically this latter can be implemented as a parabolic or cubic interpolator (4 taps) in order to limit the distortions to the minimum. Matched filtering follows, at two samples per symbol. The number of taps of this filter depends on the roll-off factor. In the simulations an impulse response that spans 20 symbol periods was assumed with no particular optimization. As it will be seen, this leads to a performance degradation of less than 0,1 dB. Then, two distinct feed-forward units perform fine frequency and phase compensation. Digital automatic gain control (DAGC) is then performed in order to adjust the level of the incoming symbols to the reference constellation and further carrier phase adjustment is carried out by a DPLL. The de-rotated symbols are finally passed to the decoder where the pilot symbols are first discarded and the channel intrinsics are computed on the data symbols.

All the synchronization units are fully pilot-aided, i.e. do not make any use of the data symbols, except for the clock recovery, the frame synchronizer and the last DPLL. This latter works on the data symbols only and its presence is required to lower the phase error RMS for high-order constellations (16 and 32APSK). The frame synchronizer uses a unique word correlator that works on symbol-by-symbol basis and feed with its final frame alignment the two demultiplexer of the demodulator.

During initial acquisition the synchronization tasks are performed with the following order:

1) Clock recovery is activated first; in fact the Gardner algorithm can work with relatively large frequency errors.

2) Once the clock recovery has converged, frame synchronization can be carried out using techniques that are relatively insensitive to the maximum specified carrier frequency error.

3) Coarse and fine carrier frequency recovery is then carried out.

4) Finally, phase recovery is performed.

The requirement of 100 ms acquisition time for channel zapping can be met down to QPSK 1/2. For lower code rates, a slightly longer convergence time is required.

In the following of the annex the key algorithms for a DVB-S2 modem are described, from signal pre-distortion techniques to combat the channel non-linear effects, to the clock and carrier synchronization algorithms and finally the digital AGC algorithm. The following notation is adopted: $z(k)$ are the samples at the signal matched filter output (SMF), $z^P(k)$'s are the $z(k)$ samples which refer to pilot symbol location within the DVB-S2 physical layer frame, $c(k)$'s are the complex information data symbols belonging to a QPSK, 8PSK, 16APSK or 32APSK constellation, $c^P(k)$'s are the pilot symbols and L_0 is the pilot symbols periodicity in number of symbols. DVB-S2 allows for inserting pilot fields of $L_p = 36$ symbols every 16 slots, i.e. $L_0 = 1\,476$ symbols in both the broadcast and unicast profile.

C.1 Modulator with Pre-Distortion

The selected Amplitude Phase Shift Keying (APSK) modulation for DVB-S2 is characterized by the fact that constellation points lie on concentric circles. This circular symmetry is particularly suited to non-linear amplification as it is easier to maintain the APSK circular constellation shape over a non-linear HPA than for classical squared Quadrature Amplitude Modulation (QAM) constellations. In [i.26] it has been shown that by proper APSK constellation parameters optimization it is possible to achieve performance that is very close or even slightly superior to QAM over AWGN channels. PSK modulation formats (QPSK and 8PSK) result to be a particular case of APSK corresponding to the case when the points are all lying on a single circumference. For 16APSK two rings of points are present with 4 points on the inner ring and 12 points on the outer ring. In the case of 32APSK three rings are present with 4 points on the inner ring, 12 points on the middle ring and 16 points on the outer ring. Over non-linear channels the APSK constellation, when observed at the demodulator symbol matched filter decimated output, is affected by two main kinds of impairment:

1) The constellation centroids (see note 1) warping due to the AM/AM and AM/PM HPA non-linear characteristic.

NOTE 1: By centroid the compilation of received constellation cluster centre of mass is considered, conditioned to each constellation point.

2) The clustering effect due to the inter-symbol interference (ISI) experienced at the demodulator matched filter output.

The warping phenomenon is responsible for the reduction of the distance among APSK rings (AM/AM compression) as well as a differential phase rotation among them (AM/PM differential phase). The ISI causing the constellation clustering is related to the demodulator SRRC filter mismatch on the received signal due to the combination of the signal band limiting introducing memory in the channel, the IMUX filter linear distortion, the HPA memoryless non-linearity, the OMUX linear filter distortions, resulting in a non-linear channel with memory.

Clearly the warping effect has no impact on single ring constellations such as QPSK and 8PSK (see note 2) but is causing important degradations for 16APSK and 32APSK. This is because the decoder log-likelihood ratios are typically computed using the "standard" APSK constellation and do not take into account the centroid locations distortion caused by the HPA. In [i.25], two kinds of pre-distortion techniques have been considered for APSK: "static" and "dynamic". The static pre-distortion technique simply consists in modifying the APSK constellation points to minimize the demodulator SMF samples centroids distance from the "wanted" reference constellation. The static pre-compensation is preferably performed off-line in the absence of AWGN once the satellite channel characteristic are known according to the following steps [i.11]:

1) Generation of a S blocks of W symbols over which the SMF centroids are computed.

2) Computation of the error signal at the end of each block.

3) Pre-distorted constellation point update.

NOTE 2: The phase and amplitude PSK distortion will be compensated for by the demodulator AGC and phase recovery sub-systems.

The static pre-distortion is able to correct for the constellation warping effects but it is not able to compensate for the clustering phenomenon.

The dynamic pre-distortion algorithm takes into account the memory of the channel conditioning the pre-distorted modulator constellation not only to the current symbol transmitted but also to the $(L-1)/2$ preceding and $(L-1)/2$ following symbols (L symbols in total). This calls for an increased look-up table size of M^L points. By exploiting the APSK constellation symmetry the amount of memory size can be reduced to $3M^L/16$ for $M = 16$ and 32.

The clustering effect reduction is obtained at the expenses of an increased outer constellation points amplitude, with two main drawbacks:

a) the augmentation of the HPA Output Back-Off (OBO) which negatively affects the overall system efficiency;

b) the possible impact on the HPA (TWTA) safe operation due to the higher peak-to-average ratio making the instantaneous signal power occasionally well beyond the saturation point.

Based on the previous considerations an improved dynamic pre-distortion approach has been devised, as illustrated in [i.11]. The quantity to minimize is in fact not the r.m.s. of the centroids conditioned to a certain data pattern but rather the total link degradation D_{TOT} given by:

$$D_{TOT}(s)[\mathrm{dB}] = \left[\frac{E_s}{N_0}\right]_{req}^{NL}(s)[\mathrm{dB}] - \left[\frac{E_s}{N_0}\right]_{req}^{AWGN}(s)[\mathrm{dB}] + OBO(s)[\mathrm{dB}] \quad \text{(C.1)}$$

being $\left[\frac{E_s}{N_0}\right]_{req}^{NL}$ and $\left[\frac{E_s}{N_0}\right]_{req}^{AWGN}$ the average symbol energy over noise density required to achieve the target Frame Error Rate (FER) in the non-linear and linear channel respectively and OBO the HPA output back-off. This approach ensures the best trade-off between ISI minimization and the OBO penalty due to the increased peak-to-average ratio caused by dynamic pre-compensation.

C.2 Clock Recovery

Symbol clock recovery can be performed first using the well-known Gardner's algorithm [i.28]. This algorithm is non-data aided and thus can be run without any frame synchronization in place. The performance of this algorithm is quite insensitive to the modulation format at least over the range of E_s/N_0 of interest as well as to a carrier frequency error up to 0,1-0,2 times the symbol rate. That means that for 25 Mbaud symbol rates, the timing recovery can work with a carrier frequency error up to 5 MHz. For lower symbol rates (down to 10 Mbaud) a possible technique is to use two timing recovery algorithms working in parallel. The first with a signal pre-rotated in frequency by +1/4 of the symbol rate (R_S) and the second with -1/4 of R_S. Then, after pre-determined time left for the transient, the algorithm that has converged can be selected. The jitter RMS of the algorithm depends on the signal roll-off factor. In particular, it worsens as the roll-off decreases. For the DVB-S2 range of roll-offs and E_s/N_0, a normalized (to the symbol rate) loop bandwidth of 5×10^{-5} seems to be required for negligible impact to the receiver performance. With this loop bandwidth and using a second order loop, a clock frequency error of 10 p.p.m. can be tracked with no residual error bias. Also, the overall acquisition transient of the timing recovery unit would be around 10^5 symbols, which corresponds to 5 ms at R_S = 25 Mbaud.

C.3 Physical Layer Frame Synchronization

C.3.0 General elements

After the receiver symbol timing has reached steady state the next step to be performed is frame synchronization by searching for the physical layer header. This can be performed even in the presence of a strong carrier frequency error through differential detection. Reference [i.12] shows that the mean acquisition time is around 20 ms for 25 Mbaud transmissions at -2 dB and less than 4 ms at 0,7 dB. At 99 % probability the acquisition time for frame synchronization is around 130 ms at -2 dB and 10 ms at 0,7 dB (see note). In case of the unicast profile exploiting ACM, until the carrier frequency and phase synchronization estimators are not in steady-state condition the physical layer frame configuration field (MODCOD) [i.8] cannot be decoded. Hence pilot locations for successive frames are determined based on PLHEADER synchronization verification at the four possible locations (one per modulation format). Once carrier phase synchronization has been established, then the position of the pilot symbols is also known (by decoding the MODCOD fields of the PLHEADERs of each physical layer frame [XFECFRAME]).

NOTE: Those acquisition times can be largely improved by using more complex frame detection schemes.

C.3.1 An algorithm for Frame Synchronization

Figure C.2 illustrates a scheme to correlate on both the SOF and PLSCODE differentially. The shift registers in the circuit can be partitioned into two sections. The first is associated with SOF, the second with PLSCODE. There are in total 57 taps associated with the 89 registers. In the first part, 25 of them are associated with the pair-wise difference of SOF. In the second part, 32 nonzero taps are associated with PLSCODE since only 32 out of the 64 differentials are known. The taps associated with the shift register for computing the correlation can be obtained as follows. First set all the registers to zero, then shift the modulated SOF and a modulated and scrambled codeword of PLSCODE into the circuit. Once the rightmost register becomes nonzero, the tap associated with a register is just the complex conjugate of the content of the corresponding register. Given that the modulated SOF and PLSCODE take only ± 1, $\pm i$, the taps only take these four possible values as well. Clearly these are trivial multiplications from the implementation point of view.

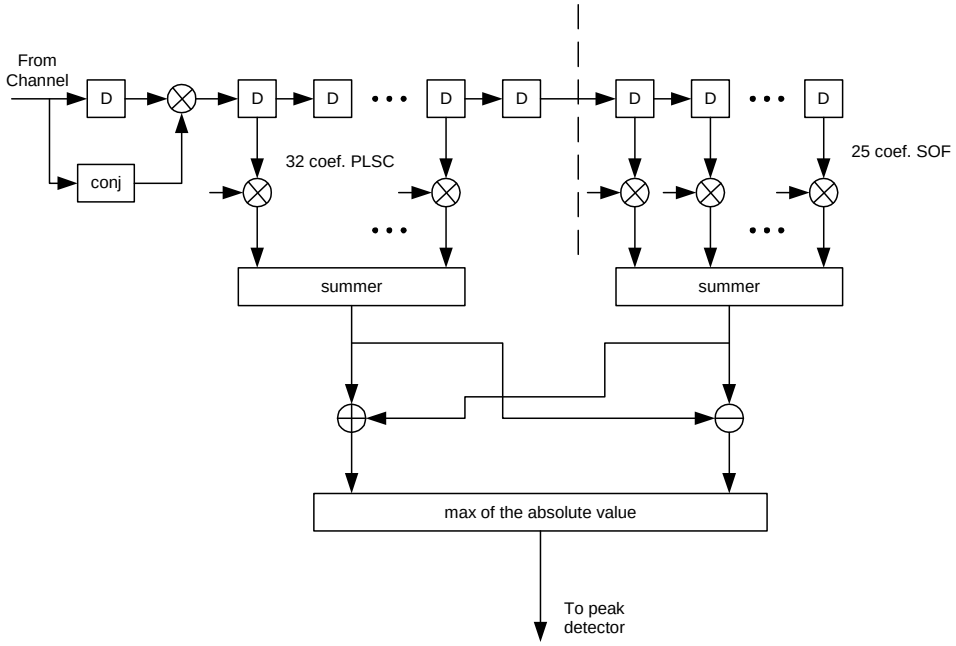

Figure C.2: Differential detection of the SOF and PLSCODE

When used for frame synchronization, the incoming signal arriving at the correlator is sampled at one sample per symbol. It is first differentially decoded and the resulting samples are then sequentially shifted into a shift register of length 89. The contents of the shift register are multiplied with the taps. The first 25 and the last 32 values at the output of the multipliers are separately summed together in two different branches. The outputs of the two summers are respectively added and subtracted to produce two values. The maximum of the absolute value out of the two branches is the final output of this correlation circuit.

The output is then further processed by a peak search algorithm. The conventional approach is to compare the output of the correlator with a predetermined threshold. If the value is larger than the threshold, it is declared that preliminary frame synchronization has been achieved. Post verification may then follow. In [i.12], an algorithm is presented for rapid search and verification.

C.3.2 An Alternative Frame Synchronization Algorithm

C.3.2.0 Introduction

When the initial frequency uncertainty is small, the acquisition of frame synchronization may use a simple finite state machine using correlators which exhibit a good probability of acquisition after a few number of physical frames. The solution described hereafter is proposed to show that an acceptable performance may be achieved for all noise levels used by the standard. This solution also has the advantage of being compatible with CCM, VCM or ACM modes, with or without pilot insertion. Tuneable parameters are also introduced in this process, in order to allow fine optimization of the acquisition, assuming specific operating conditions.

C.3.2.1 Acquisition procedure description

The acquisition of the carrier frame structure may only rely on the detection of the SOF and PLSCODE sequences in the incoming frame. The symbol rate acquisition is assumed to be already locked, the whole process may be achieved with 1 sample/symbol.

The carrier and fine frequency acquisition may not be used for frame acquisition as they often depend on the modulation which is not known before determining the PLSCODE value. Symbols are assumed to have an arbitrary phase and a small residual frequency deviation that will impact the correlator performance. The proposed procedure may be summarized as follows:

1) Unlocked state, the demodulator looks for the 26 symbols of the SOF sequence on the fly on the incoming carrier plus noise samples.

2) Tentative state, the correlation of the samples with the SOF sequence exceeds a specified threshold T_{ST} (Threshold on SOF in Tentative state), the demodulator tries to decide which PLSCODE follows on the next 64 symbols. If the maximum correlation result over the 128 PLSCODE values exceeds a second threshold T_{PT} (Threshold on PLSCODE in Tentative state), the demodulator goes in locked state, deciding when the next SOF should occur on the value of the PLSCODE. Otherwise, the demodulator remains unlocked.

3) Locked state, the demodulator tests that a SOF sequence is present at the expected position by comparing the correlation to a T_{SL} (Threshold on SOF in Locked state) value. If the threshold is not exceeded, the demodulator goes back to unlocked state.

4) Locked state, the demodulator determines the maximum correlation result with the 128 PLSCODE pattern values and compares it to a threshold T_{PL} (Threshold of PLSCODE in Locked mode). If the value exceeds the threshold, the demodulator remains in locked state and computes where the next SOF should occur, otherwise is goes unlocked.

It is described with the state machine presented in figure C.3. Using this model, the behaviour of the acquisition depends on the combination of thresholds [T_{ST}, T_{PT}, T_{SL}, T_{PL}] which determine the transition from one state to the other.

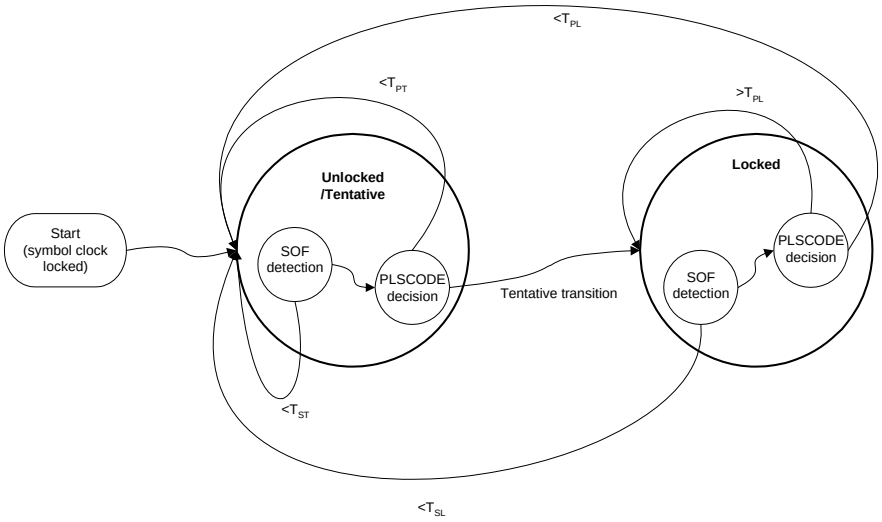

Figure C.3: Acquisition state machine

The procedure is in fact reduced to 2 states which mainly differs in the fact that correlation with SOF symbols is done "on the fly" in unlocked state when it is done at a defined location in the frame in locked state.

C.3.2.2 Performance Analysis

The performance of the procedure resides in the time needed to obtain a true locked state with a given channel, characterized by its C/N and other impairments like frequency deviation or symbol clock error. For the following analysis, only C/N is considered as frequency deviation and clock error mainly result in a reduction of the correlation energy between the received signal and the known patterns and therefore may be approximated as a corresponding increase of the Gaussian noise.

The performance analysis considers that the incoming carrier is always present as it deals with acquisition. False acquisition in the absence of carrier is out of scope. To simplify computations, the signal is assumed to be composed of random QPSK symbols separated by consistent (e.g. the number of "information" symbol corresponds to the PLHEADER code value) PLHEADER symbols. This reduction to QPSK corresponds to the C/N range assumed for worst case acquisition and is also supposed to be a worst case for false alarms as correlation of QPSK PLHEADER symbols with higher order modulations symbols exhibit a lower energy on average.

As the actual performance in terms of absolute time is largely dependent on system parameters such as symbol rate, block length, blocks distribution, the performance analysis presented here is limited to the number of PLFRAMEs required for acquisition.

Considering a given channel, the thresholds [T_{ST}, T_{PT}, T_{SL}, T_{PL}] are selected upon the following criteria:

1) Provide a low false detection probability, i.e. low probability of getting in locked state after a given number of PLFRAMEs as the demodulator is in fact not locked on frames

2) Provide a low non-detection probability, i.e. low probability of staying in unlocked state after a given number of PLFRAMEs.

The probability of exceeding, or not, the thresholds in the presence of QPSK signal and additive Gaussian noise (with one sample per symbol), has been derived from the method described in [i.30], applied to the corresponding patterns. The results are then obtained by combining those probabilities, estimated by a quasi-analytical method. Monte-Carlo simulations are on-going to verify the quasi-analytical results.

C.3.2.3 Acquisition parameters optimization

The Probability of False Alarm (PFA) and Probability of Non Detection (PND) for the transition from the unlocked state to the locked state as a function of thresholds for C/N = -2 dB are shown in figure C.4 hereafter. The values of thresholds are normalized to 1,0 (meaning all symbols are correlated).

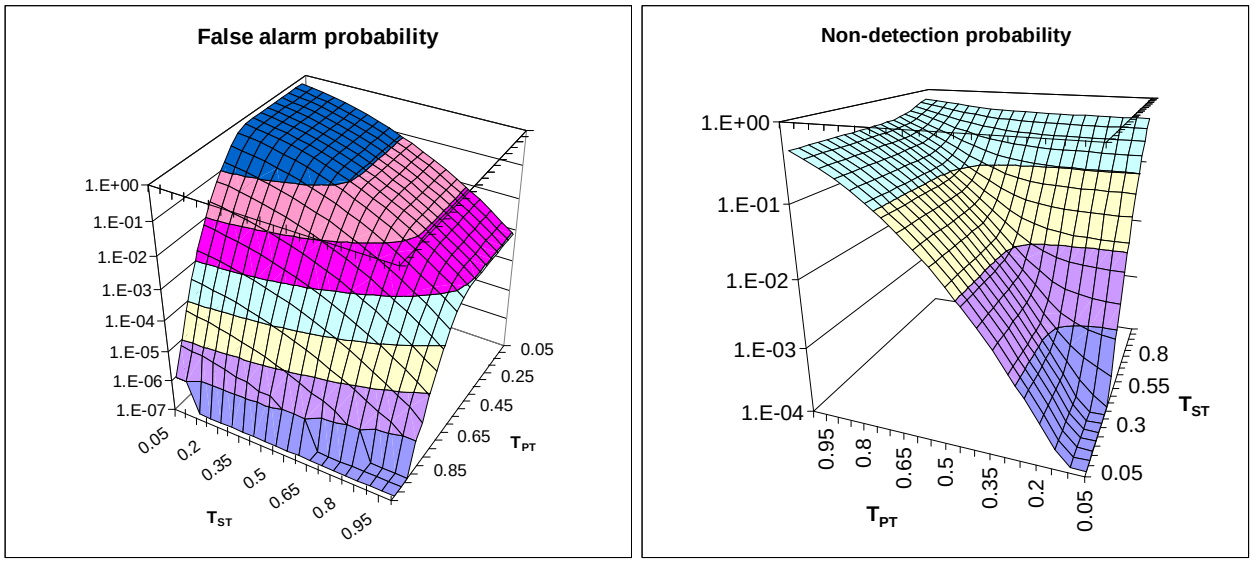

Figure C.4: PFA and PND variations with T_{PT} and T_{ST} for C/N = -2 dB

False alarm means a transition that occurred when no start of frame was present (only random symbols and noise) and non-detection means that a correct PLHEADER was present but no transition occurred. As can be seen on those charts, the threshold on PLSCODE should be higher than the one on the SOF to avoid too many unwanted transitions due to false alarm. As expected, a trade-off is required to avoid too many false alarms while preserving a low number of frames needed to achieve detection.

As the frame contains, in the worst case, nearly 1 000 times more data symbols than PLHEADER symbols, the tentative thresholds pair (T_{ST} and T_{PT}) should be selected to give a low false alarm probability even if there are many non-detections.

For the locked state, if false alarm is low due to the first transition, a higher false alarm should be accepted as it degrades fewer the overall false alarm probability of the system. Concurrently, a lower non detection rate is admitted as it guarantees that the demodulator gets locked after some frames, even with a high input noise.

Table C.1 shows the result for a possible optimization of the thresholds values (Thresholds combination [T_{ST} = 0,61, T_{PT} = 0,88, T_{SL} = 0,36, T_{PL} = 0,65]).

Table C.1: PFA and PND for optimized thresholds values

C/No [dB]	PFA	a = Number of frames for a 1E-7 PND	PND for K frames		
			K = 10	K = a	K = a+1
10	4,684 E-33	2	5,234 E-30	1,4 E-6	1,643 E-9
1	3,553 E-14	8	8,525 E-9	3,485 E-7	5,451 E-8
0	5,69 E-12	10	1,005 E-7	1,005 E-7	2,015 E-8
-1	6,763 E-10	11	9,146 E-7	2,291 E-7	5,741 E-8
-2	5,136 E -8	13	7,7 E-6	2,298 E-7	7,131 E-8

Considering the obtained results, it seems that the simple procedure presented here gives acceptable performance in terms of low detection time and low false detection probability. It should be noticed that this procedure is applicable seamless for uniform or variable coding (e.g. CCM or VCM modes) by the demodulator. A few parameters remain tuneable for specific system conditions and should be accessible for the demodulator user.

C.4 Carrier Frequency Recovery

A significant portion of DVB-S2 deployment replaced/enhanced the DVB-S users. In this situation, it is highly desirable that the outdoor equipment including the LNB is retained. Extensive simulation studies have been carried out, using the critical phase noise model of consumer LNB from ETSI EN 302 307-1 [i.2], Annex H.8, and implementing variants of three baseline carrier recovery techniques:

- decision directed digital phase locked loops with "blind" phase error detection (DD-PLL), operating on the modulated symbols;
- pilot-symbol aided DD-PLL (phase estimations extracted from the pilot symbols and from the PLHEADER are used to reset the DD-PLL circuit, which otherwise operates on the modulated symbols);
- pilot-symbol interpolation techniques (phase estimations extracted from the pilot symbols are interpolated over the modulated symbols).

With the receiver algorithms taken into consideration, the simulation results demonstrate that carrier synchronization can be achieved in presence of phase noise and worst-case thermal noise for any DVB-S2 mode. Some of the transmission modes, such as for example 8PSK rate 3/5 and rate 2/3, 16APSK rate 3/4, 32APSK 4/5 required the use of pilot symbols to avoid cycle slips. For ACM operation, the use of pilot symbols can guarantee continuous receiver synchronization.

As the carrier phase recovery unit (the linear interpolator in particular) tolerates residual normalized carrier frequency offsets up to $3{,}5 \times 10^{-4}$, the task of this unit is to bring the precision of the recovered carrier frequency down to that max value. Assuming that the frequency error is Gaussian distributed, the normalized standard deviation of the frequency jitter has to be lower than $5{,}3 \times 10^{-5}$, for a probability of exceeding the maximum value lower than 10^{-11}. For an initial maximum frequency uncertainty around ±5 MHz, which represents 20 % of the symbol rate at 25 Mbaud, Carrier frequency is acquired through a two-step procedure: coarse estimation and fine tuning/tracking.

In [i.24], a simple pilot-aided carrier recovery technique is proposed, which can perform a first coarse frequency recovery. The algorithm can be implemented in a feedback structure where a second order loop filter drives an NCO and is fed by a frequency error detector (FED) that implements the following equation:

$$e(k) = \mathrm{Im}\left\{z^{(p)}(k)c^{(p)*}(k)z^{(p)*}(k-2)c^{(p)}(k-2)\right\} \qquad \text{(C.2)}$$

where $z^{(p)}(k)$ are the signal samples at the matched filter output corresponding to the pilot symbols $c^{(p)}(k)$. The loop is active only during the pilot symbols and is frozen (i.e. the value of the frequency estimate is kept constant) during the data symbols. In [i.11], examples are given of the tracking performance of the coarse frequency synchronizer. Extensive simulations have shown that, for the worst case and with the required range of E_s/N_0, this synchronizer is able to brinweg the max value of the frequency error down to 100 kHz (which normalized to the symbol rate of 25 Mbaud corresponds to 4×10^{-3}) in about 100 ms by using a normalized loop bandwidth of 10^{-4}. Note that this coarse frequency acquisition in theory needs to be run only at system initialization when the max carrier frequency error can be as large as 5 MHz. For channel zapping in broadcast mode, as a result of a channel tuning the specified maximum short-term normalized carrier frequency uncertainty is less than ±100 kHz. Hence, in principle once the nominal acquisition time of the coarse carrier recovery unit is passed, this unit could be frozen and its NCO kept running with the last frequency estimate. However, due to very slow carrier frequency drifts, it is required to let this coarse frequency acquisition unit running also after initial acquisition but with a reduced loop bandwidth, say 10 times less.

A fine frequency estimation completes the carrier frequency acquisition process. This can be accomplished by a pilot-based feedforward algorithm derived from the L and R technique [i.29] and whose block diagram is depicted in figure C.5.

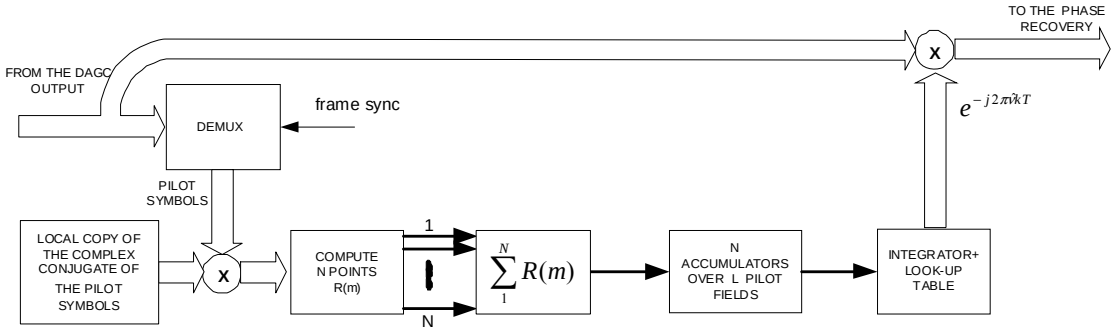

Figure C.5: Block diagram of the fine frequency estimator

The deviation from the known L and R algorithm is that here the mean N point autocorrelation function $\sum_{m=1}^{N} R(m)$ is also averaged over L consecutive pilot fields before computing the argument function. The expression of the frequency estimate thus reads:

$$\hat{\nu}T = \frac{1}{\pi(N+1)} \arg\left\{\sum_{l=1}^{L}\sum_{m=1}^{N} R_l(m)\right\} \qquad \text{(C.3)}$$

where $R_l(m)$, for $m = 1, \ldots, N$, are the N points autocorrelation vector computed over the l-th pilot symbol fields (36 symbols) [i.11]. By simulation it has been found that with $L = 1\,000$ and $N = 18$, the RMS of the residual normalized frequency error RMS is 6×10^{-5} at $E_s/N_0 = -2$ dB, $5{,}2 \times 10^{-5}$ at $E_s/N_0 = 1$ dB, $2{,}72 \times 10^{-5}$ at $E_s/N_0 = 6{,}6$ dB and $1{,}82 \times 10^{-5}$ at $E_s/N_0 = 10$ dB. Therefore, with this configuration it is guaranteed that the RMS is below the target of $5{,}3 \times 10^{-5}$ for SNRs down to about 1 dB. The acquisition time for this algorithm is 1 000 pilot fields, that is about 60 ms at 25 Mbaud. No outliers have been recorded over long simulations at SNR as low as -2 dB and with frequency error of 100 kHz. However, in this case the parameter L has to be increased to about 2 500 in order to get the required jitter RMS. Note that this algorithm can work over non-overlapped blocks of 1 000 pilot fields each.

In [i.12] an alternative frequency recovery method is described, based on a coarse frequency estimation obtained by a feed-forward algorithm that works only on the pilot symbols (referring with the term *"pilot symbols"* to both the 90-symbol PLHEADER and the aggregated pilots if any), and a fine tuning stage, where frequency estimation is achieved by another feed-forward estimator that works only on the pilot symbols in the pilot mode, or by a simple frequency estimator using both the modulated data and pilot. Unlike conventional continuous mode receivers, that usually operate continuously with no regard to the frame structure of transmit data, the new DVB-S2 receiver tracks the carrier phase of received data on a segment by segment basis like a burst mode modem. More specifically, the *segment* can be a 16-slot coded data segment in the pilot mode or a whole LDPC frame in the pilotless mode. The phase tracking loop is reinitialized with the phase estimates obtained from the pilot symbols for each segment, making its operation independent from other segments, thus, preventing any error propagation. Therefore, the block processing eliminates the impact of traditional cycle slips. From phase tracking perspective, the only difference between different modulation schemes is the phase error detector used in the phase tracking loop. The data-aided frequency estimators are independent of modulation schemes and feed-forward, thus always stable. They work very well with large frequency offset (up to 25 % of symbol rate) under extremely low SNR (as low as -2 dB). It takes the coarse frequency estimator less than 20 frames to bring the frequency offset from 25 % to less than 10^{-4} of the symbol rate, and it takes the fine frequency estimator just 1 frame to bring the frequency offset further to the range of 10^{-6} of the symbol rate, which can be very well handled by the phase tracking loop.

C.5 Automatic Gain Control

The Automatic Gain Control (AGC) represents an important demodulator sub-system. In fact, the decoder needs accurate soft information about the received symbol distance from the reference constellation points. The soft information accuracy is critically dependent on the channel estimation, i.e. symbol, clock timing, carrier phase and signal amplitude normalization. The AGC deals with the latter estimation. In DVB-S2 interactive profile the task of the AGC is complicated by the presence of a frame-by-frame variant physical layer and the wide range of SNR ($-2{,}5 < E_s/N_0 < 16$ dB). It is proposed [i.11] to use the pilot symbols exploited for the carrier phase estimation also for AGC thus adopting the data-aided version of the vector-tracker AGC (DA-VT AGC), [i.27]. This means that the AGC will only be activated in the presence of the pilot symbols and amplitude normalization frozen in between consecutive pilots. As pilot symbols are QPSK scrambled at physical layer, their constellation amplitude may in general be characterized by a different energy than the frame payload data due to the satellite HPA distortion effects. This unwanted effect can be easily removed applying the (static) pre-distortion technique to the pilot symbols too and by ensuring that the pilot symbols average energy at the HPA output is the same as the payload symbols one. Furthermore, although a DA-VT AGC has been selected, to avoid unwanted interactions with the carrier phase estimator subsystem, only the real amplitude of the complex AGC is used to normalize the signal power. A non pilot-aided AGC will need to remove the payload data by using some reliable symbol estimates to get an unbiased estimate that complicate the demodulator processing. Also in this case the modulator pre-distortion will ensure that the received constellation centroids are characterized by the same energy for all possible physical layer constellation configurations even when operating the satellite HPA close to saturation.

C.6 Carrier Phase Recovery

C.6.0 General

The carrier phase recovery unit has to cope with a residual carrier frequency error from the carrier frequency recovery unit as well as a strong phase noise. To this end, a very simple pilot-aided technique exists which provides satisfactory results at least for low order modulations (QPSK and 8PSK), while for 16 and 32APSK some extra data-tracking algorithm is needed.

C.6.1 Pilot-Aided Linear Interpolation

The pilot-aided interpolation techniques consist in deriving the phase trajectory over the data symbols by just linear interpolation of estimates performed over two consecutive pilot fields. As the symbols transmitted over the pilots are known, it is clear that the best estimator that can be used there is the Maximum Likelihood (ML) [i.24], chapter 5. Also, as the L_p is short a feedforward (FF) approach is also suggested in order to speed up the required estimation process.

The block diagram of the FF ML estimator is represented in Figure C.6 where the variables with superscript "p" indicate that the they refer to the pilot symbols.

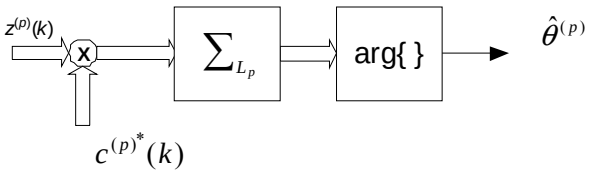

Figure C.6: FF ML Phase Estimator

The phase estimate is carried out by collecting the L_p matched filter output samples $z^p(k)$ at baud rate corresponding to the pilot fields, and performing the following algebraic operations:

$$\hat{\theta}^{(p)} = \arg\left\{ \sum_{k=0}^{L_p-1} \left[c^{(p)}(k)\right]^* z^{(p)}(k) \right\} \tag{C.4}$$

It is clear from (C.4) that just one estimate is provided every pilot field, so if the carrier phase is actually time variant due to a phase noise or an uncompensated carrier frequency error, the estimate provided will be an average of the phase evolution during the pilot field. However, if L_p is small and the phase process relatively slow, the time variation property of the carrier phase can be neglected. Under this hypothesis and with relatively high signal-to-noise ratio, it can be shown (see [i.24], chapter 5) that (C.4) can be re-written as:

$$\hat{\theta}^{(p)} \cong \theta + N_I \tag{C.5}$$

with N_I being the zero-mean Gaussian noise contribution to the phase estimate, with variance:

$$\sigma_{N_I}^2 \cong \sigma_{\hat{\theta}^{(p)}}^2 = \frac{1}{2L_p E_s / N_0} \tag{C.6}$$

which is independent from the modulation used in the pilot fields. In [i.11] it is shown that, for L_p = 36, the differences between (C.4) and (C.5) are very small down to SNR values of -6 dB. Also it is worth noting that under the assumption of ideal matched filtering (the noise samples at symbol rate at its output are white), the process consisting of the sequence of noise samples N_I relative to different pilot fields, is white, as no correlation exists between the noise in different pilots.

The linear interpolation technique makes use of the phase estimates performed over consecutive pilot fields to derive the vector of phase estimates over the data portion of the slot. In these cases, as the FF ML estimator (4) provides a phase estimate in the interval [-π, π] while the true carrier phase may grow beyond this range over a time slot period, in order to be able to consistently use the pilot-based estimates, an unwrapping technique has to be applied to these latter. This can follow the approach outlined in [i.11], [i.29] and [i.30], and depicted in figure C.7.

If the index "*l*" counts the number of pilot-based estimates, the final unwrapped pilot estimates $\hat{\theta}^{(p)}{}_f(l)$ are computed from $\hat{\theta}^{(p)}(l)$ as:

$$\hat{\theta}^{(p)}{}_f(l) = \hat{\theta}^{(p)}{}_f(l-1) + \alpha SAW\left[\hat{\theta}^{(p)}(l) - \hat{\theta}^{(p)}{}_f(l-1)\right] \tag{C.7}$$

where $SAW[\Phi] \equiv [\Phi]_{-\pi}^{+\pi}$ is a saw tooth non-linearity that reduces Φ to the interval (-π, π) and α is a parameter in the range $0 < \alpha \leq 1$, which in the following will assumed equal to 1.

It is easy to verify that equation (C.7) provides a good final unwrapped pilot phase estimate, provided the difference between the carrier phase in the current pilot field and the final estimate $\hat{\theta}^{(p)}{}_f(l-1)$ on the previous slot is less than π. If that condition is not met, it can be thought of the feedback algorithm of figure C.7 as in a cycle slip. This can be the case, for example, when as a result of a residual carrier frequency offset Δν, the carrier phase grows linearly over two consecutive pilot fields of more that π, i.e.:

$$2\pi\Delta\nu L_s T \geq \pi \Rightarrow \Delta\nu T \geq \frac{1}{2L_s} \tag{C.8}$$

where L_s is the distance between pilot fields in number of symbols, i.e. 1 476.

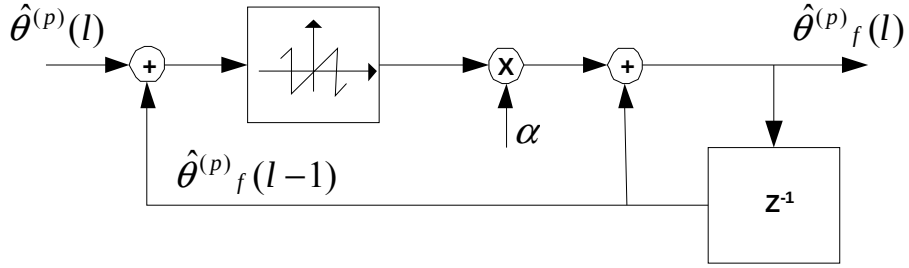

Figure C.7: The unwrapping algorithm

In [i.11] more details on the cycle slip probability of the algorithm are given.

The performance of this very simple algorithm has been assessed in terms of phase error jitter RMS in the presence of phase noise and with a normalized carrier frequency error of 10^{-4}, for 25 Mbaud transmission rate. The error RMS decreases with the E_s/N_0 value, but it tends to reach a floor at about 3 degrees for large values of E_s/N_0. This is due to the reason that even in absence of noise, the phase estimator is not able to track the phase noise trajectory within the data portion of the pilot repetition period. A more efficient technique would be to use a Wiener filter interpolation technique over the data symbols, even though the expected performance improvements do not justify the added complexity. Therefore, it is expected that for high order and more phase jitter sensitive modulations like 16APSK and 32APSK a data symbol phase tracking algorithm needs to be used to limit the performance degradation. This is addressed by the Fine Phase recovery unit which is described in the next clause.

C.6.2 Fine Phase Recovery for High Order Modulations

The best Non-data aided (NDA) algorithms found in literature for 16 and 32APSK are described in [i.26]. They consist of Q-th power close-loop NDA phase synchronizers whose block diagram is depicted in figure C.8.

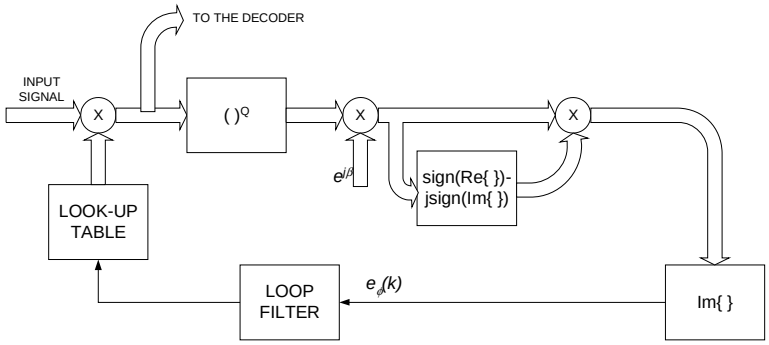

Figure C.8: Fine phase recovery unit

The corresponding phase error detector algorithm has the following form:

$$q(k) = [z(k)]^Q e^{j\beta} \tag{C.9}$$

$$e_\phi(k) = \mathrm{Im}\{q(k)(sign[\mathrm{Re}\{q(k)\}] - jsign[\mathrm{Re}\{q(k)\}])\} \tag{C.10}$$

where β is a fixed phase rotation of 0 radians for 16APSK and $\pi/4$ for 32APSK, while Q is 3 for 16APSK and 4 for 32APSK.

Raising a 4+12 APSK constellation to the 3rd power (in the complex domain), the original 4+12 APSK constellation transforms into a QPSK-like one. It is easy to see that the external ring points fall into a QPSK ring, while the internal points collapse towards the origin. Hence, a four-quadrant closed loop phase estimator can be efficiently applied to the cubic non-linearity output. Same considerations apply when raising the 32APSK constellation to the 4th, although now a $\pi/4$ phase shift is required to have the same decision zones as before. Note that most remarkable features of this algorithm are its simplicity and that it is relatively insensitive to amplitude errors due to the quadrant slicing operation involved. This would not apply to a full hard decision-directed scheme implementing the 16 and 32APSK constellation hard decision rules.

An alternative method is illustrated in [i.12].

C.7 Performance Results

This clause shows a summary of the end to end performance results for QPSK, 8PSK, 16APSK and 32APSK modulations reported in more details in [i.11]. There results concern the non-linear channel with and without pre-compensation, and with the proposed carrier synchronization algorithms in the presence or not of phase noise and the carrier frequency error. Timing is considered ideal, as the inclusion of the timing recovery algorithm within the end-to-end simulation program would have significantly slowed down the simulations. However, its impact into performance is minimal for all the modulation schemes, as long as the design guidelines outlined in clause C.3 are met.

The assumed baud rate is 25 Mbaud, which represents a realistic value for the minimum symbol rate value for the forward link of a broadband satellite transponder and the roll-off factor of the SRRC filters equals 0,35. Lower symbol rates are expected to have slightly worse performance, as the phase noise impact to the performance is higher. However, lower Baud rates are associated to professional applications for which better RF front-ends are typically used. The assumed initial carrier frequency error is 5 MHz and both the coarse and fine frequency recovery is active. The overall impact of imperfect carrier synchronization has been assessed by means of simulations. The $\Delta E_s/N_0$ degradation on AWGN channel is very small for QPSK ½ and 8PSK 2/3 (about 0,1 dB for QPSK ½ and 0,25 dB for 8PSK 2/3) even though only the linear interpolator is used as carrier recovery circuit, thus confirming that no data tracking phase recovery system is needed for these modulations. For 16APSK the loss is about 0,4 dB at BER = 10^{-7} with the fine phase DPLL running. An additional loss of 0,2 dB is paid if the fine phase DPLL is turned off. 32APSK shows a loss of about 1,05 dB at BER = 10^{-7} with an additional loss of 0,2 dB if the DPLL is deactivated. To note that for 32APSK a better phase noise mask should be adopted considering the more professional type of applications to be supported. When a phase noise mask with 3 dB reduction in power is considered and the DPLL is active, the 32APSK loss reduces to 0,3 dB. Over the time spans of the simulation runs, no cycle slip event have been recorded, thus confirming the robustness of the proposed design. Numerical results show that the distance between pilot symbol fields has been optimized for QPSK and 8PSK constellations, thus some performance degradation is paid for higher order constellations requiring higher phase tracking accuracy. For these modulations, a shorter periodicity (given the same overhead) would have been more efficient.

The simulations with the satellite channel derived for each configuration the optimal IBO and the results are summarized in table 1. In [i.11] the results for the static pre-distortion algorithm are reported in details.

As expected, results for QPSK show that the overall loss for the optimized dynamic pre-compensation amounts to 0,52 dB obtained at IBO = 0 dB. Only 0,05 dB gain is achieved using dynamic pre-distortion compared to static. However, not using the dynamic pre-compensation optimization scheme there will be a loss of 0,1 dB. In case of 8PSK, the overall loss for the optimized dynamic pre-compensation amounts to 0,6 dB obtained at IBO = 0 dB. The optimized dynamic pre-compensation loss is 0,35 dB less than static pre-compensation and 0,35 dB compared to non-optimized dynamic pre-compensation. For 16APSK the degradation for the optimized dynamic pre-distortion amounts to about 1,5 dB at IBO of 1 dB; the advantage for exploiting dynamic pre-compensation amounts to about 0,8 dB compared to static pre-compensation while the dynamic optimization brings about 0,2 dB improvement. It is worth to notice that when the dynamic optimization scheme is implemented, the total distortion curve is rather flat for IBO smaller than 1 dB. For 32APSK the total distortion for the optimized dynamic pre-distortion amounts to about 2,8 dB at IBO of 3,6 dB; the advantage for exploiting dynamic pre-compensation amounts to about 1,83 dB compared to static pre-compensation and about 3,4 dB compared to non predistorted constellations.

[i.11] reports also the probability density function (PDF) and cumulative distribution function (CDF) of the signal envelope at the modulator output for the optimized dynamic pre-compensation. The peak-to-average ratio is 5,4 dB for QPSK, 6,2 for 8PSK, 8,4 for 16APSK and 10,8 for 32APSK. Without the optimization of the dynamic pre-distortion algorithm the peak-to-average ratio would be approximately the same for QPSK while would be higher by 4,5 dB and 4,4 dB for 8PSK and 16APSK respectively.

Annex D:
Capacity assessment in ACM modes

D.0 General

Point-to-point multi-beam satellite systems based on the DVB-S standard are currently designed for link closure in the worst-case propagation and location conditions. Capacity is estimated on the basis of worst case link budgets (e.g. targeting service availability of about 99 % of the worst month, or 99,6 % of the average year).

The situation is different for DVB-S2 ACM unicast networks: in fact, the point-to-point nature of link connections allows exploiting spatial and temporal variability of end-user channel conditions for increasing average system throughput. This is achieved by adapting coding rate and modulation format (ACM) of the downlink Time Division Multiplex (TDM) frame addressed to a specific user (or a subset of users experiencing the same SNIR condition) to best match the current user link SNIR. As a consequence, the received downlink carrier bit rate is location and time dependent, while the Baud rate is instead constant to ease the frequency resource allocation. The individual users bit rate at which packets are received is dependent in a complex way from the instantaneous carrier bit rate and the resource management policy implemented at the gateway [i.13]. If a proper ACM dynamic physical layer adaptation algorithm, capable to track the instantaneous SNIR variation at the terminal is implemented, then link margins can be greatly reduced compared to a CCM system. Due to the physical layer adaptation loop latency, some physical layer threshold margin is still in order ETSI EN 302 307-1 [i.2]. In this reference a possible approach to design the ACM physical layer configuration control loop is provided. It is shown that by proper control loop design, ACM loop implementation losses can be kept reasonably small.

Assuming a fixed beam power allocation, there are several key parameters responsible for SNIR variability within the satellite coverage. Geographically dependent parameters include:

- (Multi-beam) Satellite antenna gain, non-uniform over the coverage (e.g. a difference of 5 dB could exist between the peak antenna gain, at the centre of the beam, and the edge of beam gain).
- Interference level, variable over the coverage, function of the antenna performance (beam isolation) and frequency reuse pattern (e.g. a C/I range of nearly 20 dB could exist over the coverage of a multi-beam system based on a 4-colour frequency reuse scheme and uniform power beam loading). More extreme situations can occur when, due to the non-uniform traffic loading over the coverage region, different powers and number of carriers are associated to the different beams.
- Atmospheric attenuation (mainly rain attenuation), variable, for a given availability, over the coverage due to the different climatic zone (e.g. in Ka-band over Europe, for a target availability of 99,7 %, the range of attenuation over the coverage is nearly equal to 5 dB).
- User terminal antenna gain, consequence of the different terminal antenna sizes used in the system. ACM allows to automatically match the physical layer parameters to the user terminal characteristics thus avoiding system over sizing.

Timely dependent parameters, the major of which is the atmospheric attenuation (mainly rain attenuation), i.e. the fading difference between clear sky and rain conditions (e.g. in Ka-band over Europe and for a target availability of 99,7 %, the difference between clear sky and rain fading could be up to 6 dB). It is remarked that the ST SNIR variation range is smaller than the propagation fading depth due to the co-channel interference effect. In fact, downlink co-channel interference fades with the useful signal thus smoothing the channel fading impact on the ST SNIR. This fading mitigation effect grows with the interference over thermal noise power spectral density ratio [i.17].

It is therefore apparent that the evaluation of the system capacity achievable through the use of the DVB-S2 ACM profile cannot be performed through conventional one-dimensional link budgets. The same concept of capacity for an ACM system is much less defined than for a CCM one. In fact, the physical layer throughput in each beam is in general different and time variant. The presence of geographically and timely dependent system parameters calls for a more comprehensive physical layer throughput analysis methodology, illustrated in detail in [i.17].

D.1 System Sizing Issues

The traditional system design involves fixing a priori the system throughput together with the link availability requirement to be achieved and the target service area. Based on these requirements, system sizing is then performed. System sizing involves the definition of several system aspects, the most important being the number of satellite beams for covering the service area, the on board EIRP per beam (typically defined at the Edge Of Coverage (EOC) as this represents the worst case) and the G/T requirement of STs. To avoid too much EIRP oversizing it is often accepted not to meet the link availability target in all locations in the service area. Hence the link availability requirements are often formulated as: achieving the link closure for, e.g. 99,7 % of the time for a subset of the service area corresponding to, e.g. at least 95 % of the coverage surface (the remaining 5 % of the coverage having either a lower time availability or a higher terminal antenna size).

The great advantage of ACM compared to CCM when operating at frequency bands whose link fading attenuation gets large in the presence of (heavy) rain, is that it allows to individually adapting the ST physical layer configuration (hence the SNIR modem threshold) thus maintaining the service active even under very unfavourable fading conditions. In this way the service provision to the "unlucky" active users has minimum impact on the aggregate throughput, as there is only a very small percentage of them affected at the same time by heavy fading over the satellite coverage region. Also, the long-term (e.g. yearly) system throughput statistics are very marginally impacted by fading events considering their limited time duration.

When defining the service availability, it should be kept in mind that it refers to a per-user QoS thus is also dependent on the resource management policies put in place in the system [i.13]. Concerning the service availability for the most common case of best effort service (like ADSL Internet access offer), thanks to the wide DVB-S2 operating SNIR range it will typically be equal or very close to 100 %. This is because ACM allows keeping users connected to the satellite network even under the worst link conditions with negligible impact on the other users. CCM systems will instead pay a too high cost for providing a very high availability being the physical layer configuration common to all users in the coverage region.

The minimum bit rate associated with the service availability has to be related to a per-user definition. This complicates the analysis as the user bit rate also depends on current beam carrier traffic and on the policy of the resource manager. In ACM systems the latter can counteract the effects of poor propagation conditions by allocating more resources to users in deep fading conditions (removing resources from users in clear-sky conditions, receiving a carrier bit rate much higher than in CCM systems), considering that heavy fading events are typically affecting only a limited geographical area. Reference is made to [i.13] for further discussion about this important issue.

D.2 Methodology Description

The methodology described in [i.16] consists in simultaneously simulate the link budget of thousands of Satellite Terminals (ST) dispersed over the target coverage area. For each ST location, fading attenuations are generated according to long-term statistics (one year), so that each ST can experience during the simulation all the possible propagation conditions. This allows deriving precise global and local (e.g. beam) statistics about the total system throughput as well as statistics about unavailability (both temporal and spatial) that can be used to assess if the link availability and service area targets have been achieved.

The input parameters consist in the satellite system fixed characteristic parameters as well as time and spatial varying parameters within the satellite coverage area enabling a statistical analysis: Satellite Terminal G/T characteristics, ST required $E_S/(N_0+I_0)$ for each ACM operating modes (also including the required implementation margins), TDM carrier Baud rate, Adjacent Channel Interference (for both up and down-link), Inter-system Interferences, satellite EIRP maps and G/T maps, number and position of the GWs and associated RF characteristics (max EIRP per carrier), Frequency plan, frequency reuse patterns and polarization reuse (if any), Satellite longitude and coverage area limits.

Capacity assessment is performed through the following steps:

1) Generate a sufficient number of STs distributed over the coverage area. If some zone of the coverage area is deemed more important than others (because more traffic will be likely generated in those areas), STs density might be made higher in those zones to give higher weight to performance in those areas.

2) For a given time instant, randomly generate fading at each ST and each GW. For this purpose ITU-R model for rain, gas (oxygen, water vapour) and scintillation fading can be considered. The generated random fading correctly reproduce the fading CDF (Cumulative Distribution Function) at the considered location (see note). It is to be noted that for the purpose of average capacity evaluation, the fading model is not required to reproduce the correct time and spatial correlation. In case of polarization reuse, effect of propagation on XPD should also be considered.

NOTE: Such fading will be dependent, in addition to the carrier frequency, on the station geographical location and satellite position.

3) For each ST perform a link budget (both up-link from GW to satellite and down-link from satellite to ST) taking into account the intra-system interference. The co-channel intra-system interference can be exactly computed as all parameters which influence it are known. Adjacent channel interference can be evaluated approximately assuming nominal level for adjacent carriers and the channel isolation (to be provided as input parameters for both up and down-link).

4) For each ST compare the current link budget result, i.e. the obtained $E_s/(N_0+I_0)$ with the one required by each operating mode. If the obtained value is lower than the one required for the most protected operating mode than the link is unavailable. Otherwise the link is available. The corresponding throughput can then be logged assuming to adopt the highest spectral efficient protection mode which can be supported by the obtained $E_s/(N_0+I_0)$.

5) Repeat step 2 to 4 for a sufficient number of iterations. The number of iterations required depends on the target system availability. As a rule of thumb, a number of iterations at least equal to 10 times the inverse of target unavailability should be considered (e.g. for an availability of 99,9 % of the time, the number of iterations should be larger than 10/0,001, i.e. 10 thousands).

The post-processing phase consist in the following steps:

- Compute for each ST the link availability (obtained as the ratio of the number of times the ST was available with the total number of simulation iterations).
- Compute the spatial availability by computing the percentage of STs fulfilling the required link availability target.
- Compute for each ST the average throughput, by averaging the throughput obtained at each simulation step over all the simulation iterations.
- Compute the average system throughput by averaging the aggregated throughput of all the STs during the whole simulation.

D.3 Study Case Results

The aim of this clause is to provide reference scenario examples where the gain of ACM compared to CCM has been assessed using the described methodology. This scenario, considered as a representative possible scenario of a broadband system over Europe, remains one possible system implementation. Other implementations may lead to different results even though the same general conclusions apply. However, a sensitivity analysis to some parameters is also proposed at the end of the clause.

The following assumptions have been introduced:

- Only the physical layer throughput is considered, even if the effective user throughput is also dependent on the particular radio resource management (RRM) policies implemented. While this is true also for conventional CCM systems such as DVB-S, DVB-S2 interactions with RRM is certainly more complex to assess [i.13].
- The required margin for loop control inaccuracy is not included. As the propagation conditions of a satellite link cannot be estimated and reported to the Gateway instantaneously with an absolute accuracy, a margin should be implemented in order to ensure that the received traffic is demodulated and decoded by the ST. However, it is important to mention that simulation results taking into account realistic propagation events, signalling delay and physical layer adaptation margins, show that the throughput degradation does not exceed 15 %, while the link availability is not impacted [i.14].
- No encapsulation inefficiencies of the received traffic into the DVB-S2 FEC frames are considered.

- The method assumes IBO on-board the satellite adjustable on a frame-by-frame basis according to the transmitted modulation format (the resulting different OBOs are the ones defined in table H.1.1 of DVB-S2 standard), to provide the maximum capacity that can be supported by ACM systems. A more realistic approach should be to define a single compromised OBO value that can support the different modulation formats with a small degradation in performance. As shown in [i.11], the impact to the system throughput would be negligible as a near-optimum compromised IBO value of 1,2 dB can be found for QPSK, 8PSK and 16APSK.

NOTE: Operational results indicate that for 16APSK at least 1,5 dB OBO is required.

- The system throughput has been computed assuming a uniform distribution of STs over the coverage, and equal time allocation to all STs regardless of the location of the STs (e.g. beam edge or beam centre) and regardless of the experienced fading. It implies that, for example, more traffic is provided at beam centre than at beam edge. If a uniform traffic distribution over the coverage should be considered, then the time allocation to all STs should not be uniform and should consider the location and fading of each STs. However, no major impact on the system throughput is expected due to low probability of extremely robust modes utilization (a preliminary assessment has only shown 1 % of system throughput decrease).

- As practical systems will have to support a non uniform beam loading whose distribution is going to change over the satellite lifetime, the capability of ACM to self-adapt in each location to changing interference patterns (e.g. non uniform frequency reuse patterns) is a key property. In this more practical operating conditions the ACM advantages have to be assessed on a case-by-case.

- No attempt has been done to optimize the system design when exploiting ACM. In fact, with ACM the system parameters are to be optimized following a different approach than the conventional one. Furthermore, satellite multi-beam antenna have to be designed having in mind average performance rather than worst-case figures (gain, C/I). This may also lead to simplified payload design. ACM may also help to cope with the satellite and ST antenna mispointing errors.

- Another main benefit of ACM systems with respect to CCM systems that has not been considered in the simulations is that ACM systems can take advantage of different ST antenna sizes to increase the provided throughput, which is impossible in CCM systems. It implies that an ACM system is much more scalable than a CCM system as if a user would like to increase the data rate of its link, then, it could use a bigger antenna.

As a reference system a DVB-S QPSK carrier with a coding rate equal to ¾, dimensioned for 99,7 % target link availability over 95 % of the coverage region has been used.

The reference system is based on a 40 Ka-band spot beams. The antenna pattern is a 40 Ka-band spot beams system over a European coverage (see figures D.1 and D.2). Figure D.3 shows the contour-plot of the C/I_0 (taking into account only the antenna pattern, no intra-system interference) (note that actually $C/I \sim = C/I_0 - 80$, therefore the C/I ranges from about 16 dB to 38 dB). The beam width is approximately equal to 0,6°.

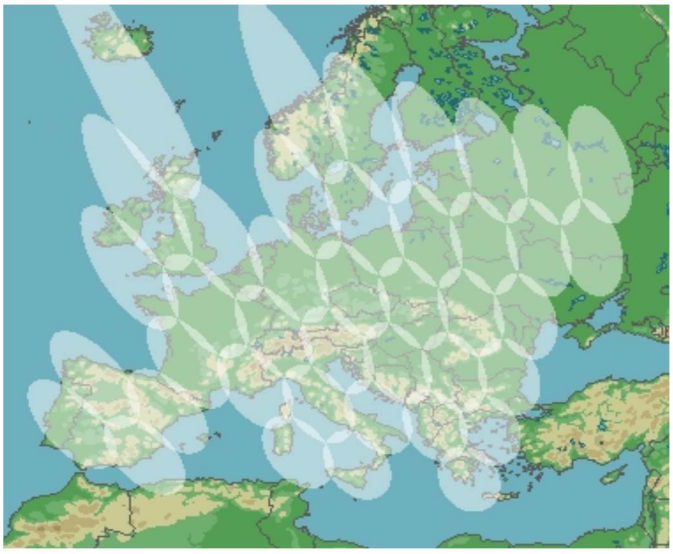

Figure D.1: 40 Ka-band spot beams spread over a typical European coverage

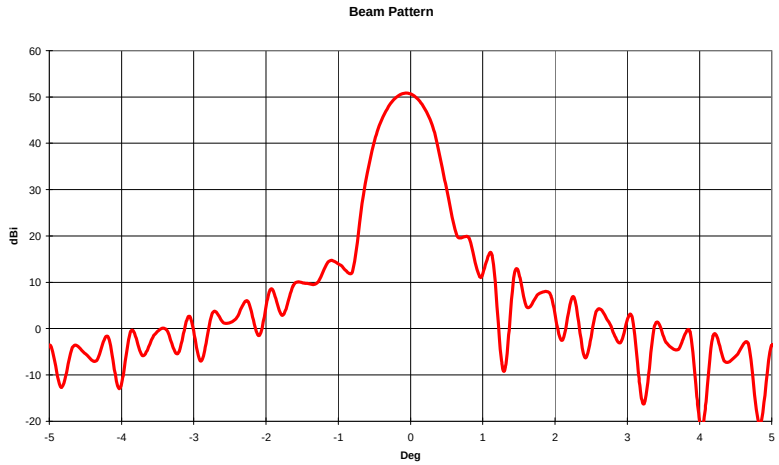

Figure D.2: u-cut of the beam Pattern for a central beam (Beam 24)

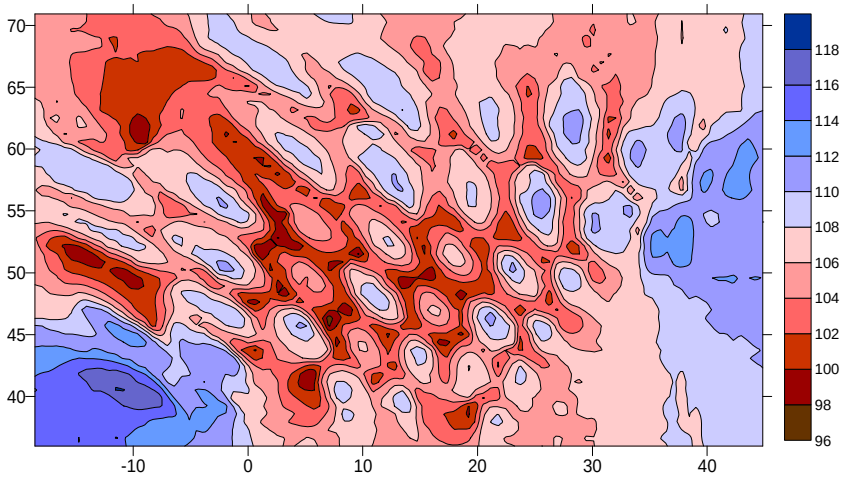

Figure D.3: Contour-plot of the C/Io for the down-link of the transparent Forward-Link scenarios

The link is divided in channels of 125 MHz bandwidth supporting one carrier of 90 Msymb/s. Only one channel is allocated per beam: a gateway transmits four channels of 125 MHz, all in the same polarization (in order to have a simple gateway RF transmit section). Therefore, the feeder link bandwidth is equal to 500 MHz (4x125 MHz in one polarization).

On-board, downlink channels are converted in frequency and transmitted to the right polarization according to the frequency plan. The user bandwidth is equal to 250 MHz (2x125 MHz in two polarizations), see figure D.4.

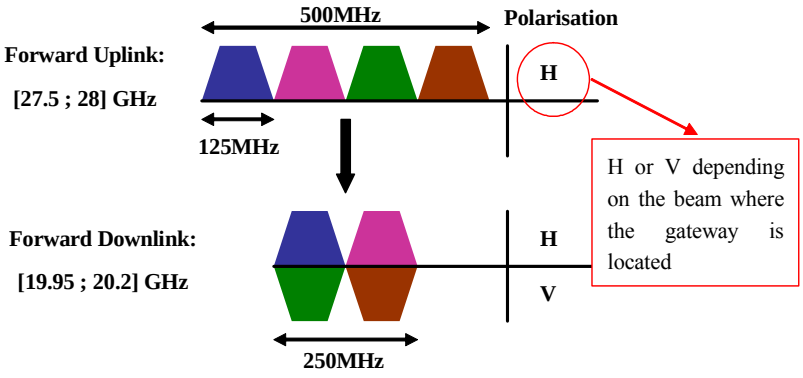

Figure D.4: Forward link frequency plan

Table D.1 lists the main system parameter values considered for the reference system scenario. The total capacity throughput of the reference system is 4,97 Gbps.

Table D.1: List of main system parameters

Carrier Rate	90 Msymbol/s
Uplink frequency	28,2 GHz
Gateway parameters	
Gateway antenna diameter	4,5 m
Gateway HPA	120 dBW
Gateway EIRP per carrier	74 dBW
Gateway NPR	21 dB
Satellite parameters	
Satellite EIRP per carrier (EOC)	60,5 dBW
OBO	0,5 dB
EOC Gain	49,5 dBi
Satellite Input Losses	3 dB
Terminal parameters	
Terminal Antenna diameter	0,75 m
Terminal G/T	16,5 dB/K
Intersystem Interferences	
Adjacent Satellite Systems	25 % (of thermal noise level)
Intra-system interferences	
Co-frequency Co-polarization (95 % of coverage)	21 dB

It should be noted that the feeder link has been dimensioned in order not to contribute significantly to the overall link budget.

The performances of DVB-S2 physical layer considered in the simulations are summarized in table D.2.

Table D.2: modulation and coding schemes and required E_s/N_0 considered in the simulations

Mode	Spectral efficiency including all overhead [bit/s/Hz]	Required E_s/N_0 [dB]
QPSK 1/4	0,357	-1,5
QPSK 1/3	0,616	-0,3
QPSK 2/5	0,745	0,6
QPSK 1/2	0,831	1,9
QPSK 3/5	1,132	3,1
QPSK 2/3	1,261	4,0
QPSK 3/4	1,390	4,9
QPSK 4/5	1,476	5,6
QPSK 5/6	1,562	6,1
QPSK 8/9	1,691	7,1
8PSK 2/3	1,885	7,8
8PSK 3/4	2,078	9,1
8PSK 5/6	2,335	10,5
16APSK 3/4	2,762	11,5
16APSK 4/5	2,933	12,3
16APSK 5/6	3,104	12,9

The above performances correspond to short FEC frame, considering dynamic pre-distortion, implementation margin and channel degradations derived from [i.11]. The efficiency refers to all DVB-S2 framing overhead including pilot symbol insertion.

In addition the output power back off (OBO) at the optimum operating point for the different modulation schemes have been considered in the link budget [i.11]. Dynamic pre-distortion has been assumed at the optimum IBO value while both synchronization jitter-induced and modem implementation losses have been taken into account.

The $Es/(N_0+I_0)$ value relative to the target link and space availability lead for the DVB-S2 CCM system to 8PSK modulation format and 2/3 coding rate. The short FEC frame has been considered (without pilot symbols). The total system throughput is equal to 6,92 Gbit/sec, which implies a capacity increase of 39 % with respect to the DVB-S system.

To ease the comparison with the reference system, the ACM performance has first been computed assuming the same system parameters. The DVB-S2 ACM system could experience both higher availability and throughput than the DVB-S2 CCM system. The higher availability is guaranteed by the utilization of spectral efficiencies lower then 8PSK 2/3 when in presence of deep fade events, provided the minimum required user bit rate is met. The higher throughput results by using high spectral efficiency modes in clear sky conditions.

Using the tool previously described, the following modulation and coding histogram has been obtained.

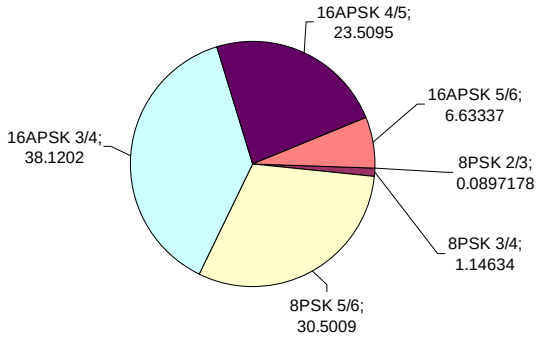

Figure D.5: Distribution of modulation and coding usage

The spectral efficiencies lower than 8PSK 2/3 are very rarely used (not even shown in the pie-diagram of figure D.5) by the ACM system, but they allow to increase the link availability to 99,9 % for a space availability of 98 %. A total average system throughput of 9,66 Gbit/sec is achieved, which means a capacity increase of 40 % with respect to the DVB-S2 CCM system and 94 % versus DVB-S. It should be noted that in the current example the 32APSK modulation is never used.

The gain of the ACM system heavily depends on system parameters. If the target link availability is changed to 99,8 % (instead of 99,7 %) for QPSK modulation and ½ coding rate (instead of 8PSK 2/3) over 95 % of the coverage and the satellite EIRP per carrier is equal to 57,8 dBW EOC (instead of 60,5 dBW, adjusted in order to satisfy this new required operating point), the total system throughput for DVB-S2 CCM mode is in this case equal to 2,99 Gbit/sec (instead of 6,92 Gbit/sec). the assessment method indicates that the usage of lower spectral efficiencies allows to improve the system availability but do not have impact on the system throughput. The total average system throughput of the ACM system is equal to 8,65 Gbit/sec, implying a capacity increase of 190 % with respect to the DVB-S2 based CCM system.

This result shows that:

- If the reference system has been sized for a just slightly higher availability (99,8 % instead of 99,7 %), then the potential gain of ACM is greatly increased. The reason is that high availability means system capability to cope with deep fading: important link margins should be put in place for CCM to provide the required service availability. The satellite RF power used for static margins is completely wasted as for the large majority of the time the users will experience higher SNIR that what required by the demodulator. ACM instead can exploit the available SNIR at any time implying a significant increase of average throughput.

  Similar conclusions would apply when considering larger space availabilities.

- While the satellite EIRP is decreased by 46 %, the average throughput of the ACM system is only decreased by 10,5 % (the gain of ACM system with respect to the CCM system is higher in the second system scenario than in the first one, but the absolute capacity is lower). The main reason is that the higher the spectral efficiency of the modulation and coding scheme, the lower the power efficiency (due to the impact of the flattening of the capacity curve at high value of SNIR).

If the system does not implement all the modulation and coding schemes of the DVB-S2 standard, then the efficiency of the system is somewhat impacted. For example, referring to the system considered in the last example, if only the following modulation and coding schemes are implemented: QPSK ½, QPSK 2/3, QPSK 5/6, 8PSK ¾, 16APSK 4/5, then the total average system throughput is equal to 7,53 Gbit/sec, which implies a decrease of 13 % with respect to the implementation of all modulation and coding schemes. In this case, the ACM capacity increase is equal to 152 % with respect to CCM system. If the selection could be optimized, the impact on the capacity could be decreased. For example, if the following modulation and coding schemes are selected: QPSK ½, 8PSK 2/3, 8PSK ¾, 8PSK 5/6 and 16APSK ¾, then the capacity decrease is only 0,3 %.

It means that the ACM system is not very sensitive to the number of modulation and coding schemes implemented (i.e. the step between the different required $Es/(N_0+I_0)$) if the range is kept identical. The implemented physical layer configurations can be optimized to best fit the SNIR simulated distribution, and depend on the particular system sizing.

Other simulations have been run in order to assess the impact of implementing only QPSK and 8PSK modulations. The results are shown in figure D.6 for the reference system with scaled satellite HPA power and with full power.

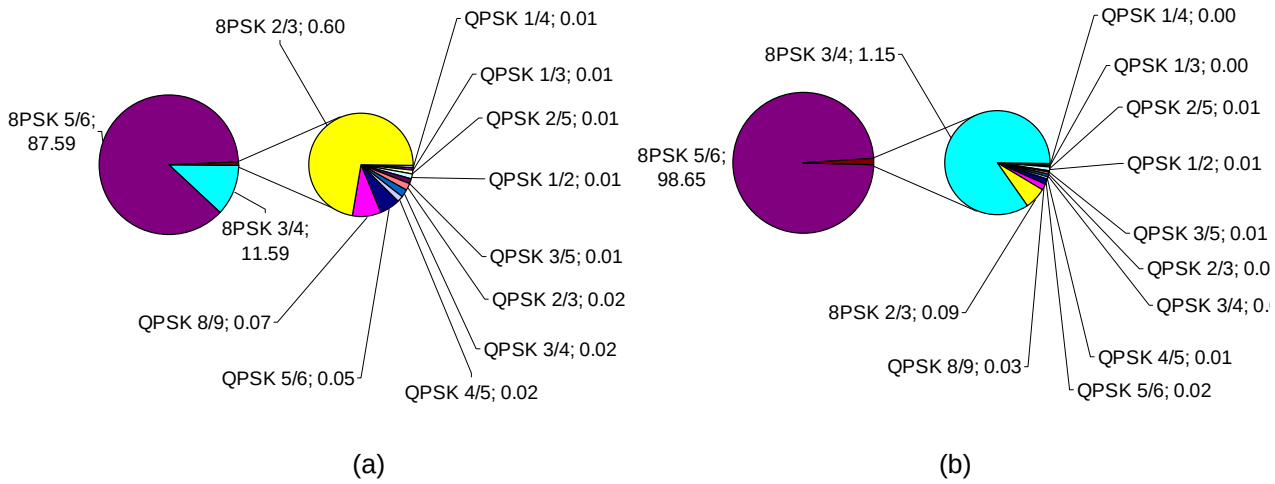

Figure D.6: Distribution of Modulation and coding usage for the reference system (a) with reduced satellite HPA EIRP (57,8 dBW satellite EIRP EOC) and (b) with full power (60,5 dBW satellite EIRP EOC) implementing only QPSK and 8PSK

For the case of figure D.6(a) the throughput is now 8,30 Gbit/sec to be compared with 8,65 Gbit/sec when all the modulations are supported (here are however considered all QPSK modes down to rate 1/4 whilst before the lowest mode was QPSK 1/2 but this should not impact the throughput in a significant way).

The throughput for the case of figure D.6(b) is 8,40594 Gbit/sec which should be compared with 9,66 Gbit/sec when the whole set of modulations are supported (figure D.5). Now the loss is more significant due to the higher use of 16APSK modes.

The previous results show that the impact of supporting only QPSK and 8PSK modulations may be significant (about 15 % for the system of figure D.6(b)) depending on the particular system sizing.

In CCM systems the satellite multibeam antenna is typically specified through its minimum performance over the coverage region (or a subset of it) in terms of gain and C/I. This is because the CCM physical layer is dimensioned on the worst-case location for the worst-case time of the year. Thus, knowing the satellite RF power limitations the antenna design should ensure that the CCM physical layer efficiency is acceptable for the worst-case location. For ACM instead, the average antenna performance has more relevance than the worst-case. This is because as for the fading attenuation, worst-case C/I's or gain variations, if limited in area extension, may be accommodated by the ACM intrinsic adaptability with minimum impact on the overall throughput performance. This is an essential issue as it allows to:

- Relaxing the multibeam antenna design in terms of minimum C/I for example reducing the number of feeds required/beam in a multi-feed/beam (AFR) antenna architecture. This has the advantage of simplifying the payload RF front-end and at the same time easing the introduction of digital processors with DBFN.
- Increasing the beam overlap to one side reduce the gain ripple within the beam while reducing the antenna mispointing errors impact.

Accept variable frequency reuse over the system coverage region to cope with uneven traffic distributions.

Those features are considered pivotal for designing very efficient broadband satellite networks. The capacity gain factor of ACM systems with respect to CCM systems is not impacted by the number of beams assumed in the coverage, meaning that the absolute ACM capacity increase gets significantly higher for systems with a large number of beams.

Simulation tests have been carried out for system study cases with different number of beams, from 60 up to 205 beams. Results show that the ratio between the average ACM system spectral efficiency and the correspondent CCM efficiency remains the same regardless of the number of beams. This makes the ACM system capacity increase with the number of beams noticeably higher than the one of the CCM system. In the particular study case considered, the increase in terms of absolute capacity from 60 to 205 beams of ACM systems corresponds to 3 times the one of CCM systems. Considering the sensitivity of the ACM gain to the number of beams, simulation results show that the capacity improvement achieved by ACM system over conventional systems moves from 10 Gbit/sec (60 beams) up to 30 Gbit/sec (206 beams).

Additional parameters directly impacting system throughput are frequency and polarization reuse. Simulation results show that for ACM systems an additional gain of about 50 % can be obtained by the use of the two polarizations. The utilization of a more pushed frequency reuse pattern 1:3 can bring with respect to a more conventional 1:4 frequency reuse pattern a gain of about 15 %.

Annex E:
Physical layer adaptation in ACM systems

E.0 Introduction

In annex D the benefits of ACM systems over non-adaptive systems have been shown. However, results have been obtained considering ideal channel estimation and physical layer adaptation. In order to fully exploit the potential advantage of physical layer adaptation, there is the need for devising efficient techniques for accurately estimating the satellite channel and consequently adapting the transmission parameters with minimum capacity loss, while keeping under control the link outage probability. In the following some results are reported from [i.14] about a possible way to implement physical layer adaptation for ACM systems. For notation simplicity it is assumed that the pilot symbols used for the channel estimation are concentrated at the beginning of each slot of the frame. To be remarked that in the numerical example provided the frame parameters are not in line with the DVB-S2 ones.

E.1 Channel estimator

Various channel estimator algorithms have been investigated for our application. The SNORE channel estimator algorithm, originally devised by NASA for deep-space missions [i.19], has been recently shown to be derived from maximum-likelihood (ML) estimation theory [i.32]. In figure E.1, the block diagram of the selected channel estimator algorithm is reported.

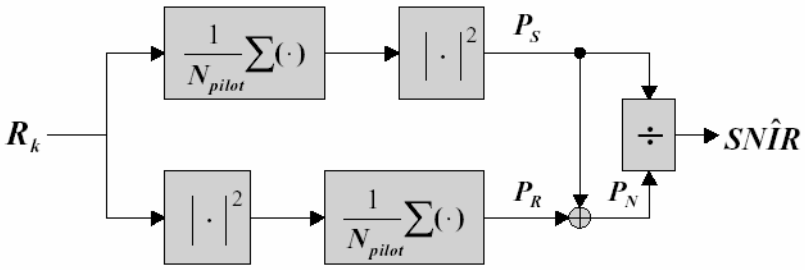

Figure E.1: SNORE channel estimator functional block diagram

As discussed in [i.19], the SNORE algorithm can work in *data-aided* (DA) or *decision-directed* (DD) operating mode. In any case, the SNORE estimator does not rely on the AGC correct operation for SNIR estimation. In case of QPSK modulation, the latter scheme suffers from an important estimation bias for values of the chip (see note) energy over the noise plus interference power ratio E_c/N_t lower than 8 dB. This problem is even more pronounced for higher order modulation schemes. The DA version is instead bias-free until very low E_c/N_t < -20 dB. The pilot presence allows to use the DA version of the SNORE algorithm operating on the periodic pilot time slots and has therefore been selected for our application. The pilot [E_c/N_t] can be generically expressed as:

$$\frac{E_c}{N_t} = \frac{P_S}{P_{N_t}} \tag{E.1}$$

where P_S represents the pilot sequence transmitted power and P_{Nt} represents all noise plus interference received power. The useful signal power at time $t_k = kT_{\text{slot}}$ can be estimated as:

$$\hat{P}_S[k] = \left\{ \frac{1}{2N_p W} \sum_{l=0}^{W-1} \sum_{m=1+(k-l-1)N_{slot}}^{(k-l-1)N_{slot}+N_p} [r_p(m) d_p(|m|_{N_{slot}}) + r_q(m) d_q(|m|_{N_{slot}})] \right\}^2 \tag{E.2}$$

where $r_p(m)$ and $r_q(m)$ correspond to the in phase and quadrature pilot component samples at the chip matched filter output after carrier phase error removal at time $t_m = mT_c$, and $d_p(m)$ and $d_q(m)$ constitute the original pilot spreading sequence. The operator $|\ |_N$ corresponds to the modulo N operator and N_{slot} to the slot duration. The integer $W \geq 1$ represents the number of pilot slots coherent averaging and it is upper bounded by the fading bandwidth to be tracked (f_c). In practical implementations the sliding window can be replaced by a simpler IIR type of filter. The SNORE estimation time T_{est} can be computed as $T_{est} = N_{slot}\, W/R_c$ and the condition $T_{est} << 1/f_c$ has to be verified.

NOTE: By chip it is intended here the elementary channel signalling duration. The name chip is used as the channel symbols do not necessarily contain coded information bits (e.g. pilot symbols) and are scrambled by pseudo-random sequences.

The total received power, P_R, can be expressed as follows:

$$\hat{P}_R[k] = \frac{1}{2N_p W} \sum_{l=0}^{W-1} \sum_{m=1+(k-l-1)N_{slot}}^{(k-l-1)N_{slot}+N_p} \left\{ r_q^2(m) + r_q^2(m) \right\} \tag{E.3}$$

The noise plus interference power estimate is then derived as:

$$\hat{P}_{N_t}[k] = \hat{P}_R[k] - \hat{P}_S[k] \tag{E.4}$$

and the estimate $\left[\frac{\hat{E}_c}{N_t}\right][k]$ is given by:

$$\left[\frac{\hat{E}_c}{N_t}\right][k] = \frac{\hat{P}_S[k]}{\hat{P}_{N_t}[k]} \tag{E.5}$$

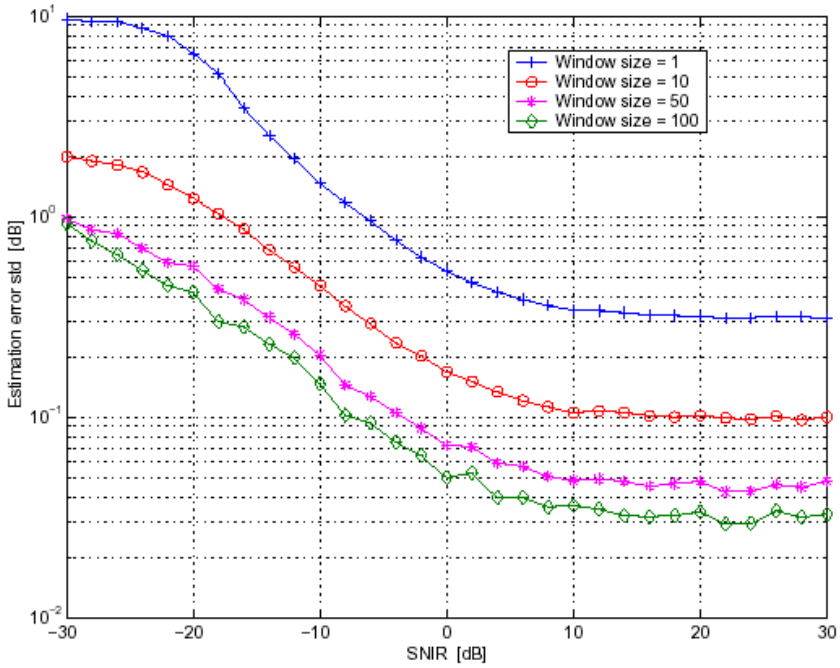

Figure E.2: SNORE channel estimator simulated standard deviation: N_p = 202, N_{slot} = 2 204 chips

Figure E.2 shows the simulated estimation error standard deviation for various averaging factors W when N_p = 192 and N_{slot} = 2 204 which corresponds to a pilot overhead of about 9 %. It appears that $W \geq 10$ is required to achieve an acceptable estimation error standard deviation (e.g. less than 0,1 dB). As shown before the upper limit on W is determined by the maximum fade dynamic the estimator is able to track. In general, the pilot overhead selection is driven by the phase error estimation requirements rather than the channel estimation accuracy.

It can also be observed that in order to achieve a standard deviation of the estimated SNIR error less than 0,2 dB over the DVB-S2 SNIR range [-3 to 15 dB] Np = 128 and W = 50 are required. According to the current frame and overhead assumptions there will be 2 pilot symbols every 90 symbols. Thus the DA-SNORE estimation time at 25 Mbaud corresponds to:

$$T_{est} = \frac{1}{R_s}\left(\frac{N_p^{slot} + N_{symb}^{slot}}{N_p^{slot}}\right)N_p^{SNORE}W = \frac{1}{25\cdot 10^6}\left(\frac{2+90}{2}\right)128\times 50 = 11{,}8\ \text{ms} \qquad \text{(E.6)}$$

Which is still acceptable considering that it should be able to cope with channel variations of 0,5 dB/s (e.g. only 0,005 dB/10 ms) for which the dominating control loop delay is due to the GEO satellite propagation time. Assuming that the channel is quasi-stationary over the SNORE estimation time, the SNORE will use pilot samples corrected by the phase estimator that can be coherently combined also if spaced by hundreds of symbols.

Other estimators relying on the demodulator AGC capability of keeping the total noise plus interference plus useful signal power constant showed less attractive performance as the estimated SNIR standard deviation showed a symmetrical behaviour around the 0 dB point. This means that the SNIR is growing for both SNIR $\rightarrow$ -∞ and $\rightarrow$ +∞. This unwanted property together with the estimator accuracy dependency on the real AGC errors let us opt for the SNORE DA estimator scheme.

E.2 Physical Layer Selector

E.2.0 General

The physical layer configuration selector contained in the user terminal estimates at any time the optimal physical layer configuration. To guarantee reliable and efficient system operation, the physical layer selector accounts for:

a) SNIR estimation errors;

b) Propagation delay and possible channel variations occurring between the user request and the updated physical layer.

Concerning point a) it is assumed that following clause E.1, the SNIR errors are unbiased and distributed according to a Gaussian distribution with variance depending on the actual SNIR, the pilot duration and the averaging window. Those dependencies can be formulated as:

$$\frac{\hat{E}_c}{N_t} \cong N\left(\frac{E_c}{N_t}, \sigma_s^2\left(\frac{E_c}{N_t}, N_p, W\right)\right) \qquad \text{(E.7)}$$

where $N(\cdot)$ represents a Gaussian process with mean and variance E_c/N_t and $\sigma_s^2\left(\frac{E_c}{N_t}, N_p, W\right)$ respectively.

Related to point b), it is observed that the GEO orbit assumption suffers from a large propagation delay (see note 1). In the following selector algorithm derivation, supported by experimental evidence reported in [i.14], it is assumed that the atmospherical attenuation is a slow fading process compared to the satellite propagation delay, thus $[E_c/N_t][k] \cong [E_c/N_t][k\text{-}2D]$. Under this hypothesis, the main contribution to the channel estimation error is related to the channel estimation algorithm.

NOTE 1: For GEO bent-pipe satellites the round-trip time, D, is about 250 ms.

Denoting $F_l[t_k]$ and $\hat{F}_l[t_k]$ the discrete physical layer configurations associated with the true and the estimated value of E_c/N_t at time $t_k = kT_{slot}$, respectively, the two following unwanted events are possible:

If $F_l[t_k] > \hat{F}_l[t_{k-2D}]$ $\rightarrow$**Slot efficiency loss event**

If $F_l[t_k] < \hat{F}_l[t_{k-2D}]$ $\rightarrow$**Slot payload loss event**

where the *Slot efficiency loss event* corresponds to the event that the available link capacity has not been exploited in the current time slot. The *Slot payload loss event* is associated to the event that the received slot payload will be not correctly decoded (see note 2). It is apparent that, while the first event is causing a capacity reduction, the second one will affect the ST Frame Error Rate (FER) and has to be accurately controlled. In Figure E.3-a and -b, a graphical explanation of the phenomena mentioned above can be found.

NOTE 2: For any physical layer configuration $F_l[t_k]$ the payload is assumed to be lost if $[E_c/N_t][k] < [E_c/N_t]_{req}(F_l[t_k])$.

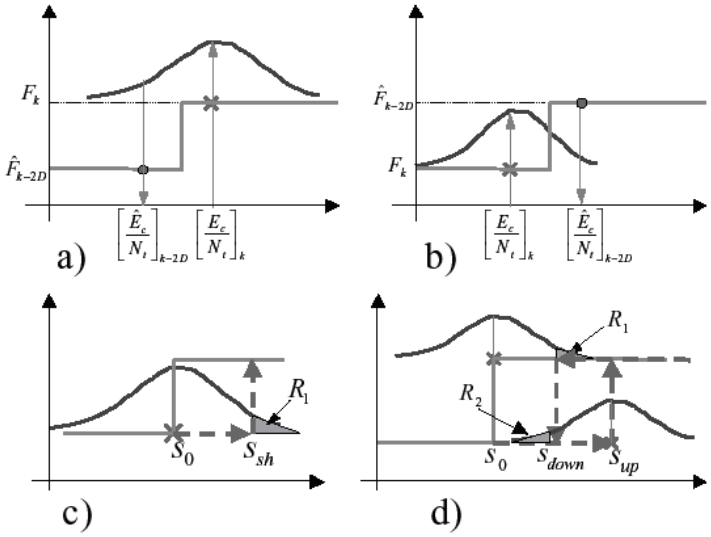

Figure E.3: a) Slot efficiency loss event - b) Slot payload loss event - c) Shifted threshold technique- d) Hysteresis technique

The ideal physical layer configuration dependency on $[E_c/N_t]$ is indicated by a step function. The cross represents the current true SNIR $[E_c/N_t][k]$ and the estimator Gaussian-like $[E_c/N_t]$ pdf is super imposed. The dot represents the estimated $[\hat{E}_c/N_t][k - 2D]$. In case a), as the estimated value is lower than the true one, a slot efficiency loss event will occur. On the contrary, in case b) the estimation is higher than the true value, thus a more efficient physical layer is associated to the current channel condition. In this case a slot payload loss event will occur. In the following, two possible techniques to control the two above unwanted effects are proposed. It has to be underlined that any technique aiming at the *slot payload loss event* reduction will increase the *slot efficiency loss event*.

E.2.1 Shifted Threshold

The first countermeasure to ST demodulator channel estimation errors is to shift to the right the physical layer configuration threshold to guarantee that $\Pr\{\hat{F}_{l[tk-2D]} > F_{l[tk]}\} < R_1$. This conditioned probability can be derived as follows:

$$\Pr\left\{\left[\frac{\hat{E}_c}{N_t}\right][k-2D] > S_{sh} \middle| \left[\frac{E_c}{N_t}\right][k] \le S_0\right\} \le R_1 \qquad \text{(E.8)}$$

where S_{sh} and S_0 represent the new shifted threshold and the original threshold value, respectively and R_1 represents the required slot error rate.

Recalling the assumed short-term channel invariance and Gaussian E_c/N_t estimator error from the last expression the new value of the *Shifted Threshold* can be derived as follow:

$$\Pr\left\{\left[\frac{\hat{E}_c}{N_t}\right][k-2D] < S_{sh} \middle| \left[\frac{E_c}{N_t}\right][k] = S_0\right\} = 1 - R_1 = 1 - Q\left(\frac{S_{sh} - S_0}{\sigma_s(S_0)}\right) \quad \text{(E.9)}$$

from which:

$$S_{sh} = S_0 + \sigma_s(S_0)\, Q^{-1}\,(R_1)$$

The graphical representation of this approach is reported in figure E.3-c. The computation has to be repeated for each possible physical layer transition as σ_s is dependent on the E_c/N_t corresponding to the threshold level.

E.2.2 Hysteresis

The shifted threshold technique allows to control the probability of *slot payload loss event*. However, let assume as working point a value close to one of the shifted thresholds computed according to the previous procedure. Due to the channel estimator random errors the SNIR value will be jittering around its true value that is close to S_{sh}. Thus the ST physical layer will often ping-pong between the two adjacent physical layer configurations causing a large amount of unwanted reverse link signalling. Nevertheless, the shifted threshold approach will keep the probability of slot payload loss below the design value R_1.

The problem described above can be mitigated by introducing a second threshold and operating the switch through an hysteresis cycle according to the graphical representation of figure E.3(d) The up and down thresholds indicated with S_{up} and S_{down} are derived as follows:

The **down-threshold** is related to the constraint to limit the *slot payload loss event*:

$$\Pr\left\{\left[\frac{\hat{E}_c}{N_t}\right][k-2D] > S_{down} \middle| \left[\frac{E_c}{N_t}\right][k] \le S_0\right\} \le R_1 \quad \text{(E.10)}$$

The **up-threshold** is related to the purpose of reducing the amount of reverse link signalling:

$$\Pr\left\{\left[\frac{\hat{E}_c}{N_t}\right][k-2D] \le S_{down} \middle| \left[\frac{E_c}{N_t}\right][k] \ge S_{up}\right\} \le R_2 \quad \text{(E.11)}$$

Adopting the same logic of the *shifted threshold* computation, the hysteresis thresholds can be derived:

$$S_{down} = S_0 + \sigma_s\, Q^{-1}\,(R_1) \quad \text{(E.12)}$$

$$S_{up} = S_{down} + \sigma_s\, Q^{-1}\,(R_2) \quad \text{(E.13)}$$

For all the cases where $S_{down} < E_c/N_t < S_{up}$ the decision on the physical layer configuration to use will be based on the slope of two consecutive E_c/N_t estimates. If the slope sign is positive the S_{up} threshold will be applied. Vice versa in case the slope is negative, the S_{down} threshold applies. Two considerations are in order. First, the hysteresis reduces further the *packet loss event*. Second, a severe constraint on the reverse link signalling reduction further increases the *efficiency loss event*.

E.3 Performance results

In [i.14] the proposed channel estimation and physical layer adaptation for the downlink of a broadband multibeam satellite system has been deeply investigated. An overall system model able to accurately represent the ACM system physical layer adaptation has been devised. The simulator is capable of reproducing the useful and other beams interference signals, channel fading impairments, channel estimation and physical layer selection. Particular attention has been devoted to the modelling of the other beam interference and the fading channel. The latter has been implemented by means of a time domain simulator representative of experimental results for both fading amplitude and spectral characteristics.

The DA-SNORE channel estimator has been proposed for tracking typical Ka-band channel variations with enough accuracy to drive the physical layer selector. For this unit the simple threshold design approach has been complemented by a more practical solution exploiting shifted threshold and hysteresis that allows to control the outage probability due to the estimator errors and to limit the reverse link signalling.

The performance of the proposed solution has been verified resorting to a realistic Ka-band multi-beam study case. Simulation results for optimized algorithm parameters indicate that for both heavy and light fading conditions, effective physical layer adaptation can be achieved with acceptable losses compared to the ideal system. The technique proposed although investigated for systems at Ka-band can be easily adapted to other frequency bands such as Ku and Q/V-band.

A DVB-S2 test-bed with ACM has been developed to run extensive tests in a laboratory environment [i.15], and subsequently over satellite link [i.16]. The main characteristics of the forward link are as follows:

- 10 Mbaud DVB-S2 carrier with 25 % roll-off, normal frame size (64 800 bits), pilot symbols activated.
- Number of MODCOD activated for ACM: 22 (full DVB-S2 set excluding 6 sub-optimal MODCOD at overlap between modulations) or 4 (reduced set maximizing spectral efficiency, based on statistical results of multi-dimensional link budget simulations).
- IP traffic: web browsing, file transfer, video streaming, voice, telnet, background traffic, coupled with 3 different quality of service (signalling, high priority and best effort).

The MODCOD thresholds have been set based on the characterization of the demodulator performance under stable conditions, adding on top satellite channel margins and ACM margins. ACM margins account for possible variations of C/(N+I) as perceived by the demodulator during the ACM loop time (1 second). The two main contributors to variations are the atmospheric conditions in Ka-band and the demodulator C/(N+I) measurement inaccuracy (following a Gaussian distribution). ACM decision for changing MODCOD depends on the up or down threshold being crossed.

It is important to calibrate the ACM margins properly, in order to avoid outage events (i.e. uncorrectable frames due to being C/(N+I) lower than MODCOD threshold) while being spectrally efficient (i.e. keeping MODCOD as high as possible). The ACM loop response time needs to be short enough to be able to track accommodate C/(N+I) variations due to fading with acceptable margins. Considering that the maximum fade slope corresponding to heavy rain events at Ka-band does not normally exceed 0,5 dB/s, a - 1 second ACM loop updating time is usually considered achievable sufficient. To be remarked that there is no need to send continuous ACM control commands. Rather one can limit the associated signalling by sending ACM MODCOD change requests only when the user terminals observe a C/(N+I) change exceeding a certain MODCOD threshold (i.e. 0,3 dB). In order to limit the number of MODCOD changes, an offset of 0,3 dB has been added on the up threshold compared to the down threshold, resulting in a hysteresis effect.

When analysing the synthetically generated time series of an extreme fading case as the one reported in (figure E.4), it is observed that the C/(N+I) up and down variations across 1 second intervals are correlated with the C/(N+I) values. In other words C/(N+I) is jittering less in clear sky conditions than that under bad weather conditions. This suggests than margins can be individually optimized per MODCOD selecting larger faded conditions margins to better cope with the increased C/(N+I) speed of variation. To be remarked that by doing so the impact on the system capacity is very reduced being the deep fading event spatially and time limited while the probability of loosing packets due to the ACM reduced adaptation speed is minimized.

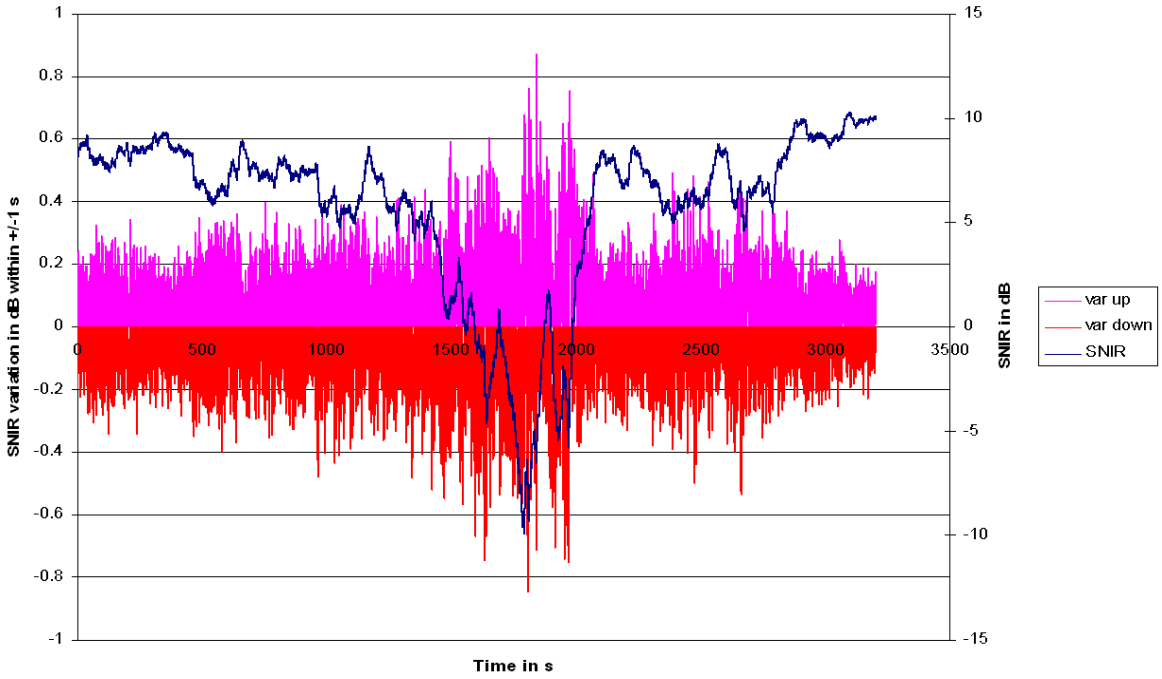

Figure E.4: Example of simulated Ka-band "extreme fading" event C/(N+I) time series and C/(N+I) variation in one second of simulated Ka-band "extreme fading" event

Figure E.5 illustrates the laboratory measured behaviour exploiting the ACM test bed described in [i.15] of the ACM loop under a "deep fading" time zoomed event. After an initial period of relatively stable conditions, where a few MODCOD transitions occur, the fading event begins and C/(N+I) drops sharply and the MODCODs changes quickly down to the most robust MODCOD corresponding to QPSK r = 1/4. Conditions become even worse during the 17th minute, where the link is lost. C/(N+I) then globally improves with up and down variations, and the link is eventually back to the initial conditions. During the fading event, the ACM loop correctly adapts to the link both on up and down transitions. No outage event occurs until, in that C/(N+I) remains is always above MODCOD threshold. The demodulator unlocks when C/(N+I) is below -2 dB, which should be considered as part of the link unavailability (i.e. the beyond 99.9% domain).

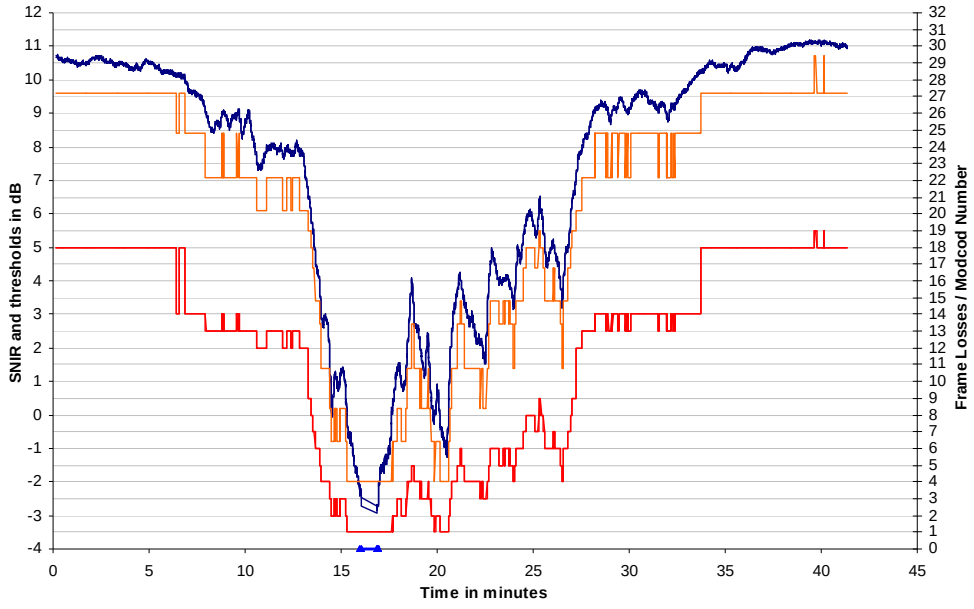

Legend: Top blue curve correspond to the current= C/(N+I) value in dB, bottom red curve corresponds to the= MODCOD number, middle orange curve = corresponds to the ACM ing threshold in dB.

Figure E.5: ACM loop adaptation to a deep fading event

Different strategies detailed in [i.15] have been tested and compared for setting the ACM margins:

- Fixed margin: all MODCODs use the same margin for handling variations of SNIR on a 1 second period. The ACM loop with fixed margin works correctly, although spectral efficiency is not optimal.
- Variable margin: each MODCOD has a different margin, which optimizes the ACM loop and spectral efficiency (approximately +10 % compared to fixed margin). The margin can be calibrated for each MODCOD.
- Adaptive margin: consists of reducing the ACM margin progressively until a frame is lost. Adaptive margin gives a further gain in efficiency, while bursts of packets may be lost because of the slow margin adaptation loop characteristics. The resulting PLR ranges from 1E-3 to 1E-2, depending on the number of MODCODs and the fading severity. This performance may be acceptable for certain types of UDP applications which are usually tolerant against packet losses, but not for all types of applications. The adaptive algorithm could be improved with a better channel estimator for the distance to QEF - based for instance on the number of bits corrected by the LDPC decoder - and making sure that the selected MODCOD threshold is always higher than channel SNIR.

Fixed margins: identical for all MODCOD;

Variable margins: calibrated per MODCOD;

Adaptive margins: margin reduced until an error event occurs, then reset.

ACM performance tests have been run in a laboratory environment on the combination of different time series (5 fading events ranging from "clear sky" to "deep fading", simulated from a representative Ka-band 100-beam satellite system over European coverage detailed in [i.15]), MODCOD set (basic or reduced) and ACM margins (3 types). It was found that spectral efficiency is primarily a function of the type of event, and secondly of the MODCOD set and type of ACM margin (see figure E.6). A fixed margin per MODCOD significantly reduces the overall performance as the most common MODCODs corresponding to clear sky conditions are "forced" to use the same extended margins as the MODCODs used for guaranteeing availability under fast changing channel conditions corresponding to fading events., Thus as discussed before, so it is worth calibrating the ACM margin per MODCOD. With fixed and variable margins, assuming they are correctly calibrated, no outage event is encountered. With adaptive margins, frame errors appear when the ACM threshold becomes lower than the CCM threshold. This effect could be limited by an early reaction when approaching the zero link margin by means of better the estimation of the distance of the FEC decoder to QEF and by putting a low limit on the threshold. Link availability is equal to 100 % for the 3 first types of fading events tested. It is around 99,85 % for the extreme and deep fading events, because C/(N+I)_for a short period becomes lower than QPSK r = 1/4 MODCOD threshold.

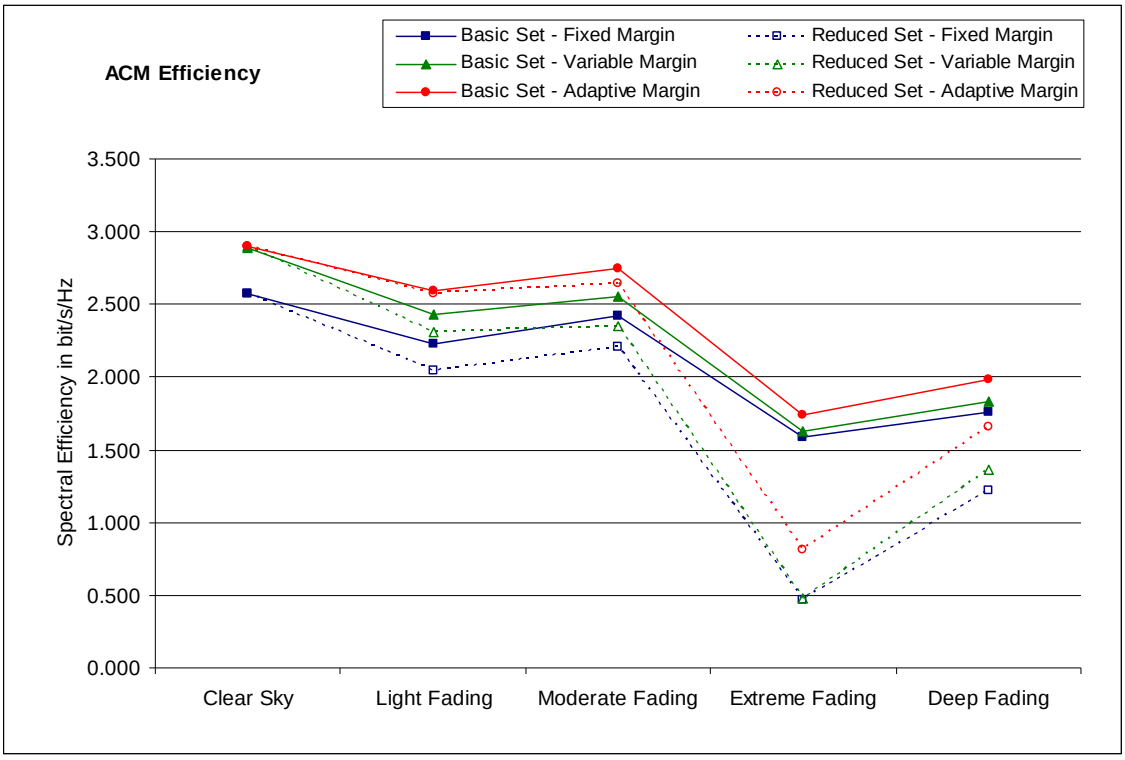

Figure E.6: Spectral efficiency in bit/s/Hz

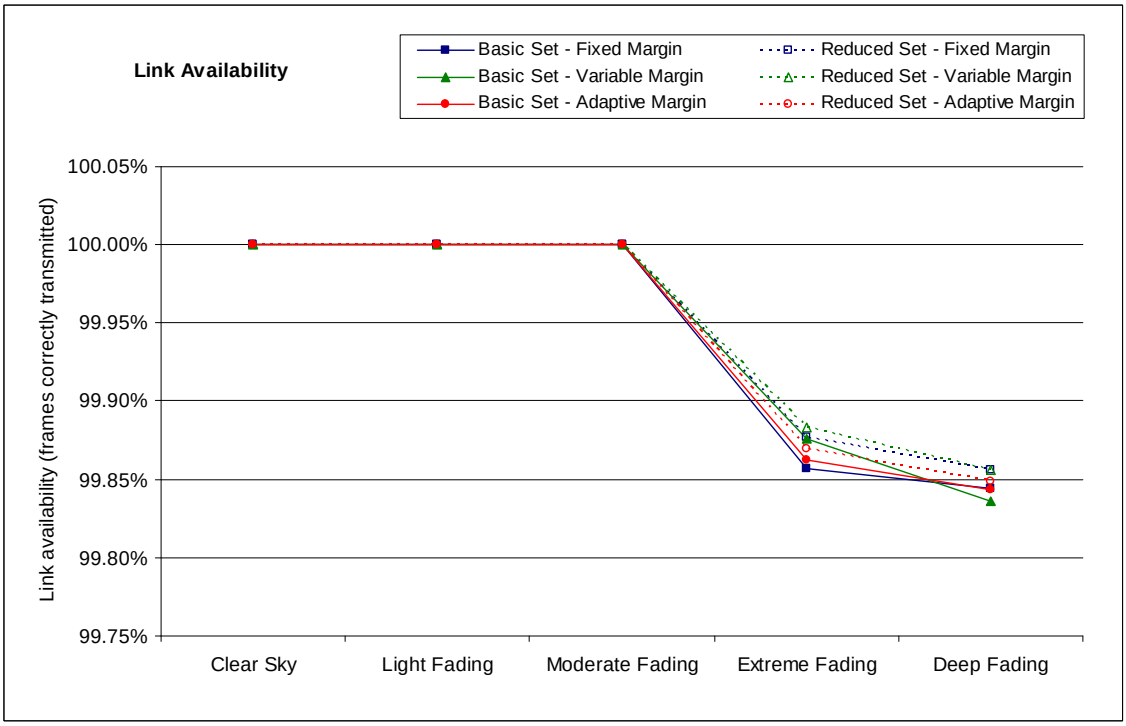

Figure E.7: Link availability

The main results obtained are summarized below. The spectral efficiencies have been calculated as a weighted average of the 5 discrete fading events of one hour each: Clear Sky: 50 %, Light Fading: 30 %, Moderate Fading: 18 %, Extreme Fading: 1,9 % and Deep Fading: 0,1 %. It is noted that the results naturally depend on the system scenario simulated and its multiple parameters, and it is not easy to extrapolate to yearly performance based on short samples.

- With 22 MODCOD activated and variable ACM margins, under clear sky conditions, no frame loss occurs and the gain of spectral efficiency is equal to +130 % compared to CCM MODCOD 7 (corresponding to 99,9 % availability) and to +53 % compared to CCM MODCOD 12 (99,7 % availability).
- Compared to an ideal ACM loop which would react immediately and without any up/down margin/hysteresis, the measured loss of efficiency of ACM implementation with variable margin is 2,4 %.
- The measured loss of efficiency when quantizing the number of MODCOD from 22 to 4 is between 3 % and 5 %.

With fixed and variable margins, frame error rate due to ACM outage event is below 10^{-7}, which demonstrates that the ACM margins are correctly set. With adaptive margins, spectral efficiency increases by 3 to 5 %, at the cost of a higher frame error rate - such use could be justified if the above communication layers are tolerant to sporadic errors.

The performance of applications together with the variable link capacity due to ACM has also been assessed. Under normal circumstances, the ACM loop adapts to the quality of link and can sustain the data rate required by the applications for each terminal. In this case the available capacity is sufficient and the link is error free at IP level (no traffic packet loss, no impact on end-to-end delay and jitter). Congestion may occur when the forward link capacity is globally insufficient to serve the aggregated demands from the terminals. Another issue could be that, for a given terminal, the MODCOD spectral efficiency multiplied by the symbol rate is lower than the required data rate – ACM directly limits capacity. In such congested events, where demand is higher than capacity, throughput delay increases due to saturation of the transmit queues and packets are eventually lost. The effects depend on the transport layer protocol: UDP packet losses directly impact the applications, while TCP retransmission mechanisms minimize the impact on applications. It was observed that most Internet applications are usually tolerant to variable capacity links, and therefore adapt correctly to capacity variations caused by ACM. Also, the gateway resource allocation systems are usually able to handle congestion. The novelty introduced with ACM is the variability of the capacity per terminal and globally. The use of QoS mechanisms, which have been tested together with ACM, allow to transmit high priority traffic in a reliable way, while lower priority traffic can cope with delay increase or packet losses.

The tests performed by satellite have verified the behaviour and performance of ACM in real environment, confirming previous assessment performed in laboratory. As an example figure E.9, a deep fading Ku-band event has been encountered on the 2nd of July 2008 at 2.30 PM. Weather conditions (see figure E.8) have been described by the local weather office as "storm with thunder, heavy rain and water accumulating on ground". Wind was moving from west to east, i.e. in perpendicular direction of the satellite link, at about 20 km/h. The SNIR time series and associated MODCODs for the two sites (Rambouillet (RMB) near Paris also acting as uplink station and Toulouse (TLS)) are shown in figure E.9.

It is important to note that, since the gateway and terminals in Rambouillet are co-localized, the fading event impacts both to the uplink and on the downlink. A correlation is clearly observed between Rambouillet and Toulouse small antennas, by comparing the SNIR curves, which means that the feeder link is impacted by the fading event. Because satellite transponder ALC was deactivated (fixed gain mode), uplink power level variations impacted the downlink through the amplifier AM/AM response.

Toulouse terminal is only impacted by the fading event on the uplink, the downlink being under better and more stable link conditions.

When considering the satellite environment and the multiple-terminal aspect, it is emphasized that:

The ACM margins have to accommodate scintillation effects, which oscillatfluctuations are usually faster than the ACM loop response time, as well as possible variations of the signal level through the satellite channel. Such effects should not be neglected otherwise ACM margins could be insufficient and outage events may occur.

C/(N+I) values and its variations are location dependent, due in particular to different satellite EIRP and terminal dish pointing, possibly also due to different types of terminals being used. One approach for the ACM margins is to consider a single worst case value on the coverage. Another approach is to customize ACM margins per terminal, in a pre-determined way (geographical pattern) or automated way (self-calibrated terminals).

The optimization of the TWTA operating point in the case of ACM is more complex than in the case of CCM, because non-linear degradations are modulation dependent. In order to maximize the system efficiency globally, it is necessary to take into account the expected C/(N+I) distribution and corresponding MODCOD, and to optimize the TWTA operating point for the most commonly used frequent MODCODs. This way, the relative loss of efficiency for the other MODCODs remains marginal.

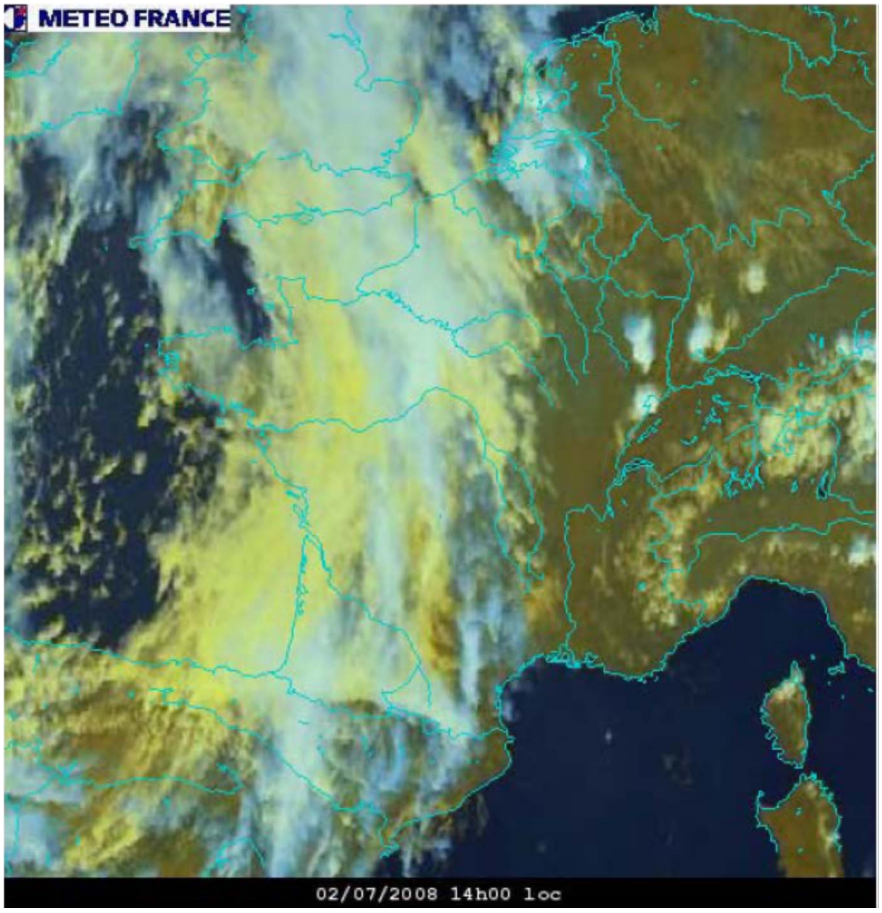

Figure E.8: Satellite weather image of the storm event observed on July 2, 2008 and reported in figure E.9

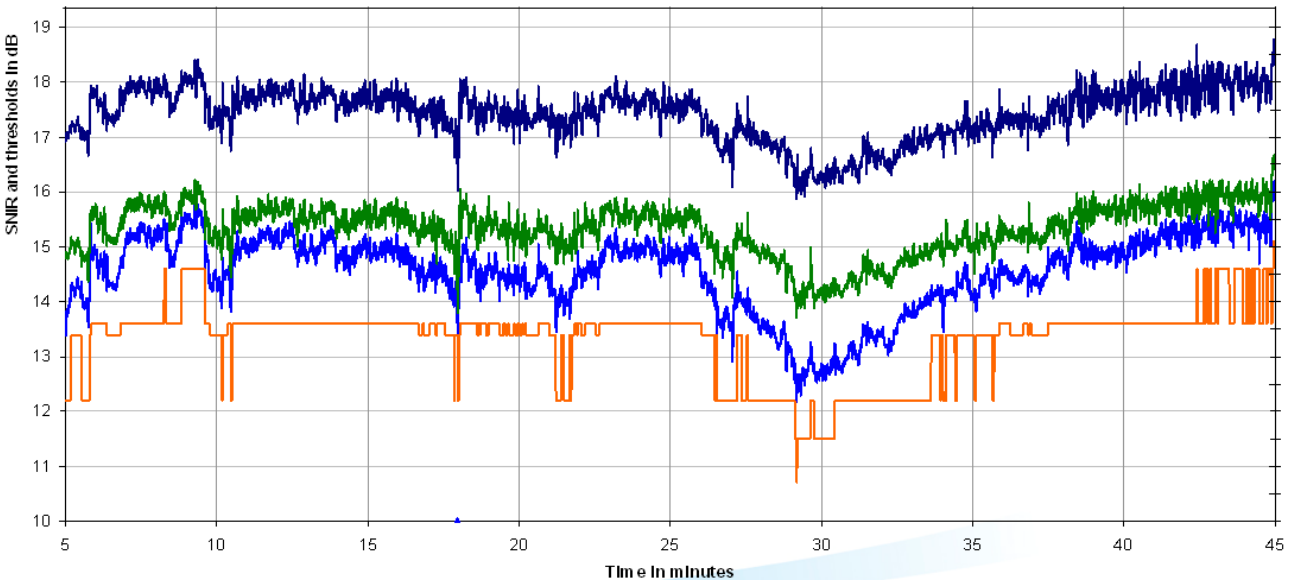

NOTE: Dark blue and green curves represent the SNIR observed in Rambouillet with the large and small antenna respectively. The light blue curve represents the observed SNIR in Toulouse with a small size terminal antenna. The orange curve represents the MODCOD threshold levels for the demodulator which C/(N+I) is drawn in light blue.

Figure E.9: Example of the SNIR impact of Ku-band a storm event as perceived by 3 terminals operating at Ku-band and the consequent ACM MODCOD selection and impact on ACM loop

When considering the satellite environment and the multiple-terminal aspect, it is emphasized that:

- The ACM margins have to accommodate scintillation effects, which fluctuations are usually faster than the ACM loop response time, as well as possible variations of the signal level through the satellite channel. Such effects should not be neglected otherwise ACM margins could be insufficient and outage events may occur.

- C/(N+I) values and its variations are location dependent, due in particular to different satellite EIRP and terminal dish pointing, possibly also due to different types of terminals being used. One approach for the ACM margins is to consider a single worst case value on the coverage. Another approach is to customize ACM margins per terminal, in a pre-determined way (geographical pattern) or automated way (self-calibrated terminals).

- The optimization of the TWTA operating point in the case of ACM is more complex than in the case of CCM, because non-linear degradations are modulation dependent. In order to maximize the system efficiency globally, it is necessary to take into account the expected C/(N+I) distribution and corresponding MODCOD, and to optimize the TWTA operating point for the most commonly used MODCODs. This way, the relative loss of efficiency for the other MODCODs remains marginal.

In conclusion, ACM has is showing very promising performances for the next generation of satellite broadband systems like Ka-band multi-beam. The system capacity and availability are greatly improved compared to static systems.
The performance of the ACM loop has been extensively verified in laboratory and by satellite. The important elements to consider are the accuracy of the demodulator Es/N0 measurements, the ACM loop response time, the ACM margins, and handling of variable capacity links by the gateway.

Annex F:
ACM receiver implementation

F.0 General

In the following two receiver schemes are proposed to regenerate the Transport Stream clock R'_{TS} under dynamic rate variations.

F.1 Type 1 receiver

With reference to figure F.1, R'_{TS} is regenerated via a PLL which maintains constant, in the steady state, the receiver FIFO buffer filling condition (the Empty/Full E/F signal is in steady state when the buffer is halfway filled up).
The DVB-S2 receiver, after receiving a useful packet (UP) and storing it in the FIFO buffer, reads the DNP field, and inserts DNP null-packets in front of it. The NCO (Numerically Controlled Oscillator) is driven by the E/F signal via a low pass filter (LPF), and generates a steady state frequency R'_{TS} locked to R_{TS} (clock at the transmitting side), independently of the source bit-rate. During the source rate transient the situation is different. As shown in figure F.1, a step in $D_{TX}+D_{RX1}$ (delay increase produced by a bit rate reduction) is immediately absorbed by the FIFO buffer (since the NCO frequency variation is very slow), which starts to empty up. When the PLL reacts to the rate reduction, R'_{TS} slightly slows down till the buffer recovers the halfway filling condition, and R'_{TS} may return to the steady-state R_{TS} condition. After the transient, the end-to-end delay of the TS is increased by ΔD (in fact, in steady state, the reception buffer delay is constant by definition).

Therefore Type 1 receiver does not guarantee the "constant delay" and "constant bit rate" conditions for Transport Streams, although, by increasing the PLL time constants, rate variations may be smoothed.

This analysis has driven the design of a DVB-S2 subsystem called "input stream synchronizer", allowing the implementation of a "type 2" receiver not affected by delay and bit-rate variations.

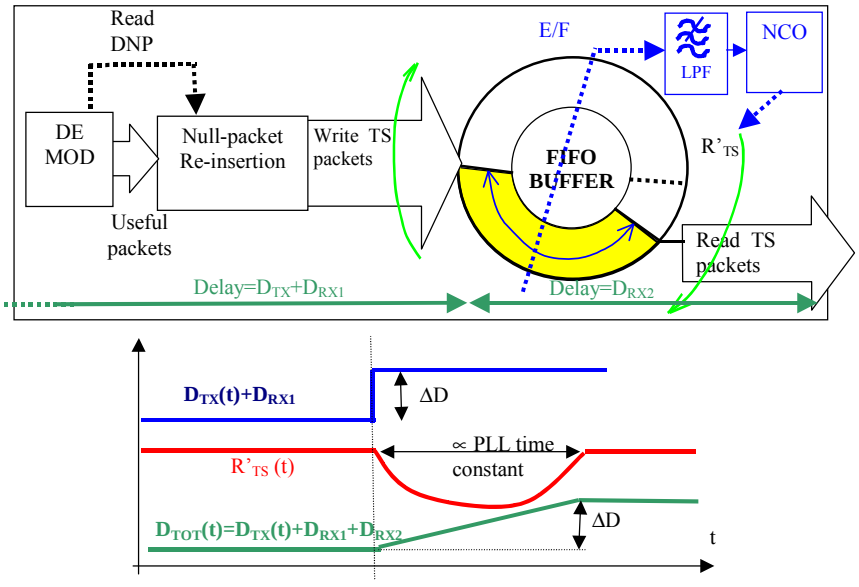

Figure F.1: Example Type 1 Receiver: delay and bit-rate variations at the receiving buffer input and output

F.2 Type 2 receiver

With reference to Figures F.2 and F.3, R'_{TS} is directly locked to the transmission R_{TS}, by introducing a "time-stamp" mechanism using the symbol-rate R_S as a common frequency reference (R_S is recovered by the receiver and is not affected by the packet delay variations). In this way the reception FIFO buffer filling condition can change and automatically compensate the chain delay variations, provided it is sufficiently large and suitably initialized to avoid overflows/underflows. Figure F.2 shows the principle scheme of the input stream synchronizer (transmitting and receiving side): in the modulator, a counter runs at speed R_S, and its content (ISCR field, Input Stream Clock Reference) is appended to each TS packet as soon as it crosses the input interface, before null-packet deletion. In the receiver, a similar counter runs at R_S speed (R_S is generated by the clock recovery subsystem), and its content is compared to that of the ISCR field of the packets when they are read out of the FIFO buffer to feed the demultiplexer. The R'_{TS} clock is generated by a PLL, which is driven by the phase error between the local counter and the transmitted ISCR. Figure F.3 gives some receiver details: since the reception FIFO buffer is not self-balancing as in the Type 1 receiver, the initial receiver FIFO buffer state may be reset by the transmitter via the BUFSTAT field. Furthermore the maximum receiver buffer size assumed by the transmitter may be signalled to the receiver (BUFS field), in order to minimize end-to-end delay when required.

For a Type 2 receiver the "constant delay" and "constant bit rate" conditions for Transport Streams are met, at the cost of a slightly increased complexity and a capacity loss of about 1 to 1,5 % for the transmission of ISCRs (2 or 3 bytes are appended to each TS packet). More information can be found in [i.15].

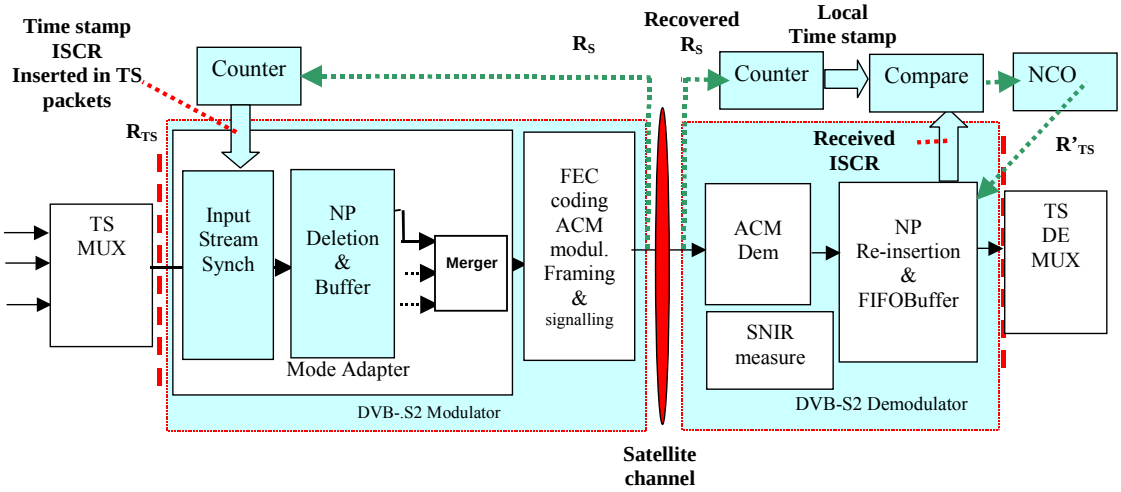

Figure F.2: ACM DVB-S2 model using time stamps to lock RTS and R'TS

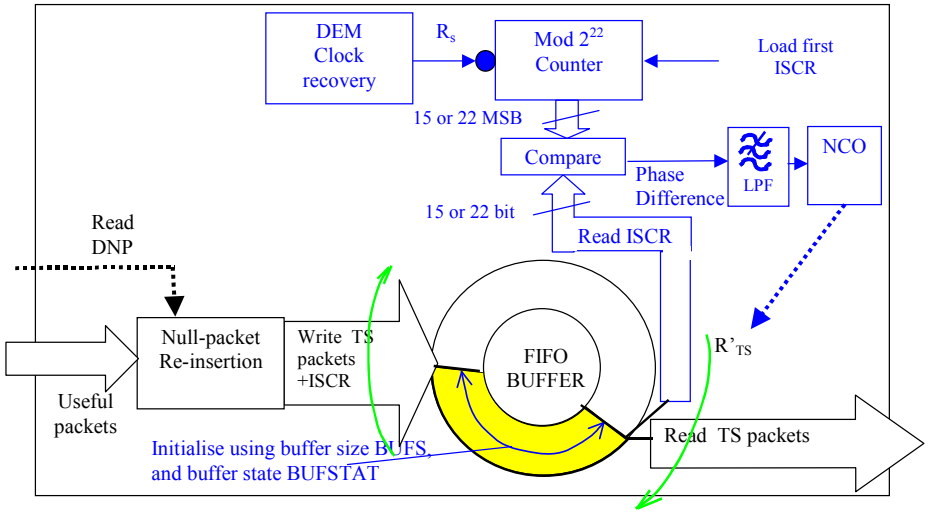

Figure F.3: Example Type 2 Receiver

Annex G:
Time slicing

G.0 Introduction

The purpose of time slicing is to reduce FEC decoding speed of a receiver. A receiver has to decode the PL-Header of each PL-Frame and decide, if this PL-Frame contains the target TSN. Signalling of Classical MODCOD and S2X MODCOD may change PL-Frame by PL-Frame. The sequence of time-sliced transmission is not specified in ETSI EN 302 307-1 [i.2] and ETSI EN 302 307-2 [i.44].

Various sequence setups are possible: simple setups and sophisticated setups. In this clause only simple setups are considered.

G.1 PL-Header for time slicing

PL-Header for time slicing (Annex M of ETSI EN 302 307-1 [i.2] and Annex M of ETSI EN 302 307-2 [i.44]) are different from the normal PL-Header. PL-Header for time-slicing lasts 180 symbols (normal 90 symbols) allowing to signal TSN.

PL-Header consists of:

- PL-Header.SOF 26 symbols
- PL-Header.PLScode 154 symbols

SOF (Start Of Frame) will be transmitted without scrambling, duration and content is equal to SOF of normal PL-Header. PLScode will be protected by convolutional code and afterwards scrambled by a dedicated sequence.
16 information bits are transmitted in the PLScode (u0 .... u15). MODCOD, Type, TSN will be signalled. Information bit u0 is important for differences in signalling MODCOD and Type.

Remarks for S2X MODCODs:

- With u0=1 fec frame type is dedicated to MODCOD in all cases.
- VL-SNR MODCODs are transmitted with pilot state = on.
- Some combinations of MODCOD signalling are reserved. For these settings pilot state is dedicated.

u0 = 0 (classical MODCODs):

u0 = 0

u1...u5 = MODCOD (see table 12 in ETSI EN 302 307-1 [i.2])

u6, u7 = type (fec frame type, pilots)

u8...u15 = TSN

u0 = 1 (S2X MODCODs):

u0 = 1

u1...u6 = MODCOD (see table 17a, 17b in ETSI EN 302 307-2 [i.44])

u7 = Pilots

u8...u15 = TSN

G.2 Simple time slice setups

G.2.1 Time Slice Sequence

Although very complex sequences are allowed a very simple sequence is chosen to explain implementation.

G.2.2 Simple Scheduling Assumptions:

- TimeSliceCycle: a timeslice cycle consists of num_timeslice pl frames;
- periodical repetition of this time-slice cycle: the TimeSliceCycle is static;
- static order of time-slices: every active TSN is transmitted in one pl frame and transmitted one time in one TimeSliceCycle;
- order of time-slices: the transmit order of TSN is static;
- static parameters of each time-slice: each TSN uses constant MODCOD and Type.

G.2.3 Examples of TimeSliceCylces

EXAMPLE 1:

num_timeslice = 4

active TSNs: TSN1, TSN2, TSN3, TSN4

transmit order of 1 timeslice cycle: $1 \rightarrow 2 \rightarrow 3 \rightarrow 4$

EXAMPLE 2:

num_timeslice = 3

active TSNs: TSN1, TSN2, TSN3

transmit order of 1 timeslice cycle: $1 \rightarrow 2 \rightarrow 3$

EXAMPLE 3:

num_timeslice = 8

active TSNs: TSN1, TSN2, TSN3, TSN4, TSN5, TSN6, TSN7, TSN8

transmit order of 1 timeslice cycle: $1 \rightarrow 2 \rightarrow 3 \rightarrow 4 \rightarrow 5 \rightarrow 6 \rightarrow 7 \rightarrow 8$

G.3 Calculation of symbol rate of a simple time slice setups

G.3.0 General

In a simple time slice setup (with assumptions listed), average symbol data rate of each time-slice can be calculated:

- with S(i) = S of time-slice(i) (number of Slots - see table 11 in ETSI EN 302 307-1 [i.2] and table 16 in ETSI EN 302 307-2 [i.44])
- with pilot_state(i) = 0 when pilots of time-slice(i) are off
- with pilot_state(i) = 1 when pilots of time-slice(i) are on

(1)

num symbols of time-slice(i) = 90,0 × (S(i)+2,0) + pilot_state(i) × 36.0 × ((int)floor((S(i)-1,0)/16,0

(2)

num symbols tsl cycle = sum (num symbols of time-slice(i)) , i = 1...num tsl

(3)

average symbol rate of time-slice(i) = (num symbols of time-slice(i) / num symbols tsl cycle) × symbol rate

Average maximum useful data rate of each time slice can be calculated in a similar way.

G.3.1 Examples of calculation of symbol rate (simple time-slicing setups)

EXAMPLE 1: time-slicing setup with 4 time-slices

num tsl = 4: 1 time-slice cycle consists of 4 time-slices

periodical repetition of this time-slice cycle

static order of time-slices

static parameters of each time-slice

Table G.1

	tsl 1	tsl 2	tsl 3	tsl 4
MODCOD	8PSK (S2 classical or S2-X)	8PSK (S2 classical or S2-X)	8PSK (S2 classical or S2-X)	8PSK (S2 classical or S2-X)
FEC Frame	normal	normal	normal	normal
Pilots	on	on	on	on
TSN	0x11	0x22	0x33	0x44
S	240	240	240	240
num symbols	2 2284	22 284	22 284	22 284
num symbols tsl cycle	89 136			

average symbol rate of time-slice 1 = (22 284/89 136) × symbol rate

average symbol rate of time-slice 2 = (22 284/89 136) × symbol rate

average symbol rate of time-slice 3 = (22 284/89 136) × symbol rate

average symbol rate of time-slice 4 = (22 284/89 136) × symbol rate

EXAMPLE 2: time-slicing setup with 3 time-slices

num tsl = 3: 1 time-slice cycle consists of 3 time-slices

periodical repetition of this time-slice cycle

static order of time-slices

static parameters of each time-slice

Table G.2

	tsl 1	tsl 2	tsl 3
MODCOD	16APSK (S2 classical or S2-X)	8PSK (S2 classical or S2-X)	QPSK (S2 classical or S2-X)
FEC Frame	normal	normal	normal
Pilots	on	on	on
TSN	0x11	0x22	0x33
S	180	240	360
num symbols	16 776	22 284	33 372
num symbols tsl cycle	72 432		

average symbol rate of time-slice 1 = (16 776/72 432) × symbol rate

average symbol rate of time-slice 2 = (22 284/72 432) × symbol rate

average symbol rate of time-slice 3 = (33 372/72 432) × symbol rate

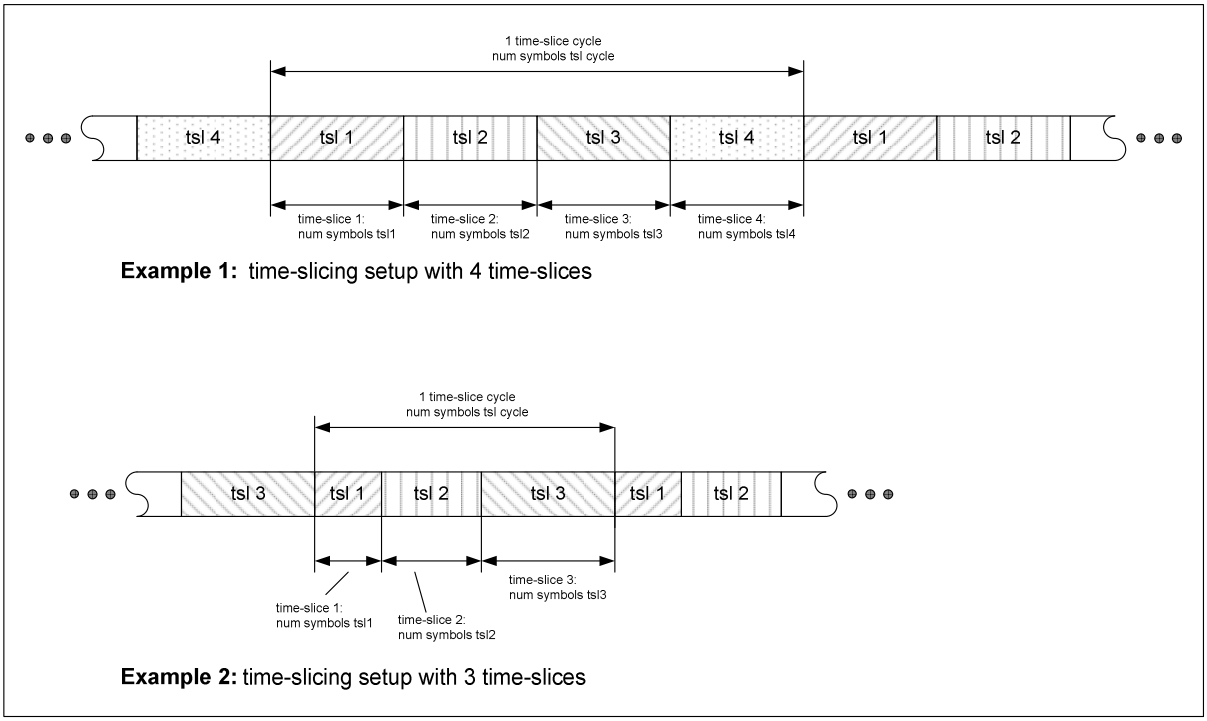

Figure G.1: Timing of example 1 and example 2

Annex H: Bibliography

- ETSI TR 101 154: "Digital Video Broadcasting (DVB); Implementation guidelines for the use of MPEG-2 Systems, Video and Audio in satellite, cable and terrestrial broadcasting applications".
- ETSI EN 300 468: "Digital Video Broadcasting (DVB); Specification for Service Information (SI) in DVB systems".
- M. Eroz, F.-W. Sun and L.-N. Lee: "DVB-S2 Low Density Parity Check Codes with near Shannon Limit Performance", International Journal on Satellite Communication Networks, Volume 22, Issue 3.
- U. Reimers (2nd edition): "Digital Video Broadcasting - The DVB Family of Standards for Digital Television", 2nd ed., 2004, Springer Publishers, New York, ISBN 3-540-43545-X.
- G. Karam and H. Sari: "A Data Pre-distortion Technique with Memory for QAM Radio Systems", IEEE Transactions on Communications, Volume COM-39, No. 2, pp 336- 344, February 1991.
- Jack K.Holmes: "Coherent spread spectrum systems", Wiley Interscience, pp 395 to 426.
- ETSI EN 300 744: "Digital Video Broadcasting (DVB); Framing structure, channel coding and modulation for digital terrestrial television".
- S. Mirta, T. Schierl and T. Wiegand , P.Inigo, C.LeGuern, C.Moreau, L.Guarnieri and J.Tronc: "HD Video Broadcasting using Scalable Video Coding combined with DVB-S2 Variable Coding and Modulation", In the Proc. of the 2010 5th Advanced Satellite Multimedia Systems Conference and the 11th Signal Processing for Space Communications Workshop, Cagliari, Italy, 13-15 September 2010 , pp. 114-121.
- H. Schwarz, D. Marpe and T. Wiegand: "Overview of the Scalable Video Coding Extension of the H.264/AVC Standard", IEEE Transactions on Circuits and Systems for Video Technology, Special Issue on Scalable Video Coding, Volume 17, No. 9, pp. 1103-1120, September 2007.

History

Document history		
V1.1.1	February 2005	Publication as ETSI TR 102 376
V1.2.1	November 2015	Publication